BIOGENIC SILICA NANOPARTICLES DERIVED FROM RICE HUSK BIOMASS AND THEIR APPLICATIONS

by

Haoran Chen

A dissertation submitted to the Graduate Council of
Texas State University in partial fulfillment
of the requirements for the degree of
Doctor of Philosophy
with a Major in Materials Science, Engineering, and Commercialization
December 2013

Committee Members:

Luyi Sun, Chair

Clois E. Powell

Chang Ji

Benjamin Martin

F. Benjamin Zhan

FAIR USE AND AUTHOR'S PERMISSION STATEMENT

Fair Use

Duplication Permission

DEDICATION

This dissertation is dedicated to the unique Ph.D. program of the Materials Science, Engineering, and Commercialization in Texas State University.

ACKNOWLEDGMENTS

The author would like to express his heartfelt acknowledgment to Professor Luyi Sun for his thoughtful supervision, resourceful advice, and patient guidance throughout the course of this work.

The author would like to gratefully convey his gratitude to all committee members, Dr. F Benjamin Zhan, Dr. Benjamin Martin, Dr, Chang Ji, Dr. Clois Powell, Dr. Luyi Sun, for their time and efforts on reviewing and commenting this dissertation.

The author wants to express his appreciation to his parents for their understanding and endless support throughout the duration of his studies. Their unconditional love is the source of his faith to a better life. He is forever indebted to them.

The author is particularly grateful to his wife, Lijuan Jia, who did more than her share around home. Without her support and gentle prodding, pursuit of this degree would never have been started. The author fondly wishes his wife should receive credit for more than his share of this work.

TABLE OF CONTENTS

Page

LIST OF TABLES

Table **Page**

LIST OF FIGURES

Figure **Page**

LIST OF SCHEMES

Scheme **Page**

ABSTRACT

According to the Food and Agriculture Organization of the United Nations (FAO), the global paddy rice production in 2013 is estimated to be 746 million tons. Based on this, the amount of rice husks (RHs) are estimated to be ca. 160 million tons. Applications of RHs have been very limited. Therefore, RHs are often considered as a biowaste. RHs could be a suitable candidate of feedstock for silica based materials because of their high silica content (15−28 wt %) and large availability. In recent years environmental demand and sustainable development have become increasingly important. It is important to study and utilize RH biowaste, and convert RHs into valued materials. This is the focus of this research. The work is reported and summarized in seven chapters in this dissertation.

Chapter 1 is an overview of the preparation of silicon based materials from rice husk biomass. Researches have been conducted on using RHs as a raw material to synthesize a number of silicon compounds, including silica, silicon carbide, silicon nitride, silicon tetrachloride, zeolite, and elementary silicon. The applications of such materials are very comprehensive. Synthesis of these silicon based materials from RHs and their applications are reviewed in this chapter.

In Chapter 2, efforts on comprehensive utilization of RH have been made to obtain both lignocellulose and high quality porous silica nanoparticles. RHs are mainly composed of lignocellulose (ca. 72-85 wt %) and silica (ca. 15-28 wt %). The majority of previous explorations focused on the preparation of silica or other silicon based materials

from RHs. The lignocellulose in RHs was usually burnt and wasted. In this study, most of the lignocellulose in RHs was extracted by ionic liquids which are environmentally benign solvents. The dissolved lignocellulose was separated and collected. The RH residue after extraction contains a high concentration of silica and was thermally treated to synthesize amorphous porous silica nanoparticles with a high purity and surface area. During the extraction of lignocellulose using ionic liquids, some metal cations (e.g., K^+) that can compromise the synthesis of silica are removed, which is synergistic for this comprehensive approach to make full use of RH biomass.

Chapter 3 studied the effects of different sources of silica on synthesizing lithium aluminum silicate (LAS) powders via a sol-gel method. Silica from the ash of untreated rice husk (RHA), silica from HCl treated rice husk (Silica-RH-HCl), and fumed silica were used to prepare LAS powder with various calcination temperatures, i.e., 400, 600, 800 and 1000 °C. X-ray diffraction (XRD) characterization showed that, in terms of apparent reactivity in the LAS synthesis, fumed silica has the highest reactivity. The silica from HCl treated rice husk has a similar but slightly lower reactivity when compared to fumed silica. RHA has the lowest reactivity among the three silica sources. This apparent reactivity is mainly determined by the intrinsic structure, including surface area and crystallinity of silica, which can be characterized by XRD and BET measurement. Overall, a higher surface area and low crystallinity are favored for the proceeding of reactions. More details about the intrinsic structure of silica are discussed in this chapter.

In Chapter 4, platinum nanoparticles (Pt-NPs) supported on silica derived from HCl treated RHs were prepared. Pt-NPs based catalysts have received attention in the past decades because of their unique catalytic properties in many important industrial processes. Experimentally and theoretically the size of Pt-NPs plays a crucial role in governing the catalytic activity. Smaller Pt-NPs exhibit higher catalytic activity. Silica has been extensively used as a support to synthesize metal nanoparticles for heterogeneous catalysis applications. However, the silica used was mostly prepared from silanes, such as tetraethoxysilane (TEOS), via a sol-gel process, which is expensive and non-environmentally friendly. Moreover, the silica particles from the sol-gel process typically possess a smooth surface, which is not ideal for the supporting of metal nanoparticles. In Chapter 4, we report a facile method to synthesize Pt-NPs based heterogeneous catalysts using the silica from RHs as the support. The biogenic silica from RHs offers a rough surface, which appeared to be much more ideal for supporting Pt-NPs than the TEOS derived silica particles.

In Chapter 5, fluorescent silica was prepared from acid treated RHs with various conditions. The fluorescence intensity of some samples was strong enough to be viewed by naked eyes in daylight at room temperature when irradiated by 365 nm UV light. The fluorescence intensity of the silica samples was roughly proportional to its carbon content. The higher carbon content resulted in stronger the fluorescence intensity. The fluorescence mechanism of the silica from RHs was discussed based on the experimental data in this chapter and the results from the literature.

In Chapter 6, four colored ceramic pigments green, blue, yellow, and red/coral, were prepared using three different silica precursors which are fumed silica, the silica from HCl treated RHs, and commercial crystalline silica. Studies showed that the silica from HCl treated RHs has a similar apparent reactivity to fumed silica, and can be a suitable substituent material for the pigment preparations. Among the three silica precursors, commercial crystalline silica exhibited the lowest apparent reactivity in terms of $ZrSiO_4$ conversion rate. The apparent reactivity of the three silicas has a similar pattern to that of the silicas studied in Chapter 3. Overall, higher degree of silica crystallinity results in a lower reactivity for the pigment synthesis.

In Chapter 7, a brief summary and the outlook are discussed. Categorization of biomass is defined and discussed. Biomass was divided into three categories, which are food competitor, non-food competitor, and biowaste. RHs are a "true biowaste" based on our definition. Compared to the other two categories of biomass, true biowaste would be the most economical resource to take advantage of since the investment on the raw material would be virtually "zero". As such, RH biomass is still worthy of further investigation and exploration, because it has great potential in terms of both sustainability and business profit.

CHAPTER 1

Silicon Based Materials from Rice Husk Biomass

1.1 Introduction

Rice husk (RH) is a byproduct of rice production.[1-3] RH contributes ca. 20–25 wt % of the total dry weight of paddy rice.[1, 4] The global rice production in 2012 was estimated to be 489.1 million tons,[5] which means approximately 122–163 million tons of RH biomass was generated in 2012. The utilization of RH has been limited because of their tough and abrasive nature, low nutritive value, and low bulk density.[6-8] The most common RH disposal approaches is open field burning, which results in waste of energy, air pollution, and greenhouse gas emission.[9]

The main components in RH are lignin, cellulose, and hemicellulose, which are generally named lignocellulose. RH also contains ca. 15 to 28 wt % of silica.[10-12] The high content of silica in RH presents opportunities for the preparation of value-added silicon based materials. Since the 1970s, various silicon based materials, including silica, silicon carbide, silicon nitride, silicon tetrachloride, zeolite, and silicates, have been successfully synthesized using RH as the silicon source.[13] This field of research has been significantly advanced and expanded in the past decade spurred by the global attention on sustainable and renewable resources. A review of the advancement in the synthesis of silicon based materials from RH biomass in the past ten years is necessary to define future prospects of this field.

1.2 Structure and components of rice husk (RH)

It was not until 1938 that the existence of silica in RH was discovered.[10] Silica is used by plants for protection and also to improve drought tolerance and disease

resistance.[14] Rice plants absorb silica in the form of soluble silicic acid, $Si(OH)_4$, which enters the root of rice from the surrounding soil. Little is known about the mechanism that allows for high silicon uptake. After silicic acid is absorbed, it is transported to the stelai, sheaths, and leaves of the rice plant.[15] Through evaporation and polymerization, $Si(OH)_4$ becomes concentrated into $SiO_2 \cdot nH_2O$. This prompts the formation of cellulose/silica composite membrane. It is commonly believed that some of the silica in RH is bonded to organic compounds but so far few details are available.[16-17] Characterization of RH, including X-ray diffraction, infrared spectroscopy, thermal analysis, and scanning electron microscopy, reveal that the highest concentration of silica is found on unbroken dome-like protrusions of the outer epidermis layer.[18] High concentrations of silica in RH can also be found on hairs called trichomes on both the inner and outer epidermis and in-between epidermal cells.[19] The content of silica in RH dependents on climate, soil composition, and rice variety.[15]

Harvesting silicon based materials has been the major research focus on the application of RH, since silicon based materials have widespread applications.[20-21] It can take advantage of the high value material from RH, and minimize the environmental issues associated with the current applications/disposals of RH. Many economical and green approaches to synthesize valuable silicon based materials from RH biomass have been developed.[13]

1.3 Silica

Silica plays an important role as ingredients in food, pesticides, and personal care products; as fillers in plastics, rubbers, and coatings; and as starting materials for semiconductors, silicates, and ceramics.[22-23] Recently, silica has also been explored for

biomedical applications.[24] The application and value of silica are highly depending on its crystallinity and micro-structure. Crystalline silica is the most abundant material in the earth's crust, but its application is limited mainly owing to its low reactivity.[22-23] Amorphous silica with high surface area is important to many key chemical applications, including absorbents, thermal insulators, and catalyst supports.[25] High quality amorphous silica is mainly produced through a multi-step process starting from the carbon thermal reduction of raw natural silica, sand. The process is associated with high temperature, high pressure, and strong acidity, which is energy intensive and eco-hazardous.[26] To minimize the above issues, and meet the extensive and increasing demand on silica for widespread applications, it is necessary to seek an economical, eco-friendly, and sustainable approach to prepare high quality silica.

The term rice husk ash (RHA) has been adopted to describe various products after various thermal treatments of RH. In this review, we define RHA as the product from non-controlled burning of non-treated RH. RHA contains incompletely burned organic components and a mixture of crystalline and amorphous silica. The products from controlled calcination of RH or from treated RH are referred to as RH silica, which typically contains a very low level of impurities compared to that of RHA.

1.3.1. Preparation of silica from RH

1.3.1.1. Silica from direct calcination of RH

The direct calcination of RH is a simple method for the collection of silica. The morphology and property of the obtained silica depends critically on the calcination conditions. The effects of calcination temperature, duration, atmosphere, and instrument on the resultant silica have been extensively investigated.

Shen et al. conducted thermal treatment of raw RH at 600, 700 and 800 °C for 0.5, 1.5, 2.5 and 3.5 hours with air.[27] The silica from the calcination of RH at 600 °C was amorphous. Calcination of RH at 700 °C was both amorphous and crystalline. The silica exhibited a higher degree of crystallinity after a longer duration of calcination at 700 °C. The RH silica was completely crystalline when treated at 800 °C. The degree of crystallinity of silica from direct thermal treatment of raw RH was sensitive to the calcination temperature, duration, and presence of alkali metal impurities such as K, Ca since they can induce the silica to melt.[27]

Direct calcination of RH is simple and straightforward.[28] The silica usually contains an appreciable amount of metallic and other impurities. A typical RHA compositions are shown in Table 1.1.[29]

Table 1.1 Composition of RHA derived from calcination of raw RH at 600 °C for 12 h.[29]

SiO_2	Al_2O_3	Fe_2O_3	CaO	MgO	K_2O	Na_2O	MnO	TiO_2	P_2O_5
93.2	0.13	0.07	1.23	0.25	0.78	0.08	0.33	0.006	0.15

1.3.1.2 Silica from calcination of treated RH

1.3.1.2.1 Water pretreatment

In order to obtain high quality amorphous silica from RH, proper pretreatment is needed. Water leaching of raw RH to remove adhering soil, dust, and some metal cations was found to be one of the simplest pretreatments to obtain high quality RH silica.[27, 30-33]

Shen et al.[27] examined and compared the effects of calcination parameters on the crystallinity of silica from the raw RH and water-leached RH. The raw RH was washed with deionized (DI) water at 25 °C at a rate of 80 mL/g (H_2O/RH) for 4 hours. Then the

water-treated RH was calcined at 600, 700 or 800 °C for 0.5, 1.5, 2.5 or 3.5 hours. All the silica samples from water treated RH was amorphous, which was different from that of non-treated RH.[27] The non-treated RH tended to give crystalline silica after prolonged calcination at higher temperatures.[19, 27] The conversion from amorphous to crystalline (α-cristobalite) of silica derived from water-treated RH was found to start at ca. 850 °C.[33] Wang et al. used elemental analysis to show that the simple water rinse can effectively remove most minerals except for K and Ca in RH.[30] Compared with raw RH, the water rinsed RH is beneficial for obtaining amorphous and high-purity silica.[27, 30] There are still metal impurities and carbonaceous residue remaining in the synthesized silica. In order to prepare even higher purity and more amorphous silica from RH, pretreatment of RH with acid or base is needed.[30]

1.3.1.2.2. Acid pretreatment

Many efforts have been made to reduce metal and carbonaceous impurities to synthesize high quality RH silica. Certain minerals in RH, such as K and Ca, were found to be responsible for the residual carbon and crystallinity in the synthesized RH silica. The eutectic reaction between minerals and silica during the calcination of RH is responsible.[34-35] Acid-leaching is widely used prior to calcination to effectively remove metal impurities from RH.

Hydrochloric acid (HCl) treatment has been widely adopted for the preparation of silica from RH. In general, RH was boiled in HCl solution for 1−3 hours followed by thoroughly water rinsing and drying.[36-40] The pretreated RH was calcined at 600−900 °C to yield silica. HCl solutions with various concentrations were used for pretreatment.[4, 41-45] Even a low concentration (0.1 N) of HCl solution is effective to remove metal

impurities.[41] According to Zemnukhova et al., after leaching by 0.1 N HCl, the RH was thermally treated first at 400 °C and then at 700 °C to synthesize high purity (ca. 99.9%) amorphous silica with a specific surface area of ca. 297 m^2/g.[41] Similar results have also been reported by several other groups.[42, 46-47] According to Yalçin et al., silica with a purity of around 99.1% was produced from the RH leached with 3% (v/v) HCl.[47] In their study, samples were calcined at 600 °C for 3 hours under flowing argon and 1 hour under flowing oxygen.

The heating rate was found to be an important parameter regarding the properties of the final silica from acid treated RH such as purity, specific surface area, and the porosity of the silica.[48-50] Increasing the heating rate led to a higher silica yield, but decreased the specific surface area of silica.[48-50] At a heating rate of 5 °C/min, the specific surface area of the prepared silica powders can be up to 235 m^2/g. The purity was higher than 99.7 %.[48-50]

It has been suggested that the minerals in RH, particularly K, significantly affect the purity and crystallinity of RH silica nanoparticles.[51-53] In order to better understand this, Wang et al. conducted a systematic investigation.[30] They first verified that HCl treatment was indeed effective to remove the metal impurities by conducting elemental analysis on the silica derived from the calcination of the HCl treated RH. Two samples of HCl treated RH were intentionally doped with Ca^{2+} and K^+ respectively. The Ca^{2+} and K^+ doped RH were calcined at 700 °C for 2 hours. The subsequent characterizations showed that the K^+ doped RH led to the formation of semi-crystalline silica, while Ca^{2+} doped RH resulted in amorphous silica. This was very similar to preparations from metal free

RH. The above control experiments offered solid evidence and confirmed that K^+ was the significant factor for preparing high-quality silica from RH.

The negative effect of K^+ comes from the promotion of the melting of silica particles. The melting of silica lowers the silica surface area, increases silica particle size, and is responsible for the encapsulation of impurities, that results in crystallization of silica upon cooling.[30]

Another major source of impurity for RH silica is the carbonaceous residue from the incomplete combustion of the organic components in RH. A sufficiently high calcination temperature of ca. 700 °C is needed to completely remove the carbonaceous impurity.[30] Figure 1.1 shows the representative optical pictures and Figure 1.2 shows the SEM images of silica samples prepared from various combination of pretreatment and calcination conditions.[30] Both pretreatment (to remove mineral impurities) and calcination condition (to remove carbonaceous materials) are critical for the synthesis of high purity silica nanoparticles with high surface area (Figure 1.2A−1.2C).[30] Figure 1.2A shows the completely melted silica from high combustion temperature and the presence of K^+, while Figure 1.2C shows the partially melted silica forming irregular porous structures. This is probably because the silica at this region started to cool down before it was completely melted and fused because of insufficient heat supply. Figure 1.2B shows the transition between the two regions. Under controlled conditions (700 °C calcination and acid treatment of RH), amorphous silica nanoparticles of 20–30 nm with narrow size distribution were prepared (Figure 1.2G).[30]

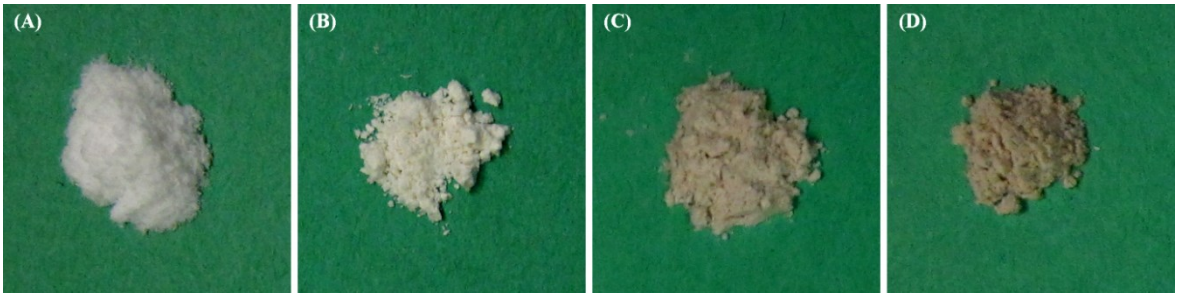

Figure 1.1 Representative silica samples exhibiting various colors; (A) white silica from HCl treated RH (700 °C, 2 h); (B) off-white silica from HCl treated RH (600 °C, 4 h); (C) light grey silica from water treated RH (800 °C, 2 h); (D) grey silica from water treated RH (600 °C, 2 h). Reprinted with permission from reference,[30] copyright 2011 Springer

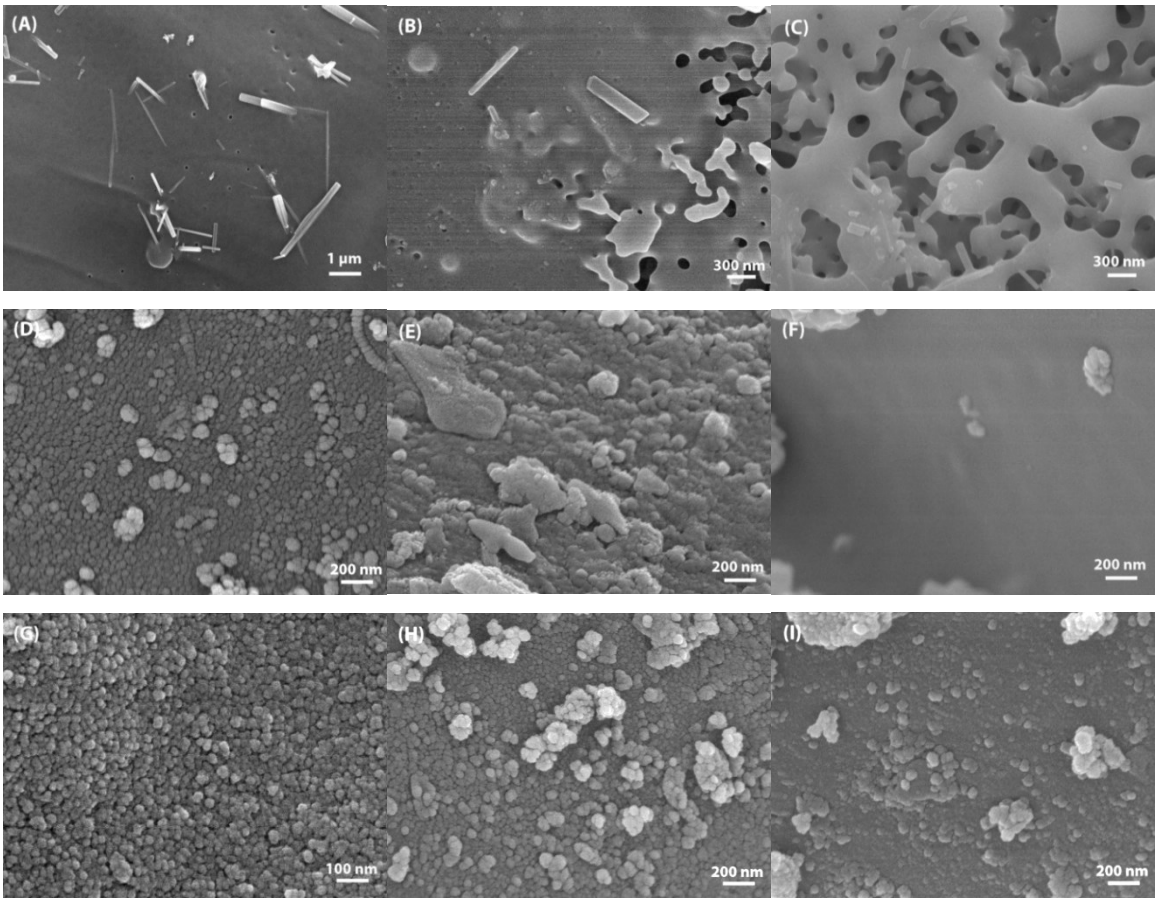

Figure 1.2 SEM images of silica samples. (A, B, C): silica from open field burning of raw RH; calcination of silica from water treated RH: (D, 700 °C, 2 h; E, 800 °C, 2 h; F, 800 °C, 8 h); calcination of silica from acid treated RH (G, 700 °C, 2 h; H, 800 °C, 2 h; I, 800 °C, 8 h). Reprinted with permission from reference,[30] copyright 2011 Springer

Besides HCl, various other acids including H_2SO_4,[34, 47] HNO_3,[54-61] and HBr[62] etc. have been used to treat RH to produce high quality silica. In order to establish a more environmentally benign process to synthesize high purity silica from RH, dilute H_2SO_4 solutions (1–5%) were used to leach RH instead of the high concentration (10-20%) H_2SO_4 solution as reported in the previous study.[34, 63] RH was first soaked in the dilute H_2SO_4 solution at 44 °C for 15 min. Following a brief rinse to remove the residual H_2SO_4 and dry at 100 °C for 1 hour. RH was calcined at 600–1000 °C for 30 min in air to produce high purity silica.[34] The results showed that dilute H_2SO_4 solution did not cause RH fragmentation as did by concentrated H_2SO_4 solution. The charring of the carbonaceous materials in RH was significant when concentrated H_2SO_4 solutions were used for the leaching treatment.[63] Low concentration H_2SO_4 solution (<5%) was sufficient to remove metallic impurities in RH. The high purity amorphous silica (99.3%) was produced when using 5% H_2SO_4 leaching treatment followed by calcination at 800 °C for 30 minutes.[34] The crystallization of amorphous silica was found to occur at 1000 °C or higher.[34]

Because of the low corrosivity, low cost, and environmental friendliness, organic acids recently have attracted attention as alternatives to the strong acids to pretreat RH. A number of organic acids, such as acetic acid,[32] oxalic acid,[32] and citric acid, [35, 64] were good candidates for the removal of the metal impurities in RH to obtain high purity silica. The strong chelate effect between the carboxyl groups of the organic acid and metallic impurities contained in RH facilitates the removal of such impurities. The amorphous silica with a purity of 93.0–96.7% has been synthesized by leaching RH using organic

acids followed by calcination at 700 °C for 2 hours.[32] Though less efficient than HCl, both oxalic and acetic acids were found effective for removing all metal impurities.

Umeda et al. soaked RH in 1−7 wt % citric acid solutions with stirring for 15−120 minutes, followed by distilled water rinse at 20 °C for 15 minutes with stirring to remove the citric acid residue from RH.[35] After drying at 100 °C for 60 min, the pretreated RH were calcined at 800−1000 °C for 30 min in a muffle furnace with an air flow rate of 0.42 mL/s. Leaching RH with 1 wt % citric acid could significantly reduce the metal impurities in RH. Na_2O and K_2O were completely removed.[35] The removal of Ca based impurities depended on the citric acid solution concentration, temperature, and stirring time. The CaO content in silica was reduced to 0.03% when RH were soaked in 5 wt % citric acid solution at 80 °C for 60 min, followed by thermal treatment at 800 °C for 30 min. The crystallization starting temperature of RH silica was 1100 °C which is significantly higher than that of RH silica obtained from raw RH (generally 700 °C or higher).[30] This was attributed to the prevention of eutectic reaction of silica with K_2O or Na_2O impurities by reducing their contents in RH.[35] The calcination time was not significantly effective regarding the crystallization of RH silica. In conclusion, the amorphous silica with a high purity of 99.5–99.7 wt % and a very low carbon content (0.02–0.03 wt %) was synthesized from 5 wt % citric acid treated RH followed by calcination at 800–1000 °C.[35]

The corrosive nature of strong inorganic acids increases the demand for anti-corrosive reactors which may not be cost effective for practical production. Organic acids (especially citric acid) are expected to be ideal candidates for future commercialization of harvesting high quality silica from RH.

1.3.1.2.3. Base or salt pretreatment

Bases have also been explored to treat RH to remove metal impurities. Sodium hydroxide (NaOH) was most commonly used. Yalçin et al. soaked raw RH in 3% NaOH solution for 24 hours at room temperature after being washed with water and dried at ca. 110 °C for 24 hours.[47] After being thoroughly washed with distilled water and dried at 110 °C to remove NaOH residue, the alkaline leached RH was calcined at 600 °C for 4 hours in static air. The RH silica with a low silica content (39.8%) was obtained. NaOH treatment was not effective in making high purity RH silica.[47] Markovska et al. studied the extraction of silica by NaOH solution. Raw RH were boiled in 2, 4, 6 or 9 N NaOH solutions for 1 or 3 hours.[65] After filtering and rinsing, the RH was dried at 110 °C for 24 hours and then used for study. The results showed that after NaOH leaching, the silica content in RH was decreased, to zero in some cases. The optimal extraction was observed by boiling RH in 2 N NaOH solution at 100 °C for 3 hours.[65] NaOH is used to treat RHA. Its use is discussed in section 3.1.3.2 as an extracting agent.

Salts, such as $KMnO_4$, has also been used to pretreat RH.[66] Javed et al. first washed RH with DI water and dried in an oven at 105 °C for 24 hours. After soaking for 30 min in 0.1, 0.05 or 0.005 M $KMnO_4$ solutions, the treated RH was dried in oven at 105 °C for 24 hours, ground for 30 minutes, and passed through a 10 mesh sieve using a vibration machine. The grounded samples were heated up to 500, 600 or 700 °C from ambient temperature (10 °C/min). After 6 hours of thermal treatment, the samples were cooled down and ground for 30 min into fine powders. The results showed that the pretreatment of RH with a low concentration of $KMnO_4$ was beneficial for the production of amorphous silica in comparison with the samples without $KMnO_4$ pretreatment. It was

hypothesized that the liberated O_2 facilitated the calcination of RH. Too high a concentration of $KMnO_4$ harms the RH silica quality. Potassium element can facilitate the formation of a glassy surface that will prevent further oxidation process and accelerate the crystallization of silica into cristobalite. The pretreatment with a high concentration of $KMnO_4$ increased carbon formation and reduced the RH silica quality. The 0.05 M $KMnO_4$ solution was found to be optimum for treating RH. Temperature is an important parameter for making RH silica. In this study, the most amorphous silica was produced by the calcination of RH treated with 0.05 M $KMnO_4$ solution at 500 °C for 6 hours.[66]

1.3.1.2.4 Pretreatment for morphology control

Most researches focused on the purity and crystallinity when synthesizing RH silica. The micro-structure of the silica has been largely ignored. Sun and coworkers recently conducted an in-depth exploration of the micro-structure of biogenic silica nanoparticles.[46] With the help of transmission electron microscopy (TEM), scanning electron microscopy (SEM), small angle X-ray scattering (SAXS), and surface area characterization, they revealed that the silica nanoparticles (20-30 nm in diameter) synthesized from the calcination of HCl treated RH at 700 °C for 2 hours were actually composed of smaller primary silica nanoparticles with a diameter of ca. 4.2 nm according to SAXS. The nanoparticles exhibit a self-similar property. The mass fractal dimension D_m is about 2.8, which shows a good match for a 3-dimensional fractal aggregate. The Barrett-Joyner-Halenda (BJH) analysis revealed that such silica nanoparticles possess a group of pores with a diameter ranging from ca. 2.0–9.0 nm. This was believed to be contributed by the gaps between the primary particles. The porosity characterization

supplements the TEM and SAXS results. 20–30 nm silica nanoparticles originated from the clustering of primary silica nanoparticles to form a porous 3-dimensional fractal aggregate.

The clustering of primary silica nanoparticles is believed to be caused by the trace amount of K^+ that are not removed by HCl treatment. This phenomenon inspired the researchers to create a tunable porous structure by partially melting the silica nanoparticles through doping the pre-synthesized 20–30 nm silica nanoparticles with K^+ cations followed by controlled thermal treatment. The characterization results showed that such a strategy worked well.[46] Figure 1.3 shows the SEM images of a series of porous silica frameworks synthesized from the calcination of KNO_3 solution treated silica nanoparticles at 800 °C for various durations. Figure 1.3A, 3B, and 3C clearly show the gradual melting and pore structure formation progress of 0.20 M KNO_3 solution doped silica nanoparticles. Two hours of thermal treatment at 800 °C led to significant clustering of the silica nanoparticles. After 4 hours of treatment at 800 °C, the nanoparticles fused and formed a porous structure with a pore size of ca. 20 nm. Extending the treatment at 800 °C for another 4 hours formed well defined pore structure, with a pore size ranging from ca. 25–40 nm. Treatment with a more concentrated KNO_3 solution (0.50 M) resulted in more pronounced fusing of the silica nanoparticles. The pore size did not change much. A much thicker wall formed (Figure 1.3D). These results support the above hypothesis that pretreatment and thermal treatment conditions yield various porous silica nanostructures from RH. The porous silica is semi-crystalline according to the XRD. With increasing crystallinity, the silica nanoparticles can be converted to desirable shapes, and possess sufficient structural integrity. The inset in

Figure 1.3C shows a coin shaped disc as an example. Porous silica frameworks are expected to find wider applications and exhibit superior performance compared to amorphous porous silica for applications such as filtering, etc.[46]

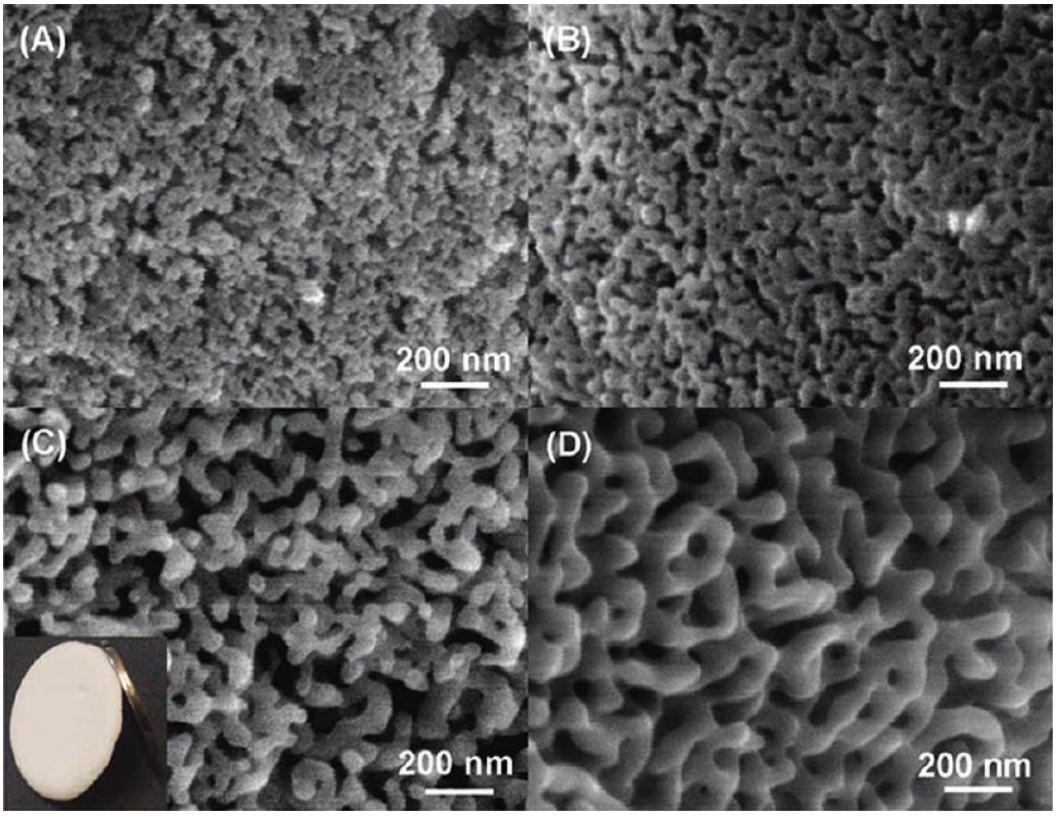

Figure 1.3 SEM images of meso/macro porous silica frameworks. (A) 0.20 M KNO_3, 800 °C, 2h; (B) 0.20 M KNO_3, 800 °C, 4h; (C) 0.20 M KNO_3, 800 °C, 8h; (D) 0.50 M KNO_3, 800 °C, 8 h. The inset in (C) shows a coin shaped disc made of the corresponding semi-crystalline porous silica framework.[46]

Sun and coworkers proposed a model to explain the formation of the hierarchical structure, their melting progress, and porous framework development of the porous silica nanoparticles from RH shown in Figure 1.4.[46] The primary biogenic silica nanoparticles from RH are amorphous and their diameter is ca. 4.2 nm according to the SAXS

characterization. Primary particles clusters form self-similar larger secondary particles with a diameter of ca. 25–30 nm, as characterized by SEM. The secondary particles pack to form large clusters. With elevated temperatures in the presence of K^+ cations, the silica particles gradually melt and fuse together to form larger aggregates and eventually form porous structures. The amorphous silica is gradually converted to semi-crystalline structure.

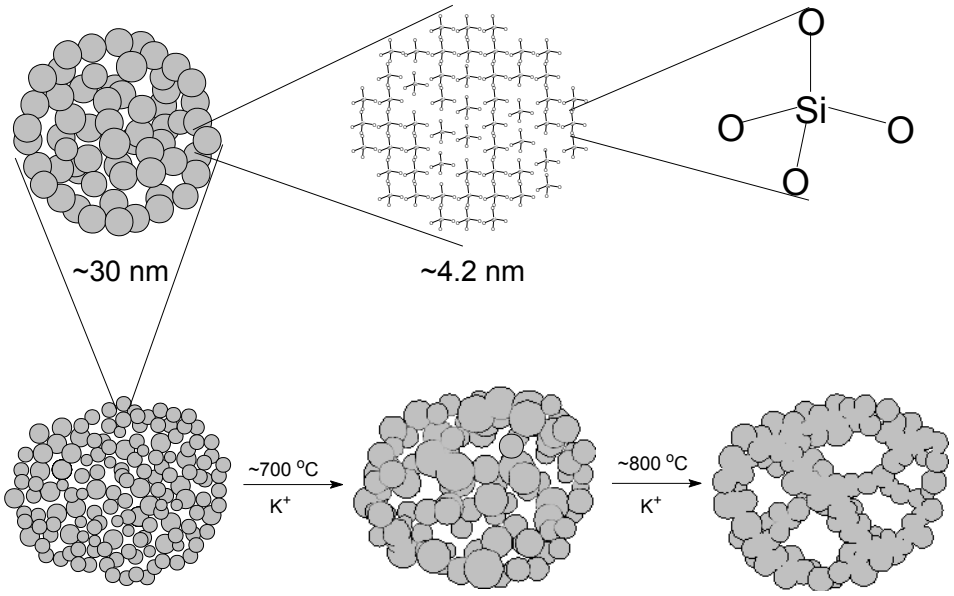

Figure 1.4 Hierarchical structure model of silica nanoparticles and the formation mechanism. Sample synthesized from RH.

1.3.1.2.5. Pretreatment for the comprehensive utilization of RH

The organic components in RH have been wasted when preparing RH silica. Recent research studied the comprehensive utilization of RH by utilizing the organic components when preparing RH silica. Sun and coworkers[12] developed a method to pretreat RH using ionic liquids before synthesizing silica. This achieved the

comprehensive utilization of RH by utilizing silica and lignocellulose from RH. In their study, the water rinsed and dried RH was treated with ionic liquids to extract lignocellulose from the RH. Under optimized conditions, more than 50% of lignocellulose in RH can be extracted and isolated. Such extracted lignocellulose is expected to have applications in biofuel and the paper industry. The ionic liquid used in the pretreatment can be easily recycled.

Without using ionic liquids to extract organic matter, Wang and his coworkers employed acid and alkali treatment of RH for a comprehensive utilization that produce high-purity silica and D-xylose or glucose.[67-68] In their studies, RH was washed thoroughly with distilled water and dried at 105 °C overnight and ground to 60 mesh.[67-68] The mixture of RH and dilute H_2SO_4 were hydrothermally treated at temperature ranging from 100 to 160 °C for 1 to 7 hours followed by filtration.[67] After filtration, the residue was washed with distilled water and dried at 105 °C overnight followed by calcination at 700 °C for 15 min under static air to produce superfine silica with a purity of 99.87%. The filtrate was neutralized by $Ca(OH)_2$ slurry to pH 3.0, and maintained at 75 °C for 1 hour followed by filtration to remove $CaSO_4$. The filtrate was treated with active carbon at 75 °C for 40 min, resulting in colorless solution. The mixture was filtered again, and filtrate was then treated with cation exchange resin (D001-CC) and basic anion exchange resin (D296) sequentially to remove metallic ion and organic acid. Following reduced-pressure distillation, the obtained syrup was dissolved into ethanol at 40 °C and treated by activated carbon once more. The filtrate was cooled to produce D-xylose with a purity of 98.5%. The optimum hydrolysis of xylan for the D-xylose synthesis was achieved by

hydrothermal treatment at 130 °C for 2 hour using 4% H_2SO_4 with the ratio of RH to acid 1:4 (g:mL). With this process, the hydrolysis of xylan from RH reached 96.22 wt %.[67]

Wang and his coworkers used concentrate H_2SO_4 to treat the pretreated RH to produce glucose, amorphous RH silica, and crystalline $Na_2SO_4 \cdot 10H_2O$.[68] The raw RH was boiled in dilute H_2SO_4 (2–8 wt %) followed by washing and drying. The acid leached RH was mixed with concentrate H_2SO_4 solution (67, 72, 77 and 82 %). The hydrolysis temperature was at 30, 40, 50 or 60 °C, while the hydrolysis time was 2, 5, 10 or 15 min. After hydrolysis, the mixture was filtered. The solid residue was calcined at 800 °C for 3 hours after washing and drying to produce amorphous silica nanoparticles with a size under 50 nm. The acid liquid filtrate was cooled down to produce glucose. The glucose yield reached 45.6 % when hydrolyzed at 50 °C for 5 min with 72% H_2SO_4 solution.[68] The above works represent good examples of comprehensive utilization of RH.[67-68]

1.3.1.3. Silica from post-treatment of RHA

The post-treatment of RHA was extensively studied for producing relatively high-purity RH silica. It is typically applied to the RHA from the combustion of RH. RHA typically contains impurities due to incomplete combustion of RH, or the encapsulation of impurities within melted silica. Post-treatment can improve the quality of RHA, but the quality of the final silica product is usually much lower than silica obtained from controlled calcination of pre-treated RH.

1.3.1.3.1. Acid post-treatment of RHA

Acid-leaching performed after calcination of RH is an effective method to remove the metal impurities and produce high-purity silica. Real et al. used RHA which was

obtained from calcination of RH at 600 °C to produce amorphous RH silica by leaching with HCl solution.[52] The product exhibited similar purity (about 99.5%) with that synthesized from calcination of HCl treated RH. However the specific surface area of the silica by acid post-treatment method was poor (1 m^2/g), much lower than that of silica produced by acid pre-treatment method (around 260 m^2/g).[52]

According to the study by Yalçin et al.,[47] RH was subjected to pre- or post-treatment by boiling in 3% (v/v) HCl solution for 2 hours. Both samples were calcined at 600 °C for 3 hour under flowing argon and 1 hour under flowing oxygen. The purity of silica obtained by post-treatment of RHA method was 95.14%. This is higher than silica from RH without treatment (91.50%) and lower than that of silica obtained by pre-treatment (99.16%). The silica had the highest purity (99.66 %) if 3% (v/v) HCl was used for treatment before and after calcination of RH.[47] Acid post-treatment can remove most of the metal impurities and was used in some areas. But the low special surface area limited its application.[69-71]

1.3.1.3.2. Base post-treatment of RHA

The unique solubility behavior of SiO_2 in base, very low solubility when pH<10 and increased solubility when pH>10, has been employed to extract SiO_2 from RHA by the alkaline dissolution followed by acid precipitation. A series of high-purity silica xerogels from RHA were successfully synthesized by Kalapathy et al. The effect of the type of acid used, and the pH value of gelation and pre-acid washing of RHA on the purity and properties of the obtained SiO_2 gel were discussed.[72-73] In general procedure, RHA obtained from raw RH was boiled in 1 M NaOH solution for 1 hour and then filtered to produce sodium silicate solution. Acid (HCl, citric acid or, oxalic acid) was

added to the sodium solution to adjust the pH value. The mixture was then incubated for certain time to obtain silica gel, which was later crushed, washed with DI water, and centrifuged to remove soluble salts. After drying at 80 °C for 24 hours, the amorphous silica xerogel was finally obtained. The contents of the impurities in the obtained silica xerogels varied as a function of the pH and the type of acid used. The silica sample produced at pH 4.0 had lower carbon content than the one produced at pH 7.0. The carbon content of silica produced by citric or oxalic acid is higher than that by HCl at pH 7.0.[72] The pH of gelation and silica concentration of gel-forming solution had significant effects on the density and the mechanical strength of the xerogels.[74] High pH led to condensed glassy solids, while high silica concentration produced highly porous silica xerogel. To reduce the metal impurities of xerogels, RHA was washed prior to alkali dissolution.[73] RHA was dispersed in distilled water. The pH was adjusted to 1, 3, 5, or 7 with HCl acid. After stirring for 2 h, filtering, and washing, the obtained RHA residues were then used to produce silica xerogel. The silica gels formed after dissolution in 1 M NaOH followed by acidification (to pH 7) using HCl. The silica gels were washed twice using DI water and dried at 80 °C for 12 hours to produce xerogels. The results showed that acid washing prior to extraction resulted in amorphous silica xerogel with a low concentration of Ca (< 200 ppm), while the final washing of the xerogel led to low Na, and K contents (total contents < 0.1%).[73]

H_2SO_4[75-77] and HNO_3[78] were also used to adjust the pH value of sodium silicate solution from RHA to produce silica gels. Wang and coworkers boiled the RHA from the calcination of RH at 600 °C for 4 hours in NaOH solution to produce sodium silicate solution, which was subsequently neutralized by H_2SO_4 to form a silica hydrogel. Then

silica aerogel was produced by supercritical carbon dioxide (CO_2) drying[75] or by drying in the atmosphere after adding the appropriate amount of tetraethyl orthosilicate (TEOS) and washing successively by water and ethanol.[76] The synthesized aerogels exhibited high surface area (597.7 and 500 m^2/g respectively).

Besides NaOH solution, Na_2CO_3 was also used to dissolve RHA because it can be recycled by Jang group.[79] To obtain high-purity silica, the RHA from a power plant was boiled in 1 M HCl solution for 2 hours. Following distilled water washing and drying at 120 °C for 12 hours, the acid-rinsed RHA was then mixed with Na_2CO_3 solution and boiled for 4 hours. After filtering, the filtrate was kept at 85 °C, into which a purified waste gas (from the same power plant, contains about 20–40% CO_2) was introduced for 60 min. The resulting slurry was aged at room temperature for 3 hours and filtered. The high-purity amorphous silica powder was finally obtained after distilled water washing and drying at 120 °C for 24 hours. Different from NaOH solution extraction, Na_2CO_3 solution can be reused by adding a small quantity of Na_2CO_3 to its initial solution. This environmental-friendly and low cost procedure is suitable for large-scale production.[79]

The NH_4F was used to synthesis 50-60 nm silica powder by the same group.[80] In a general process, RHA from a power plant was first boiled with HCl solution. The acid-rinsed RHA was added into the NH_4F solution to yield $(NH_4)_2SiF_6$ and was then filtered. The NH_3 produced during the reaction was collected by DI water to form $NH_3 \cdot H_2O$. The filtrate was added to $NH_3 \cdot H_2O$ to yield silica precipitate and NH_4F solution. The high-purity amorphous silica products were produced after washing and drying the precipitate. The NH_4F filtrate was collected and reactivated as the reactant. Although the main

reagent, NH_4F, can be recycled, the corrosive nature of NH_4F will be a negative factor during the production.

1.3.1.4. Silica from hydrothermal and steam-explosion method

Mochidzuki et al. developed a hot water autoclave method and a steam explosion method to prepare high-purity amorphous silica.[81] RH (1–3 g) was washed, dried and added into a reactor with 30 mL of DI water, which was heated in a salt bath at 180, 200, 220, and 240 °C for 18 mins (8 min for a warm-up period and 10 min for constant-temperature reaction) respectively. The mixture was then separated by filtration and the insoluble residue was washed with acetone and dried to produce RH silica. The difference between the so made RH silica and conventional RHA is the former contained fewer metallic impurities. This product consisted of Q4 ($*Si(OSi)_4$), Q2 ($((OH)_2*Si(OSi)_2$), and Q3 ($((OH)*Si(OSi)_3$) units which remained the silica structure in the original rice husk. This is very interesting since the amorphous silica having Q2 and Q3 units is assumed to be more active in aqueous-phase reactions. This hot-water-treatment method to prepare silica is applicable to the preparation of water-glass like materials that are required in some liquid-phase syntheses of inorganic materials, e.g., an advanced production system of mesoporous silicate.[81]

1.3.1.5. Bio-method for making silica from RH

Inspired by the fact that the biocycling of silica occurs through microbial activities in soil and living organism activities below marine surfaces, many scientists have mimiced natural biological processes for the preparation of silica from RH.[82-84] This method is more cost-effective and more environmental-friendly than the common chemical method.

Bansal et al. prepared crystalline silica nanoparticles via biotransformation of amorphous silica in RH through a bio-method.[82] The plant pathogenic fungus, *Fusarium oxysporum*, was cultured and used as the fungus. After washing thoroughly under sterile conditions, 20 g wet weight fungal biomass was re-suspended in 100 mL sterile distilled water containing 10 g RH. The above mixture was shaken at 27 °C for 24 hours, and then filtered to separate the fungal mycelia and RH from the aqueous component. The filtrate was treated with phenol/chloroform (1:1) mixed solvent and was centrifuged to remove the free extracellular fungal proteins from the aqueous solution. The evaporation of the supernatant under low pressure yielded crystalline silica that was capped by stabilizing proteins in the form of 2–6 nm quasi-spherical particles. X-ray photoemission spectroscopy (XPS) analysis showed that the reaction of fungus with RH leached out 96% of silica within 24 hours. The stabilizing proteins could be removed by calcination of the capped silica nanoparticles at 400 °C for 2 hours to produce crystalline porous silica often with cubic morphology. To understand its effect on RH, *Fusarium oxysporum* was also used to react with the commercial amorphous silica. The results showed that the fungus was capable of transforming commercially amorphous silica into crystalline silica. Thus, it was concluded that the amorphous silica in RH was leached out by the specific biomolecules/proteins released by the fungus and then biotransformed into crystalline silica particles. By comparative experiments, cationic extracellular proteins could just bioleach RH into amorphous silica instead of crystalline silica win in vitro conditions. In conclusion, the proteins alone did not lead to biotransformation of amorphous silica into nanocrystallite silica. The biotransformation process using microorganisms indicates that large-scale synthesis of silica at the room-temperature is possible.

Different from above study, amorphous silica (in the presence of small quartz crystallites) was synthesized from RH by using Californian-red worms.[83] This process involved the complete conversion of the annelids' diet from organic material to RH by gradually feeding them with RH for 5 months. During digestion, the muscles of the intestinal wall break down the RH while the endocrine, faring and calciferous glands provide enzymes (amylases, proteases), which degrade the organic material. Silica resisted enzyme attacks during the degradation process and was finely ground by the earthworms' digestive system. The resultant specimens' humus was collected, neutralized using $CaCO_3$ and dried at room temperature. The sample was then pyrolyzed (to eliminate organic components) at different temperatures (500, 600, and 700 °C), followed by acid digestion of HNO_3 and HCl (3:1) at 40 °C for 4 hours to eliminate metallic impurities. The sample was then filtered, washed with distilled water, and dried. The diameter of the silica nanoparticles was in the range of 55 to 250 nm depending on pyrolysis temperatures. At 700 °C, the average particle diameter was 246 nm and at 500 °C the average particle was 55. The silica content was 88% with respect to calcined humus, which is much higher than that of coffee (12%) and cane husk (8%).

Another study with a different annelid source was also carried out with *Eisenia foetida*.[84] The reproduction and stabilization time of *Eisenia foetida* was about 1 month under aeration and dark conditions with moisture of 60–85% at 20 °C. After drying and sieving (0.5 mm), the obtained humus was calcinated at 500, 600, and 700 °C for 19 hours respectively to remove the organic matter. The heat treated samples were then soaked with the mixture solution of HNO_3 and HCl (volume ratio 3:1) at 40 °C for 4 hours to eliminate impurities. The resultant silica was recovered after washing and drying.

Silica was also prepared from RH without the vermicompost bioprocess by using the same calcination and acid treatment. The vermicompost bioprocess produced silica nanoparticles that have a size of around 81 nm. This is smaller than the silica produced without biotransformation (around 233 nm). It was inferred that the size reduction occurred in earthworm gut with the contribution from several microorganisms.

1.3.2. Applications of silica derived from RH

The application of RHA as fillers in rubber, plastics, and cement has been continuously explored[85-87] The recent applications of RHA as fillers are not reported. Readers interested in this topic are referred to an earlier review article.[13]

High-quality amorphous silica nanoparticles from RH exhibit similar performance benefits when compared to commercial fumed silica nanoparticles. Fumed silica has widespread applications owing to its high surface area and the ability to select its surface chemistry via functionalization. Applications of RH silica nanoparticles to replace fumed silica have been developed in the past decade, particularly in adsorption and catalysis areas.

1.3.2.1. Adsorption material

Due to its residual metal content and porous structure, RH silica has been used to adsorb free fatty acid in soy and palm oil. Some or all of these metal centers participate in the adsorption of the fatty acid.[88-89] Based on this, RH silica modified by Al^{3+} ion was synthesized from RHA using the sol-gel technique.[31] Water-treated RH were calcined at 800 °C for 5 hours to produce RH silica which was leached by HNO_3 solution for 24 hours to removes the metal impurities. The high-purity RH silica was dissolved in 6.0 M NaOH solution. After filtering, the filtrate was titrated with 3.0 M HNO_3 containing 10 %

(w/w) Al^{3+} until the pH value was 5 and aged for 6 days to form a gel. RHA-Al was produced after filtering and drying the solid residue at 110 °C for 24 hours. The RHA-Al was a very good adsorbent for palmytic acid because of electrostatic interaction between the Al^{3+} in the silica matrix with the oxygen atoms of carbonyl group in the fatty acid.[31]

RH silica has been chosen as an adsorbent in water treatment processes because of its granular structure, water insolubility, chemical stability, high mechanical strength, and its large availability. In order to enhance the adsorption capacities for heavy metals, RHA with 87.5% silica content prepared by directly calcination of RH at 650 °C for 2 hours was used to synthesize poly inorganic silica with Fe and Al ions, which are more favorable in removal of heavy metals from waste water.[28] In this process, sodium silicate produced by refluxing RHA in NaOH solution for 1 hour was diluted with distilled water to form 1.25 M silicate solution followed by the addition of 0.25 M HCl solution to pH≈2. The above solution was mixed with a blend of $AlCl_3$ and $FeCl_3$ and neutralized by $NaCO_3$. The maximum adsorption capacity of the yield copolymer for Pb, Fe, Mn and As ions are found to be 416, 222, 158, 146 mg/g respectively.

Surface modification is another effective method to improve the adsorption performance of silica. Mesoporous silica produced from RHA by alkaline extraction was modified with silane using 1,2-dichloroethane as a spacer.[90] The modified silica contained the cylindrical pores that open at both ends, which allow free diffusion of Cd^{2+} ions to the adsorption sites on the silica surface. The silane-modified silica showed specific adsorption for Cd^{2+} of 44.52 mg/g at a Cd^{2+} concentration of 100 mg/L. Cd^{2+} adsorption was increased 100-fold compared to the non-surface modified silica.[90] Cu^{2+} selective ligand, pyridine-2-carboxaldehyde was used to modify the amorphous silica gel

obtained from RHA by NaOH extraction. The modified silica selectively absorbs Cu^{2+}. Its mechanical stability was not as good as that of the commercial product. Its selectivity for Cu over Fe was not as high as the commercial product. But this work defined the problems associated with using RHA as a starting point for composite materials in general.

1.3.2.2. Silica-supported catalysts

Many heterogeneous catalyst systems are supported by mesoporous materials such as silica.[91-92] Silica-supported catalysts are being developed at a tremendous pace because of their high catalytic behavior derived from the high surface area. Many examples have been reported on the preparation and synergies of catalysts supported by silica obtained from RH.

1.3.2.2.1. Silica-supported metal catalysts

Chang et al.[4, 44-45] use RHA as a support for nickel catalysts by an incipient-wet method. RHA was impregnated in $Al(NO_3)_3$ solution for 24 hours followed by drying at 110 °C in an oven. The dried samples were calcined in air at 350 °C for 5 hours or at 850 °C for 2 hours to produce the substrate material (RHA-Al_2O_3), respectively. The RHA-Al_2O_3 obtained at 350 °C was impregnated in $Ni(NO_3)_2$ solution for 24 hours and dried at 110 °C in an oven.[44-45] Following calcination at 500 °C for 4 hours, the samples were activated by using a reducing atmosphere of H_2/Ar (5/95) stream at 800 °C for 3 hours. On the other hand, RHA-Al_2O_3 synthesized at 850 °C was ion exchanged to produce the catalyst.[4] In this process, concentrated ammonia was mixed with the $Ni(NO_3)_2$ solution prior to the addition of RHA-Al_2O_3 support. The mixture was kept at 25 °C for 24 hours with stirring. The exchange of Ni^{2+} with hydroxyls on the surface of

the support is enhanced at pH=8.5 with dilute ammonia. The RHA-Al_2O_3 supported catalyst was produced by washing, drying, and calcining of the above ion exchanged product.[4] It was found that RHA-supported Ni catalyst exhibited high Ni surface area, easy dispersion and high selectivity when used for the hydrogenation of CO_2.[4, 44-45] The hydrogenation reactivity was almost independent of calcination and reduction temperatures for the catalysts produced using RHA-Al_2O_3 with calcination at 350 °C.[44-45] The conversion of CO_2 and the yield of CH_4 were strongly dependent on the calcination and reduction temperatures for the catalysts obtained by ion exchange method.

Adam et al.[55, 58-61, 69, 93] prepared metal loaded catalysts from RHA. Silica supported iron catalyst was synthesized from RHA via the sol–gel technique.[69] The RHA produced by pyrolysis of the water rinsed RH at 700 °C for 5 hours was treated with 1.0 M HNO_3 for 24 hours. The obtained RHA was dissolved in 6.0 M NaOH to form a sodium silicate solution. 3.0 M HNO_3 containing 10 wt % Fe^{3+} was added dropwise to the solution until the pH reached 5. The gel was aged for 4 days followed by filtering, washing, and drying to produce the RHA-Fe catalyst. The RHA-Fe catalyst showed high activity in the reaction between toluene and benzyl chloride. It was reusable without loss of activity and with no leaching of the metal.[69] Similarly, In, Al, Ga, Cr, and V were successfully incorporated with RHA as the substrate.[55, 59, 61, 93] The catalytic activity of Al, Ga and Fe catalysts supported by silica were tested in the benzylation reaction.[93] It was found that RHA-Fe demonstrated the highest catalytic activity, while RHA-Ga gave the highest selectivity.[93] However, RHA-Al was found to be inactive under the reaction conditions studied. These catalysts could be recycled and reused several times without significant loss in activity and selectivity.[93]

Bimetallic modified RH silica catalysts have attracted much attention since two or two more active metals can improve performance in a reaction system.[60] High surface area Cu and Ce incorporated RH silica catalysts were prepared by a template assisted sol–gel precipitation method.[60] RH silica was produced by calcination of HNO_3 pre-treated RH at 600 °C for 6 hours. The obtained silica was dissolve in NaOH solution to form sodium silicate solution followed by addition of cetrimonium bromide (CTAB) as the structure directing agent. 3 M HNO_3 containing Cu^{2+} and Ce^{3+} salts was used to titrate the above solution until the pH value reached 3. The gel was aged for 24 hours. After filtering, washing, and drying, the sample was calcined at 500 °C in air to produce the xerogel which was ground to a powder to get the silica supported catalyst. Study showed the catalysts have good catalytic performance with high selectivity in the reaction of converting benzene to phenol due to the synergy between the Cu^{2+} and Ce^{3+}.[60]

1.3.2.2.2. Silica-supported organic molecule catalysts

Modification of silica with organic molecules can generate silica supported catalyst. For example, 7-amino-1-naphthalene sulfonic acid was immobilized onto RH silica and followed by HNO_3 treatment for 24 hours to form strong Brønsted acid sites.[71] The catalyst showed good catalytic activity towards esterification of *n*-butyl alcohol with different mono- and di-acids with 88% conversion and 100% selectivity towards the ester.[71]

1.3.2.2.3. Silica-supported TiO_2 and V_2O_5 photocatalysts

TiO_2 is a well-known photocatalyst for photocatalytic degradation. The absorption of UV-Vis energy by TiO_2 excites electrons to a conduction band with positive holes in valence band that generates hydroxyl radicals, which oxidize organic compounds. The

photoactivity of TiO_2 is decreased by electron-hole recombination and particle aggregation. This can be overcome by dispersing TiO_2 on materials with high surface area. Artkla et al[94-95] synthesized a hybrid photocatalyst that consisted of TiO_2 nanoparticles dispersed on mesoporous RH silica. The results showed that the morphology and band gap of TiO_2 were not affected by the support. The support prevented the TiO_2 nanoparticles from agglomerating. The activity of the hybrid photocatalyst for the photocatalytic degradation of tetramethylammonium in aqueous slurry was significantly higher than that of the unsupported TiO_2.[95]

V_2O_5 is an important industrial catalyst for partial oxidation of organic compounds. Selective oxidation with rupture of C-C bonds is normally supported on different carriers depending on the type of the reaction to be catalyzed. Bulk V_2O_5 cannot be directly used as a catalyst. Sugunan and coworkers prepared RHA-CeO_2 supported V_2O_5 catalysts. The catalytic activity was evaluated in liquid-phase oxidation of benzene. Selective formation of phenol was observed. This is attributed to the presence of highly dispersed active sites of V over the support.[37]

1.3.2.3. Preparing porous silica

For the last decades, many efforts have been made to prepare porous silica with high surface area starting from RH. Jang research group and Chareonpanich research group synthesized SBA-15 mesoporous silica using RHA derived from non-treated RH.[79, 96] RHA was first converted to sodium silicate solution and then mixed with a template agent (usually a surfactant). After pH adjustment, aging, filtering, washing, and drying, the solid was calcined at 500°C for 6 hours in air to produce SBA-15. It was found that the ultrasonic mixing gives highly ordered hexagonal pore-arrangement and a narrow

pore size distribution with a much shorter hydrolysis–condensation period. The highest SBA-15 surface area was 860 $m^{2/}g$ when the ultrasonication time was 6 hours.[96]

MCM-41 was prepared and studied by researchers using RH silica.[62] Grisdanurak et al. used HBr solution to post treat RHA to get high-purity silica. The posted treated RHA was converted to sodium silicate solution with base. By using cetrimonium bromide (CTAB) as template agent, the authors produced MCM-41 with a surface area approximately 750-1100 m^2/g. The pore distribution had an average diameter of about 2.95 nm. The authors also tried to surface modify the MCM-41 with trimethylchlorosilane (TMCS) and phenyldimethylchlorosilane (PDMS). To reduce the MCM-41 surface polarity. The results showed that the surface hydrophobicity of MCM-41 obtained from RH could be enhanced by the silylation with silane.[97]

Zhu and coworkers successfully shortened the porous silica preparation time (within 10 hours) without compromising the specific surface area.[98-99] In their synthesis, the aging step was skipped and the microwave oven was used for drying to save time. During synthesis, by using a much lower pH, the amount of PEG incorporated into the silica-PEG composites increased. This resulted in higher surface area porous silica (792 m^2/g at pH 5.7 and 1018 m^2/g at pH 3.2).[99]

1.4. Silicon carbide (SiC) derived from RH

Silicon carbide (SiC) is widely used in various industry due to its excellent mechanical, electronic and chemical properties.[13] Currently SiC is industrially manufactured by the Acheson process. This involves reduction of silica sand by coke or anthracite coal in a resistance furnace.[11] SiC from agricultural byproducts such as RH, rice straw, corn stalk, sugarcane residue etc. have attracted much attention as an

alternative method for the production of SiC. These agricultural byproducts contain both carbon and silicon components which satisfy the stoichiometry for synthesizing SiC. Silicon carbide has been successfully synthesized from RH at a temperature range of 1200–1900 °C.[11, 100-102]

1.4.1. Pyrolysis method to make SiC from RH

1.4.1.1. SiC from pyrolysis of non-treated RH

In this method, RH are coked first at temperatures range of 350–900 °C to form black ash. The ash was fired at higher temperatures of 1200–1650 °C in vacuum or certain atmosphere (Ar, N_2, or H_2) to form SiC.[11] The coking step of RH is to regulate the ratio of silica and carbon by removing some of the carbohydrate. Li and coworkers prepared β-SiC whiskers from a one stage direct pyrolysis of RH.[101] RH in an airtight graphite crucible was put in an electronic furnace with an argon atmosphere. The temperature was increased to 1000 °C at 15 °C /min and then to a higher temperature of 1500 or 1600 °C at 10 °C/min. The sample was hold for 2 hours at 1500 or 1600 °C and cooled down with ambient conditions. The product was purified by calcination in air for 3 hours to remove residual carbon followed by dilute HF leaching to remove impurities.[101] The resultant SiC contained 100–200 nm β-SiC particles and 170 nm in diameter whiskers that was several to tens of micrometers in length. The nanostructured β-SiC, especially the β-SiC whiskers, showed excellent blue light emission properties.

Zhu and coworkers used pure silicon to synthesize SiC_w reinforced SiC composites from RH by direct pyrolysis.[103] The RH was first coked at 900 °C in argon for 2 hours, and then was pyrolyzed at 1550 °C for 6 hours under argon. After the formation of SiC_w/SiC, pure silicon was added and a second pyrolysis was conducted at

1450 °C, 1550 °C, and 1600 °C. The purpose of adding silicon was to react with the unreacted amorphous carbon during the pyrolysis and to form new SiC. The mechanical properties, specifically the Vickers hardness, flexure strength, elastic modulus, and fracture toughness of the SiC was greatly enhanced. This was attributed to the reaction of the added silicon with carbon. The authors showed that too high and too low temperature of the second pyrolysis would lead to high amounts of unreacted carbon, and lower the mechanical properties of the composites. The temperature of 1550 °C in second pyrolysis was the optimum temperature for the SiC_w/SiC composite to have good mechanical properties.[103] The authors were able to make very hard and tough ceramic composites. The Vickers hardness and fracture toughness of the SiC composite are about 18.8 GPa and 3.5 $MPam^{1/2}$ respectively.

Wu and coworkers prepared multi-carbides based on SiC derived from RH by adding Si, B_4C and Mo during direct pyrolysis.[104] The purpose of adding Si and B_4C is to react with unreacted carbon. The B_4C will help to form new carbides. The added Mo will react with Si to form $MoSi_2$ which improves the overall properties of the composites. $MoSi_2$ is less brittle when compared to Si and it has a high melting temperature of 2030 °C. This improves the high temperature properties of the composite. The Vickers hardness and fracture toughness are about 16.8 GPa and 3.9 $MPam^{1/2}$.

1.4.1.2. SiC from pyrolysis of pretreated RH

Pretreatment in this section mainly refers to chemical treatments of RH before pyrolysis, such as acid or base treatment. HCl is most commonly used for acid treatment. To prepare SiC, RH was pyrolyzed directly after pretreatment in argon at temperatures between 1050 and 1600 °C.[105] SiC whiskers formation decreased after acid treatment.

Raman et al. used boric acid to treat RH and PAN fibers. The mixture was dried and then heated in a tube furnace in argon at 1450 °C for 4 h.[106] It was found that the yielded SiC whiskers have a better aspect ratio.

Strong alkalis such as NaOH have been used to treat RH before preparing SiC. The purpose of the NaOH treatment is to tune the C/SiO_2 ratio to facilitate the SiC formation. The concentration of the alkali plays an important role in determining the amount of SiO_2 released from RH. Mizuki and coworker[107] reported that SiO_2 content increased from 23 wt % in raw RH to 29.0 wt % after treated with 0.25 wt % of NaOH solution and 29.5 wt % after treated with 0.5 wt % NaOH. When 1.0 wt % NaOH was used, the SiO_2 content decreased. Syed et al. found that an increase in NaOH concentration from 0.1 to 0.5 N will result in SiO_2 content increase[108] It was concluded that lower concentration of NaOH solution in treating RH was more favorable for SiC formation.

1.4.1.3. Pyrolysis with catalyst

Catalyst is commonly used in making SiC from RH. Usually catalyst is added to RH in the form of powder or solution before pyrolysis. No special treatment is needed. Several types of catalysts, including Fe, Co, Ni, Pd, Cr, S_3N_4, and sodium silicate have been studied. It was shown that catalysts decreased the crystallization of carbon and silica in RH and accelerated the formation of SiC. With catalyst, the reaction temperature decreased dramatically when preparing SiC from RH.

Martinez and coworkers studied β-SiC synthesis from pyrolysis of RH with catalyst.[102] The authors compared two different catalysts $CoCl_2 \cdot 6H_2O$ and $FeCl_2 \cdot 4H_2O$, and found $FeCl_2 \cdot 4H_2O$ give a better result in terms of β-SiC yield. Hashishin and workers

found that Fe_2O_3 was very effective in growth promotion of whiskers.[109] More specifically, Fe_2O_3 was found to contribute to the length and the yield of the SiC whiskers. The authors found that the Al_2O_3 slightly affected the improvement in the yield of SiC whiskers.

Janghorban and coworkers studied the concentration effect of catalyst in making SiC from RH.[110] Normally an increase in the catalyst concentration would promote the growth of SiC, leading to larger grain size and higher yield of SiC. The authors noticed that this effect only extends to certain concentration limits. They impregnated RH with Na_2SiO_3 as a catalyst and found that lower concentrations of catalyst were more effective. At lower concentrations, the silicates were dispersed uniformly over the RH and acted as nucleation sites for SiC whisker growth. From higher concentrations, a thick layer of silicate inhibited the SiO gas reaching C in the husk and reduced the reaction rate.[110]

Researchers have found that alkali metal oxides can also be used to accelerate the formation of SiC. Alkali metal oxides can lower the melting point of silica. This can accelerate the reaction between silica and carbon.[111] Si_3N_4 can be used as a catalyst to increase the yield of SiC whiskers and reduce the amounts of SiC particles and carbon.[112] Krishnarao and coworkers found that when RH ash was heated with 50–60 wt% of Si_3N_4 at 1400 °C, SiC whiskers were produced without any free carbon and with only small amount of unreacted silica. Nitrogen can be considered as the inert gas in the reaction to produce some Si_3N_4, which can catalyze the production of SiC whiskers.[113]

Control of the temperature is very important when catalyst is present. Krishnarao and coworkers found that when using cobalt as catalyst, rapid heating increased the

formation of SiC whiskers,[114] while slow heating (5 °C/min) stabilized the silica and carbon. This increases their degree of crystallization.[115]

1.4.2. Microwave radiation method

Microwave radiation has the advantage of very high rate of temperature increase. Increasing the rate of temperature change is important in SiC synthesis.[11] Slower heating rate result in carbon black and SiO_2 crystallization that decreases the reactivity.[116] Rapid heating can increase the SiC reaction rate and production rate because the lower degree of crystallization favors the reaction. Moreover, the heating efficiency of conventional pyrolysis to prepare SiC usually is low due to the thermal radiation or thermal conduction. Microwave can heat materials from inside out. Microwave heating has been used to prepare SiC powders.[117-118] Qadri and coworkers used microwave technology to heat RH in a boron-nitride crucible up to 1900 °C for 5min in vacuum. Raw RH was directly converted into a collection of β-SiC nanostructures. Microwave radiation is simple, ultra-fast, inexpensive, and has minimal affection to the environment.[119]

1.4.3. Plasma method

In a plasma reactor, the reaction time can be reduced greatly by increasing the temperature.[100, 120-121] The very high temperatures (~10^4 °C), steep temperature gradients (~10^6 °C/min), and high quench rates (~10^6 °C/s) associated with thermal plasmas can be a unique route for the preparation of ultrafine SiC from RH. In contrast to other methods, it is very easy to realize continuous production and to control reaction parameters in a plasma process. Singh and coworkers developed a single step reaction to prepare SiC directly from raw RH in a pot type extended arc plasma reactor using graphite electrodes. Formation of SiC is observed in 5 min.[100] Oxidation and acid treatment after plasma

reaction (with H_2SO_4, HCl, or HF) effectively removes the excess carbon, silica, and mineral oxides. Successive washings can remove chloride and fluoride ions.[120-121]

1.4.4. Chemical vapor deposition method

Chemical vapor deposition (CVD) has been widely used in the preparation of high grade SiC.[13] Various morphologies of SiC (powders, whiskers, fibers, and films) have been prepared by the CVD method. Only a few publications can be found on preparing SiC by CVD from RH. Sharma and coworkers compared SiC whiskers from RH with those obtained by CVD with SiO and CO as the primary reactants,[122] and found that they were very similar. Motojima and coworkers prepared microcoiled SiC fibers by CVD using powder mixtures of SiO and coked RH that were very quickly heated to the reaction temperature.[123] The authors showed that preparation of high grade SiC from RH using CVD should be possible. Han and coworkers characterized the products deposited on graphite substrates prepared by CVD directly from carbonizing RH. They showed that a thin SiC film was formed right beside the carbonized RH zone. SiC whiskers aggregates were found next to the SiC film zone. The CVD process to prepare SiC from RH can be simple. It usually is regarded as a complicated technique. Considering the products' superior properties, it is economical to use the CVD method to make SiC from RH.

1.4.5. Applications of SiC from RH

1.4.5.1. Ceramic and metal composites

SiC has been intensively studied as fiber reinforcement since the 1970s. One reason is the successful preparation of relatively inexpensive high-grade SiC whiskers from RH.[124] Another reason is SiC has a relatively high thermal conductivity and low

coefficient of thermal expansion, giving it superior thermal shock resistance. The strength and hardness of ceramics and alloys can be greatly enhanced by the reinforcement of SiC. Generally, the SiC whiskers are better than SiC particles in terms of reinforcing and toughening effects. A high content of whiskers is preferred in the production of SiC from RH.

Zhu and coworkers used in-situ SiC whiskers from RH to reinforce ceramic matrix composites.[103] Characterization of the composites' mechanical properties showed that the Vickers hardness, flexure strength, elastic modulus, and fracture toughness of the biomorphic SiC ceramic composites were greatly enhanced. Agglomeration must be avoid when incorporating the whiskers into the ceramics. Agglomeration may result in structural defects and lower reinforcement efficiency.

1.4.5.2. Polymer composites

The research on silicon-carbide-reinforced polymer matrix composites is limited. Carbon fibers are commonly used in resin composites which are quite expensive. The SiC whiskers from RH could be much cheaper and be a suitable substitute. An advantage of using SiC whiskers for reinforcement is the low purity requirement of the SiC whiskers. The main impurities in SiC whiskers from RH are residue carbon, silica, and SiC particles. These have little negative effect on resin composites' mechanical properties. Satapathy and coworkers used SiC derived from RH to reinforce jute-epoxy composites.[125] The incorporation of the SiC modifies the tensile, flexural, and inter-laminar shear strength of the jute–epoxy composites. The micro-hardness and density of the composites are greatly influenced by fillers content. SiC used in Satapathy's research was produced from RH by plasma processing.[100]

1.4.5.3. Semiconductor and abrasive materials

Due to its wide energy band gap, high electron saturated drift velocity, high thermal conductivity, physical and chemical inertness, SiC have been an important semiconductor for applications in high-temperature electronics, ultraviolet sensors, and high-speed devices.[13] The SiC from RH has been used as semiconductor materials.[126-127] Special purification must be carried out in the manufacturing process of making SiC from RH because of the requirements of SiC purity for semiconductor application. For abrasive material application, the requirement on purity is not so high. The purity of SiC from RH is good enough to match the requirement. The SiC can be directly used as abrasive material or hot-pressed with composites.[128]

1.4.6. Summary

The technology of deriving SiC from RH has been commercialized.[13] Further studies on the following three aspects are necessary. One is the SiC purity issues. In nature, RH contain inorganic minerals such as K_2O, Fe_2O_3, CaO etc. Those minerals are impurities in SiC after pyrolysis. Excess carbon can be another source of impurities. These impurities have little effect on low-grade SiC applications. For the high-grade SiC applications the impurities become a problem. Since high-grade SiC is needed in many fields, better separation (purification) techniques and facilities are important in SiC preparation from RH.[129] The second issue is control of the SiC whisker content. The value of SiC whiskers is higher than that of SiC particles. Improvements in the technology that increase the whisker content are desired.[129] The last one is defect control. Usually, SiC whiskers produced from RH contain a high degree of defects.[130-131] There are three kinds of defects in SiC whiskers which have been reviewed by Sun et al.[13] Such

defects greatly affect SiC's electric properties and thermal conductivity. The defects can be decreased by choosing the proper catalyst and regulating reaction parameters.

1.5. Zeolite

Zeolites are crystalline microporous aluminosilicates, which have been widely used as ion exchangers, molecular sieves, drying agents, and catalysts because of their well-defined crystalline structure, high internal surface area, uniform pore size, and high thermal stability.[101, 132-134] The majority of zeolites are synthesized using the silica from silica gel or fumed silica.[135-136] The first study on the synthesis of zeolite using RH silica was reported in 1981.[137]

1.5.1. Preparation of zeolites from RH

1.5.1.1. Zeolite ZSM-5

ZSM-5 zeolite was prepared from the tetrapropylammonium (TPA) system for the first time using the silica from RHA.[138] Significant progress has been made in the ZSM-5 zeolite synthesis during recent years.

In the synthesis of ZSM-5 zeolite, structure directing agents are commonly used as a template. TPA is a favored organic template. Based on the method developed by Rawtani et al.,[138] various procedures[139-146] for the preparation of ZSM-5 zeolite from RH silica or RHA were developed using TPA as a template. Hemalatha et al. synthesized NaZSM-5 zeolite with TPA bromide (TPAB) as a structure directing agent.[139] In their report, RHA was refluxed in 2.0 M NaOH solution at 70 °C for 24 hours to obtain a silicate solution. The silicate solution was mixed with an aqueous solution of TPAB and aluminum sulfate. After stirring for 10 min, a NaOH solution was added to produce a hydrogel. This was transferred to an autoclave and crystallized at 180 °C for 3 days with stirring at 200 rpm. After filtering and washing, the crystallized product was dried at 100

°C and calcined at 500 °C in air for 6 hours to produce NaZSM-5 zeolite (Figure 1.5a). The ceria impregnated NaZSM-5 was also synthesized by wet impregnation of NaZSM-5 with an ethanolic solution of cerium nitrate hexahydrate followed by stirring, vacuum drying, and calcining in air at 550 °C for 10 hours (Figure 1.5b).[139]

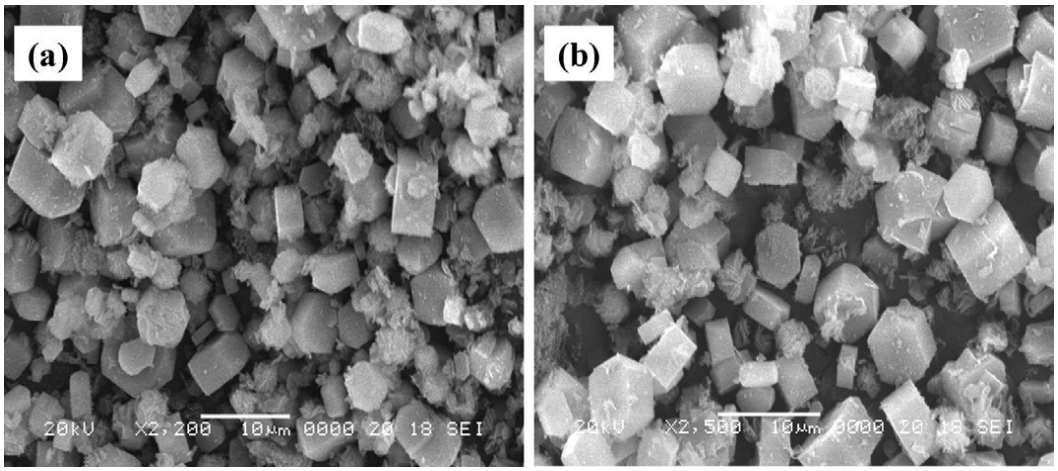

Figure 1.5 SEM images of (a) NaZSM-5 and (b) ceria impregnated NaZSM-5. Samples were made from RH silica.

Using TPA as an organic template, Naskar et al. developed a facile and single-step hydrothermal method for the synthesis of ZSM-5 zeolite.[140] RHA was mixed with sodium aluminate solution prepared by dissolving aluminum with NaOH solution. TPA hydroxide (TPAOH) was added dropwise into the above suspension with stirring. After stirring for 2 hours, the dispersion was hydrothermally treated in the temperature range from 130 to 170 °C for 12 or 24 hours. After washing and drying, the collected powders were calcined at 550 °C for 5 hours to produce ZSM-5 zeolites. It was found that the intergrowth of the crystals took place with an increase in temperature, as shown in Figure 1.6. The effect of reaction time on the formation of ZSM-5 indicated that the particles of

ZSM-5 started to form through the assembly of smaller particles at a reaction time of 12 hours. The formation of the ZSM-5 crystals was completed within 24 hours. With this method, the intermediate reaction steps can be omitted through an *in situ* reaction by directly using silica as the reactant. This is different with the conventional method in which the silica is converted to silicate and subsequently reacted with other precursors to synthesize zeolites.[140]

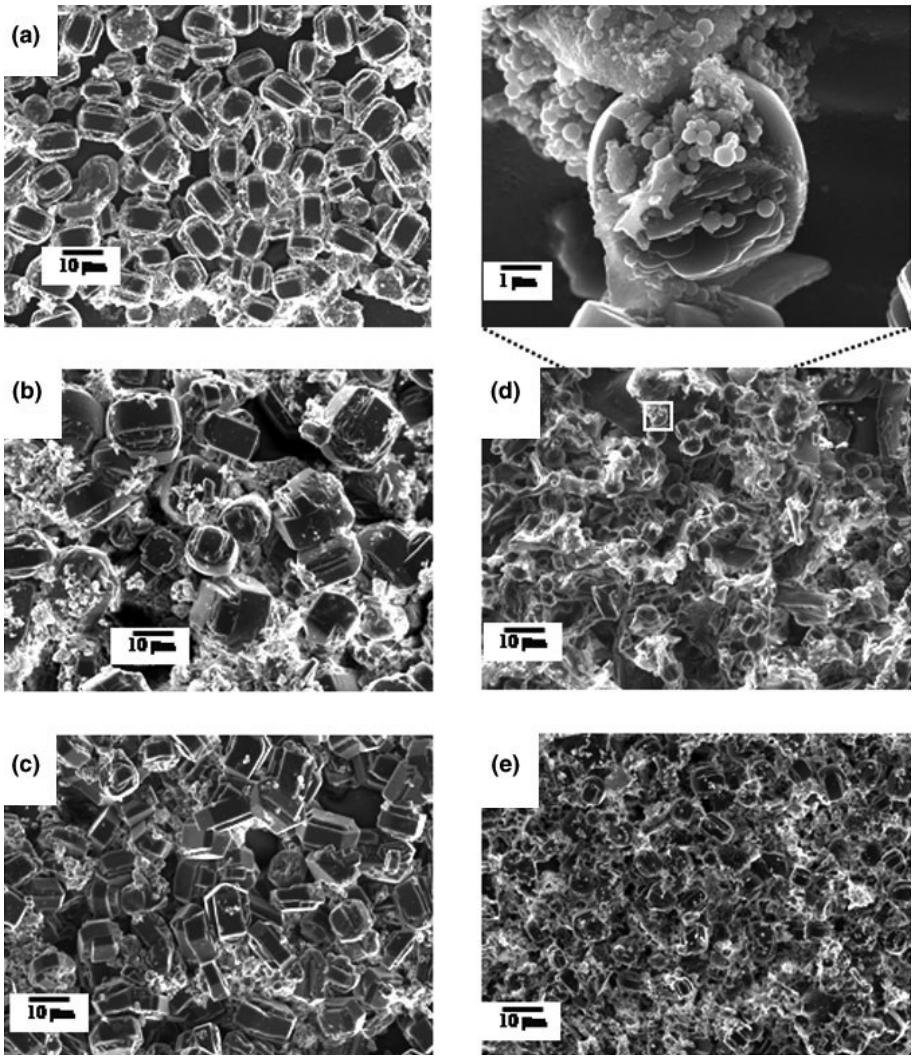

Figure 1.6 SEM images of ZSM-5 synthesized at various conditions. (a) 130 °C/120 h, (b) 150 °C/120 h (c) 170 °C/120 h, (d) 150 °C/12 h, and (e) 150 °C/24 h. Adapted with permission from ref.[140] Copyright 2011. The American Ceramic Society.

Studies show that the ratio of SiO_2/Al_2O_3 plays an important role in the formation of ZSM-5 zeolite. Mohamed et al.[141] studied the effect of the Si/Al ratio on the characteristics of ZSM-5. RHA was treated with NaOH and reprecipitate by HCl solution, which was used to obtain the silicate solution. TPAB as a structure directing agent, together with *n*-propylamine (*n*-PA), was added to the above sodium silicate solution. Aluminum sulfate solution was added and the pH was adjusted to 11. The mixture was hydrothermally treated at 150 °C for 4 days. After calcination at 550 °C for 6 hours in air, the final ZSM-5 was synthesized. Two Si/Al ratios of 40 and 80 were investigated. The products were named Z40 and Z80 respectively. Z80 sample exhibited higher BET surface area (616 m^2/g), crystallites size (44.4 nm), and crystallinity (100%) than that of Z40 sample with 536 m^2/g of surface area, 35.8 nm of crystallites size, and 79.28% crystallinity. Compared with the Z80 sample with a pore radium of 25.32 Å, the pore radius of Z40 sample was 22.92 Å. Ali and coworkers[142] followed similar procedures and synthesized ZSM-5 zeolite with SiO_2/Al_2O_3 ratio of 3.636 by using silica obtained from RH. The results showed that the ratio of Na_2O/SiO_2 had a significant impact on the crystallinity and crystal size of ZSM-5. The optimum ratio of Na_2O/SiO_2 was found to be 0.275, which resulted in 100% crystallinity and 99.36 Å crystal size of ZSM-5.[142]

The hydrothermal method under pressure is the most popular one for the crystallization of ZSM-5. The synthesis under atmospheric conditions possesses its own advantages because of the simple setup.[144] Kordatos et al. prepared ZSM-5 under atmospheric conditions. RHA, TPAB, and NaOH were mixed together and refluxed at 110 °C for 11 days and then centrifuged. After washing and drying, the solid was then calcined at 550 °C for 5 hours to remove the organic template. The resultant ZSM-5 had a

high specific surface area of 397 m^2/g. Compared to the hydrothermal treatments at elevated pressures, this method appears to be more commercially viable because of the simpler setup.[144] However, this method requires a much longer reaction time than the hydrothermal method, which typically takes several hours to a few days.

Hydrothermal reaction is much faster than refluxing under atmospheric conditions to synthesize zeolite-5. A microwave-assisted hydrothermal method was developed to shorten the reaction time.[145] In this process, microwave radiation was used for rapid dissolution of silica in the NaOH solution. It is 3−4 times faster when compared to the conventional hydrothermal process. Small size ZSM-5 zeolite crystals (0.3–5.0 μm) were obtained with the assistance of microwave radiation. The rapid dissolution of silica results in supersaturation of silica in NaOH solution and subsequent formation of zeolite crystals. Microwave assistance should bring similar benefits when it is coupled with the refluxing method under atmospheric conditions.[145]

TPA based organic templates exhibit excellent structure-directing function for the preparation of ZSM-5, but it is neither eco-friendly nor cost-effective. Thus, template free methods were developed.[147-149] Fernandes et al. developed an economically feasible route for the preparation of ZSM-5 zeolite with high purity and crystallinity without using organic templates.[147] In their process, RHA reacted with the NaOH solution, mixed with NaOH, aluminum sulfate, sodium sulfate, ethanol, and ZSM-5 seeds with vigorous stirring. The mixture was aged for 40 hours at 40 °C to give the gel and was crystallized hydrothermally at 200 °C for 50 hours. The ZSM-5 zeolite was obtained after washing and drying the solid at 120 °C for 24 hours. Fe incorporated ZSM-5 zeolites were successfully prepared using RHA without any aid of external structure directing

templates.[148] The phosphoric acid used in the synthesis formed a complex with Fe, which acted as surface directing agent in the formation of Fe incorporated ZSM-5 zeolites.

The synthesis of ZSM-5 zeolite/carbon composites was also found to be a promising environmentally-friendly chemical process compared to those involving organic templates. Vempati et al.[149] prepared ZSM-5 zeolites with various carbon content by a hydrothermal reaction without an organic template. In their synthesis, RHA containing different concentrations of combustible carbon was used as the silica source. Na-aluminate salt was used as the aluminum source to adjust the SiO_2/Al_2O_3 molar ratio (20 to 80). The ratio of SiO_2/Al_2O_3 and the combustible carbon content were very important for the formation of ZSM-5. For samples with a carbon content of 0.03%, the pure phase ZSM-5 was formed up to a SiO_2/Al_2O_3 molar ratio of 80. The pure ZSM-5 was obtained at a SiO_2/Al_2O_3 molar ratio of 20 when the samples with a carbon content of 20% and 40% were used. Carbon containing ZSM-5 could be calcined at 500 °C for 3 hours to give carbon free ZSM-5. This process does not affect the structure of ZSM-5.[149]

1.5.1.2. Zeolite Beta

Zeolite Beta is usually synthesized by the hydrothermal method with organic templates and conventional silica sources, such as aqueous silica sol, colloidal silica and TEOS.[150-151] Zeolite Beta was successfully synthesized using RH silica as the silica source and tetraethylammonium hydroxide (TEAOH) as the structure-directing agent.[152]

RHA was first converted to sodium silicate solution. Sodium aluminate dissolved in a TEAOH solution was added to the above solution with vigorous stirring and then homogenized for at least 2 hours to give a gel. The gel was hydrothermally treated at 150 °C for 0.25−12 days. Zeolite beta was obtained after the solids were calcined at 550 °C

for 16 hours. The silica could be completely transformed to Zeolite Beta after just 2 days of hydrothermal synthesis at 150 °C. The transformation mechanism of the crystalline silica to Zeolite Beta involved dissolution of the silica in the highly basic reaction mixture, formation of an aluminosilicate, crystallization of the metastable zeolite Na-P, and the pure Zeolite Beta phase.

1.5.1.3. Zeolite MCM-22

Among a wide variety of zeolites, MCM-22 exhibits a unique framework topology with two independent pore systems. The structure is attractive for adsorptive and catalytic applications. Recently, RH silica has been successfully used to prepare MCM-22.[153-154]

Cheng et al.,[153] added RH silica powder and hexamethyleneimine (HMI) to the solution of NaOH and $NaAlO_2$ with stirring. A gel was obtained after 2 hours of reaction. The gel was transferred to a Teflon-lined autoclave and was aged at 50 °C for 1 day, crystallized at 100 °C for 1 day, and then crystallized at 150 °C for 1 day to give the crystalline solid. MCM-22 was obtained after the removal of the organic template by calcining the above crystalline solid at 800 °C for 8 hours. Through this three-stage method, the crystallization time of MCM-22 was reduced from typically 9–12 days for a static process to 3 days.

1.5.1.4. Zeolite NaA, NaX, and NaY

Wittayakun et al. used RH as an effective silica source to synthesize zeolite NaY.[155] In their study, the zeolite NaY was prepared from a seed gel and feedstock gel. The sodium silicate solution was prepared from RH silica and added to a sodium aluminate solution. The mixture was aged at room temperature for 24 hours to give the

seed gel with a molar ratio of $10.67Na_2O:Al_2O_3:10SiO_2:180H_2O$. The feedstock gel with a molar ratio of $4.30Na_2O:Al_2O_3:10SiO_2:180H_2O$ was prepared in a similar fashion and was used immediately without aging. After the seed gel was slowly added into the feedstock gel with stirring, the mixture was aged at room temperature for 24 hours and then crystallized at 90 °C for 22–72 hours. The optimum crystallization time was found to be 24 hours. The pure NaY zeolite was obtained after washing and drying, as shown in Figure 1.7a. In contrast, the mixture of seed gel and feedstock gel was directly crystallized at 90 °C for 24 hours without aging. The mixed phase of NaY and NaP was obtained by this crystallization process (Figure 1.7b).[155]

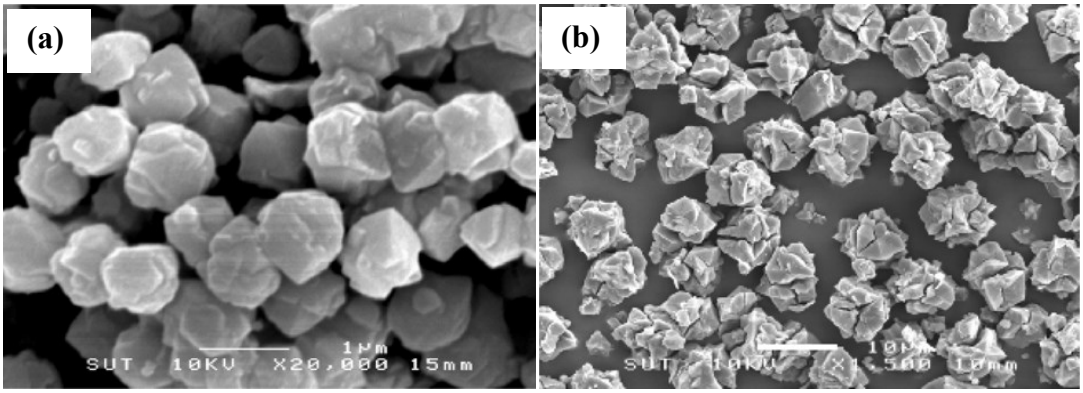

Figure 1.7 SEM images of pure zeolite Y synthesized from RH silica. (a) and transformation products from NaY containing NaP as a major component (b).

Yusof et al. investigated the synthetic conditions for zeolite NaY with high purity RH silica by seeding and ageing techniques.[156] It was concluded that the zeolite produced from RH without seeding and ageing techniques consisted of a mixture of zeolites A and Y. The zeolite synthesized by ageing but without seeding techniques was mainly a mixture of zeolite P and Y.[156]

Based on the seeding and ageing method, the effect of RH silica crystallinity on the synthesis of the NaY was examined by using amorphous RH silica from controlled calcination of RH and crystalline silica from RHA.[157] The results showed that amorphous RH silica was a better candidate because of its high efficiency in product recovery and simplicity of extraction. Furthermore, the prepared NaY could be exchanged into NH_4Y after ion-exchange and then converted to HY after calcination of NH_4Y.[157]

Zeolites NaX[158] and NaA [159-161] were synthesized by carefully mixing sodium silicate and aluminate solutions to obtain sodium aluminosilicate gel before the hydrothermal treatment. Dalai et al. used the silica from RH to synthesize NaX by a hydrothermal method.[158] RH silica was reacted with NaOH solution with shaking and heating at 80 °C for 5 hours. The sodium aluminate solution was obtained by adding aqueous NaOH solution to $Al(OH)_3$ powder followed by heating the solution to boiling. The sodium silicate and sodium aluminate solutions were mixed slowly with continuous shaking to obtain the sodium aluminosilicate gel, which was hydrothermally treated. The NaX zeolite was obtained by drying the solid in an oven at 120 °C for 12 hours. A series of NaCuX zeolites were prepared by mixing the synthesized NaX with a cupric acetate solution.

1.5.2. Applications of Zeolite

1.5.2.1. Adsorption

The zeolites synthesized from RH silica or RHA and their modified forms have been used for the removal of ions and organics from water systems because of their high ion-exchange capacity and molecular sieve properties.[153-154] The MCM-22 synthesized from RH was used as an adsorbent to remove basic dyes from aqueous solutions.[154]

MCM-22 exhibited very high adsorption of methylene blue (1.8×10^{-4} mol/g), crystal violet (1.2×10^{-4} mol/g), and rhodamine B (1.1×10^{-4} mol/g). The adsorption kinetics indicated pseudo second-order kinetics. The adsorption was a two-step diffusion process with film diffusion dominating the process. The adsorption isotherm fitted the Langmuir and the Freundlich models.[154] The MCM-22 from RH was an adsorbent for basic dye red 5GN.[153] The maximum extent of adsorption of red 5GN onto MCM-22 was at pH of 10, contact time of 60 min, with a MCM-22 dose of 1.0 g/L. The adsorption kinetics fitted a second-order equation better than Lagergren's first-order kinetics.[153] The ZSM-5 with various carbon contents synthesized from RH silica could be used for the removal of volatile organic compounds from waste water and air.[149]

Zeolites have shown different adsorption capacities for metal ions. In order to enhance the adsorption capability, the zeolites were modified by specific surfactants.[101] Yusof et al. used hexadecyltrimethyl ammonium (HDTMA) to modify the zeolite NaY synthesized from RH to remove the Cr(VI) and As(V) anionic species from aqueous solutions.[162] HDTMA-Br was dissolved in distilled water, mixed with pre-synthesized NaY, and stirred for 5 days at room temperature. After vacuum filtration, the solid sample was dried at 60 °C overnight to produce the HDTMA modified NaY. Study showed that the unmodified zeolite Y had little or no affinity for chromate (Cr(VI)) and arsenate (As(V)) anionic species. The zeolite Y modified by surfactant HDTMA exhibited strong capability of removing these anions from the aqueous solution. And the modified NaY with HDTMA in an amount equal to the 100% of their external cation exchange capacity exhibited the highest removal capacity. The pH of the solution had an influence on the adsorption capacity. The highest removal capacity for Cr(VI) and As(V)

was observed at pH 3 and 8, because Cr(VI) and As(V) were in the univalent form at those pH values. Just one exchange site from the HDTMA modified zeolite Y was needed. The adsorption of Cr(VI) and As(V) by the modified zeolite Y fits the Langmuir isotherm equilibrium.[162]

The modified ZSM-5 zeolites with different surfactants were used to remove Pb^{2+} from water.[142] The pre-synthesized ZSM-5 zeolite from RH was impregnate with a NaCl solution for 24 hours and washed two times with water.[142] The solid was filtered and dried in air to produce the NaZSM-5. The zeolite was mixed with surfactant, such as *n*-PA, TPAB, tetrabutylammonium bromide (TBAB) and CTAB. The mixture was shaken for 24 hours at 25 °C. The modified ZSM-5 was obtained after filtering and drying. The removal of Pb^{2+} from water depended on the type of surfactant. The TPAB modified ZSM-5 could absorb up to 85% of Pb^{2+} from solutions containing 50–140 ppm Pb^{2+}. The unmodified ZSM-5 or modified by *n*-PA, TBABr, or CTAB had lower absorptions of Pb^{2+}.[142]

Due to their good adsorptive and desorptive capacity, zeolite supported transition and rare earth metal oxides have been used to capture CO_2 through the interaction of the metal oxides and CO_2. Because of the strong interaction between CeO_2 and CO_2, Hemalatha et al. synthesized NaZSM-5 from RHA as the silica source and prepared CeO_2 impregnated NaZSM-5 by the wet method according to the procedures described above.[139] The CO_2 adsorption–desorption measurements showed that CeO_2 impregnated NaZSM-5 exhibited higher CO_2 adsorption capacity than NaZSM-5. The CeO_2/NaZSM-5 composite with 5% CeO_2 exhibited the highest adsorption capacity (130 mg/g). The amount of physisorbed CO_2 was higher than the chemisorbed one. The dipolar interaction

between CeO_2 and CO_2 was inferred to be responsible for the enhanced adsorption of CO_2.[139] Using the similar method, ZnO impregnated NaZSM-5 zeolite was synthesized by the same group.[163] The maximum CO_2 adsorption capacity of ZnO/NaZSM-5 composite was 140 mg/g of sorbent, slightly higher than that of CeO_2/NaZSM-5 composite.

1.5.2.2. Catalysis

Due to their high adsorption capacity, zeolites have attracted interest as catalyst support. This increases the surface area of the active site of catalysts and creates synergism. Metal oxides such as Co_3O_4 and V_2O_5[141] and transition metal ion Fe^{3+}[146] have been successfully incorporated into the framework of ZSM-5 zeolites synthesized from RH either during the *in situ* synthesis or by impregnation. Mohamed et al. prepared Co_3O_4 or V_2O_5 substituted ZSM-5 catalysts using the wet impregnation method.[141] The aqueous solution of $Co(NO_3)_2$ or NH_4VO_3 was mixed with ZSM-5 at 80 °C for 3 hours. After drying at 120 °C, the sample was calcined at 500 °C in air for 6 hours to obtain the metal oxides inside zeolites. Co_3O_4 and V_2O_5 were included into ZSM-5 zeolite by an *in situ* method similar to the synthesis of ZSM-5.[141] The study of their photocatalytic activity towards acid green dye showed that the samples prepared by the impregnation method exhibited higher activity. This was attributed to the greater exposed active sites on the catalyst surface. Using the *in situ* method, Fe-substituted ZSM-5 was synthesized by isomorphous substitution of Fe in the framework of ZSM-5.[146] The Fe-substituted ZSM-5 could be used as a catalyst for the photocatalytic degradation of p-nitrophenol (PNP) with H_2O_2 as an oxidizing agent. The Fe-substituted ZSM-5 with an Al/Fe molar ratio of 0.4 exhibited the highest photocatalytic activity. This was attributed to charge-

transfer excited complexs between Fe zeolite with the PNP ligand, in addition to the high surface area and high dispersion of Fe in the framework.

1.5.3. Summary and outlook

RHA and high quality amorphous silica from RH have been used to synthesize various zeolites. The amorphous silica from the treated RH can quickly dissolve and possess higher purity leading to higher productivity and quality of the zeolites. When RHA was used for the synthesis of zeolites, it helps achieve comprehensive applications of RH and converts waste to valuable material. Since silica can be dissolved in strong base and is typically the first step in the synthesis of zeolite, it is ideal to use a strong base to dissolve the silica in RH to form silicates, which can be used to synthesize zeolites. One can eliminate the calcination/burning process. The remaining lignocellulose after the dissolution of silica can be used for additional applications.

1.6. Silicon nitride

Silicon nitride (Si_3N_4) is one of the most important ceramic materials that exhibit high performance at both room temperature and evaluated temperatures because of their high chemical stability and excellent mechanical and thermal properties. Due to its superior properties and extensive applications, Si_3N_4 has attracted high research attention. Si_3N_4 are currently produced by several processes.[164] Besides the direct nitridation of silicon powders[165] and the reaction of chlorosilanes with a gas containing nitrogen or a nitrogen compound,[166-168] the carbothermal reduction and nitridation of silica is an alternative and the most common method for producing Si_3N_4, which can be expressed by the following overall reaction.[169-171]

$$3SiO_{2(s)} + 6C_{(s)} + 2N_{2(g)} \longrightarrow Si_3N_{4(s)} + 6CO_{(g)} \qquad (1)$$

RH is a renewable feedstock that contains both silicon and carbon which make it an attractive candidate for the production of Si_3N_4. Moreover, the high surface area of silica and carbon, and their intimate contact from the incomplete combustion of RH are beneficial for the nitridation. In general, Si_3N_4 could be synthesized from RH at temperatures between 1100 and 1500 °C under a flow of nitrogen gas[172-176] although purified and dried ammonia was also used as a nitrogen atmosphere.[177] It was showed that using RH as the raw material could lower the reaction temperature and greatly increase the rate of nitridation reaction compared to the conventional SiO_2/C mixture. Some reaction parameters, including reaction temperature, RHA purity, and atmospheric gas constituents, have been shown to be critical for controlling the yield and morphology of the Si_3N_4 product.[175] Rahman and Riley found that introducing hydrogen (95% nitrogen/5% hydrogen) could improve the rate of nitride formation, but need a higher reaction temperature (1450 °C).[178] Some metal oxides, such as Fe_2O_3 and NaF, were found to have a positive catalytic effect on the formation of Si_3N_4.[179]

Real et al. studied the synthesis of Si_3N_4 from the carbotherma1 reduction of RH by applying the constant-rate-thermal-analysis (CRTA) equipment composed of a high-temperature (up to 1600 °C) tubular furnace and a CO infrared sensor interfaced to a furnace temperature controller.[180] The reaction rate of carbotherma1 reduction could be controlled and meanwhile the CO concentration generated was maintained constant at a pre-determined value by the user. According to this procedure, the RH used were pyrolyzed at 600 °C for 3 hours in a helium atmosphere to give RHA with a C:SiO_2 ratio of 3: 1. The resultant Si_3N_4 was produced by nitriding the obtained RHA under the mixture reactive gas of 95% nitrogen and 5% hydrogen. The reaction temperature

increased as CO concentration increased. The study concluded that varying the reaction temperature between 1175–1400 °C does not alter the ratio of Si_3N_4 produced. However, increasing the concentration of CO resulted in the increase of Si_3N_4 yield from 83% at 0.0011 atm CO to 98% at 0.01 atm CO. By using this synthesis technique, the phase composition and microstructure of the resultant samples could be controlled.[180]

Based on the carbotherma1 reduction and nitridation method, three forms of Si_3N_4 containing powders, single-crystalline whiskers, and long polycrystalline fibers were prepared by Pavarajarn et al..[181] In this process, RHA which contains 50.67% carbonaceous materials, 45.56% silica, and other metal impurities was nitrided under an atmosphere of 90% N_2 and 10% H_2 at the temperature range of 1400–1470 °C for 3–10 hours to produce different types of Si_3N_4. The mechanism for the formation of Si_3N_4 was also examined. Both whiskers and long fiber forms were inferred to grow via the vapor–solid mechanism, in which silicon monoxide vapor was the reaction intermediate. The single-crystalline whiskers were formed directly from the gas phase, while the long fibers progresses through an amorphous intermediate. Increasing temperature and reaction time would be beneficial for the formation of both fibrous products because of the enhancement in the silicon monoxide generation. Moreover, both whisker and fiber products could be easily separated from the remaining RHA.[181] Using similar method, the Si_3N_4 whispers have been prepared by other group.[182] RH were pyrolyzed at 800 °C for 3 hours under argon atmosphere and then treated at 800 °C with different time intervals to produce Si_3N_4 whispers. The size of the whiskers increased as the reaction time increased.

1.7. Silicon tetrachloride

Silicon tetrachloride ($SiCl_4$) is commonly used as the starting material for the fabrication of silicon based materials that are extensively applied in the optical fiber and semiconductor industry. It also can be used as an intermediate to produce SiC, Si_3N_4, silica nanoparticles, luminescent silicon nanocrystals, as well as to catalyze certain organic reaction.[183-185]

Based on the industrial method of producing $SiCl_4$ using a SiO_2/C mixture with Cl_2 (expressed in following equation), RH was studied as a precursor to synthesize high-purity $SiCl_4$, because RH could give almost-pure SiO_2/C mixture after controlled pyrolysis at appropriate conditions. Results showed that high-purity $SiCl_4$ obtained using RH as a raw material could avoid the separation procedure and also lowers the cost.

$$SiO_{2(s)} + 2C_{(s)} + 2Cl_{2(s)} \longrightarrow SiCl_{4(s)} + 6CO_{(g)} \qquad (2)$$

Using RH as a raw material, $SiCl_4$ was synthesized through the carbonization of RH in nitrogen atmosphere followed by chlorination reaction.[186-187] The results showed that the quality of the resultant products relies heavily on the raw materials used, as well as the controlled reaction conditions. To precisely examine the influence of the precursors and the experimental conditions on the products, the pelletizing technique was introduced to pre-synthesize the RH pellets containing silica and carbon, which was used to prepare $SiCl_4$ by chlorination process.[188-189] During those procedures, the RH was first acid-leached with 1 N HCl to eliminate metallic impurities and then calcined in argon at a given temperature. The carbonized RH was pressed into pellets. Following the pyrolysis, the samples were placed in the reactor under the preset conditions: chlorine gas flow of 4.0 L/min at a pressure of 1 atm for a dwell time of 5–50 min. At the end of the

chlorination process, chlorine gas was substituted with argon gas for the duration of 10–15 min. Then the final product of $SiCl_4$ was obtained. It was found that the amorphous structure of the RH pellets improves the reaction kinetic.

Other parameters, such as reducing agent concentration, temperature, and catalysts affecting the chlorination reaction kinetics were also studied.[189] In those studies, the graphite was added as excess reducing agent to examine the influence of reducing agent crystallinity on the silica conversion.[188-189] The addition of graphite as reducing carbon did not have an ideal effect on the silica conversion as that of naturally occurred carbon: the increase of the graphite content lowered the silica conversion. It was attributed to the difference in crystallinity of the added graphite and the naturally occurring carbons. In an the previous report, K^+ was found to accelerate the rate of chlorination due to the K^+ ions diffusing into the silica lattice and consequently distorting the silica lattice.[187] Therefore, the chlorinating species such as chlorinated carbon were easy to diffuse in silica lattice. However, Seo and his coworkers found that the temperature parameter had a greater impact on the chlorination reaction kinetics, whereas the use of catalysts (CuO and TiO_2) has no significant effect on the reaction kinetic when temperatures are below 1050 °C.[189] Thus, three following intervals of experiments, 700, 900 and 1100 °C, were conducted without the addition of graphite or a catalyst to test the most efficient means of conversion. The results confirm that the optimal silica reaction yield occurred at 1100 °C with the silica conversion value of 90%.

1.8. Others

1.8.1. Silicon

Silicon is a well-known important material for optoelectronic devices, and more than 90% of photovoltaic cell is silicon-based. Although solar photovoltaic power generation is a proven technology, high cost and the shortages in the supply of solar-grade silicon have hampered its growth.

Comparing with the commercial manufacture of solar-grade silicon by Siemens process or conventional metallurgical refining process, the synthesis of low cost solar grade silicon from RH was found to be an alternative approach to meet the low-cost requirement of high-purity silicon because of the simple synthesis procedure of high-purity silica from RH. Since polycrystalline silicon of 6 N purity (99.9999%) was synthesized by magnesium reduction of RH silica at temperature of 800 °C followed by successive acid leaching refining (mixtures of HF, H_2SO_4 and HCl),[190] many other methods had been subsequently developed.[191-194] For the magnesium reduction of RH silica procedure, the reaction temperature could be reduced to 550–650 °C,[191] and the purified RH silica exhibited more potential for solar grade silicon production than unpurified ones.[193] Besides of magnesium, both calcium and carbon have been used to reduce the silica from RH.[192, 194] Although many efforts had been made in 1980's, there hasn't been a big breakthrough and only a few studies have been reported for the last decade on this subject.[195]

Based on the magnesium reduction of silica method, Larbi et al did a very detailed study for the reduction behavior of RH silica for preparation of high purity silicon.[195] In their study, the RHA obtained from a local company was first leached by

using 10 wt% HCl at 90 °C for 4 hours to removal the metal impurities and then heat treated at 700 °C in air for 1–2 hours to reduce carbon content, resulting in the resultant silica with the purity of approximate 98%. The obtained silica was mixed with magnesium granules followed by wet blending with 4% polyvinyl alcohol solution. The magnesium to silica mole ratio was varied between 2–2.5 which corresponded to 0–25 wt% excess magnesium. After drying under argon atmosphere, the samples were pelletized into 16 mm diameter cylindrical pellets. The reduction experiments were carried out under argon at selected temperatures in the range of 600–900 °C with the rate of temperature rise of 10 °C/min. After reacting at the given temperature for 1 hour, the sample was acid leached by two steps. The first step was carried out by using the mixture of 1.25 M HCl and 4.37 M acetic acid in a respective volume ratio of 4:1 at 70 °C for 1 hour. After filtering, washing with DI water and drying, the sample was then acid leached with the mixture of 2.76 M HF and 4.37 M acetic acid in a volume ratio of 1:9 at 70 °C for 1 hour. The silicon with the purity of 99.5% could be finally synthesized.

The results showed that the maximum silicon yield occurred when the magnesium to silica mole ratio was 2.1 because excess magnesium could form Mg_2Si at the cost of Si, resulting in the low yield of silicon. The yield of silicon also significantly depended on the reaction temperature. Then higher reaction temperature gave higher yield of silicon, which was attributed to the reduction of the amount of Mg_2Si at high temperature. Thus, in their study, the maximum silicon yield was obtained at the temperature of 900 °C. The mechanism of reduction reaction was also studied in this study. The reaction of RH silica with magnesium was initiated at approximately 575 °C, at which temperature magnesium has sufficiently high vapor pressure. The rapid reaction between magnesium

vapor and solid silica took place, which was then slowed down as the reduction products (MgO and silicon) limit diffusion of magnesium to the silica core. Thus the concentration gradient for magnesium from the surface to the reaction interface was created, and the Mg_2Si was easily formed at the outer layers due to the thermodynamic conditions. Therefore, the higher temperature and longer time favored further reduction of silica and also the consumption of Mg_2Si to give a higher silicon yield.

1.8.2. Silicate and related products

Silicate is a family of materials that derived from silica (SiO_2), it consist of silicate anions and is balanced by various metal cations. People have been using silicas originated from RH as a precursor to prepare all kinds of silicates.[196-200] Reasons to use RHA as a silica source in making silicates reply on its low cost and amorphous nature. Amorphous RHA has larger surface areas to volume ratio relative to crystalline silica and will favor the silicates formation as a consequence.[196-201] Zeolite is one type of the silicates and has been reviewed in a separate section due to its importance. In this section, several selected common silicates derived from silica originated from RH will be reviewed.

1.8.2.1. Calcium silicate

Portland cement consists of several components such as calcium silicates, calcium aluminates, gypsum etc., in which the calcium silicates (Ca_3SiO_5 and β-Ca_2SiO_4) are the two most important components.[196] Ca_3SiO_5 and β-Ca_2SiO_4 contribute to about 70% of cement mass. It is well known that β-Ca_2SiO_4 has advantages over Ca_3SiO_5 because its production requires less energy and raw materials.[196, 201] It has been a research interest for decades to increase the portion of β-Ca_2SiO_4 in Portland cement to save energy as well as

raw materials.[196, 201] Moreover, it has been estimated that the cement industry is responsible for approximately 6% of total CO_2 emissions in the world.[202] Higher amount of β-Ca_2SiO_4 in cement could certainly minimize this problem. Typically, commercial cement is produced in rotary kilns at temperatures around 1500 °C through solid-state chemical reactions. As a comparison, by using silica derived from RH, β-Ca_2SiO_4 can be synthesized at 800 °C through similar solid-state chemical reactions. Romano et al. prepared β-Ca_2SiO_4 doped with titanium using RHA.[196] Physicochemical and mechanical properties such as total water absorption, water absorption by capillary rise, resistance to acidic attack, and flexural strength showed that the performance of mortars containing 20% of β-Ca_2SiO_4 doped with titanium was similar to the mortars prepared from commercial Portland cement. And the β-Ca_2SiO_4 material was synthesized at 800°C. The authors also prepared manganese modified β-Ca_2SiO_4 by using RHA.[196] Briefly, CaO, MnO and RHA were calcined together at 800 °C for 3 hours and different calcium silicates containing various amounts of manganese were prepared. It showed a high potential for the utilization of RHA as a raw material in cement production. Singh prepared highly reactive β-Ca_2SiO_4 using RHA.[203] The author showed that by using RHA, highest compressive strength of β-Ca_2SiO_4 was made compared to that made from other sources of silica such as Aerosil and aerosol containing 10 wt % fly ash.[203]

1.8.2.2. Zirconium Silicate ($ZrSiO_4$)

Lee and coworkers prepared vanadium doped $ZrSiO_4$ (V-$ZrSiO_4$) using silica from RH.[197] Synthesis of the optimum V-$ZrSiO_4$ (blue color) was carried out at 750 °C for 5 hours on equimolar amount of ZrO_2 and SiO_2 mixture with the addition of 0.2 mol % of V_2O_5 and 0.5 mol % of NaF (mineralizer). The formation mechanism of the

pigment synthesis was proposed as follows: 500 to 700 °C is the temperature for an active reaction, which is the initial step reaction caused by the phase transition of α-quartz to β-cristobalite involving the reaction of V_2O_5 with NaF to produce the intermediate phase $NaVO_3$ and SiF_4. At the final step in the temperature range from 700 to 800 °C, zircon is synthesized as SiF_4 diffuses into the M-ZrO_2 lattice. As soon as it is produced, V(IV) is incorporated into the mother crystal resulting in a turquoise blue coloring of the Zirconium Silicate.

1.8.2.3. Lithium aluminum silicate

Lithium aluminum silicate (LAS) glass ceramic, one of the most important glass-ceramic systems, has attracted high attention over the past several decades, because of its low and even negative thermal expansion coefficient as well as excellent thermal and chemical durability.[198] Chatterjee et al. prepared LAS through a sol-gel technique by using three different sources of silica namely TEOS, commercial fumed silica and RHA. β-eucryptite and β-spodumene were successfully prepared from all of the three silica sources. SEM results indicated no distinguishable morphology of LAS powders for three different sources of silica, though the reactivity of RHA was slightly lower than that of TEOS and fumed silica. Notably, the RHA used in the paper was mainly crystalline form (cristobalite form) and the silica from TEOS and fumed silica were amorphous based on XRD results in their paper.[198] Presumably the crystalline form of RHA is responsible for its lower activity relative to TEOS and fumed silica.

1.8.2.4. Titanosilicate

Microporous titanosilicate is a new family of unique zeolite discovered by Engelhard in 1989,[204] and this new classes of microporous titanosilicates were named as

ETS-4 (0.4 nm pore size) and ETS-10 (0.8 nm pore size). Shamsuddin and coworkers found that RHA is a very suitable silica source in the low cost preparation of highly pure ETS-10.[199] An optimum preparation procedure of ETS-10 was obtained from the gels of molar composition TiO_2:3.75SiO_2:1.5NaOH:0.54KF:21.25H_2O at 493 K and 52 h of crystallization time. Various characterizations showed that ETS-10 derived from RHA was found comparable with that prepared using Ludox in terms of their physicochemical properties. The RHA synthesized ETS-10 exhibited a very high BET surface area of 364 m^2/g. (Figure 1.8).[199]

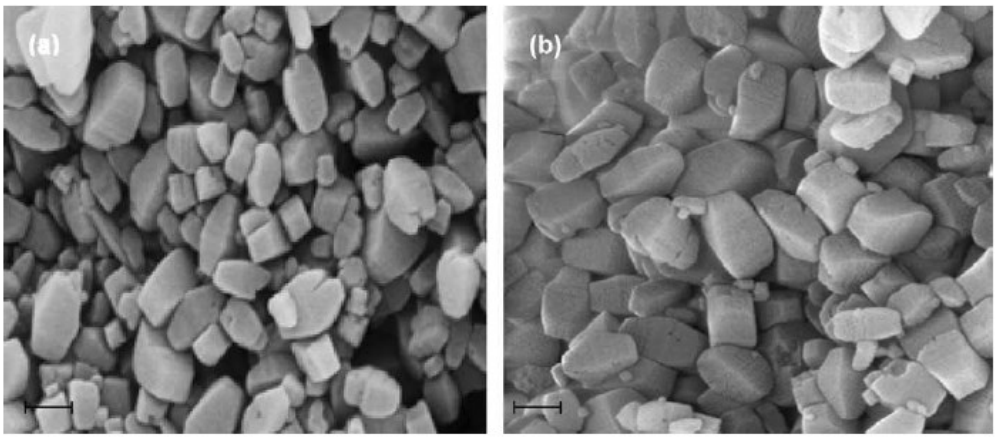

Figure 1.8 FE-SEM micrographs of ETS-10 synthesized by different silica sources. (a) Ludox-30 (b) RHA. Calcination temperature was 493 K. Scale bar: 200 nm.[199]

1.9. Conclusion

Many chemicals have been successfully derived from biomass. In many cases the feedstock is competing with food, such as lactic acid from corn and ethanol from sugar cane or grain.[205-206] Other biomasses such as switch grass or wood, though do not competition with food, will results in competitions within resources (water, nutrition etc). On the contrary, utilization of RH biomass has no competition with food or other resources which offers an advantage over other biomasses for further development

towards commercialization. As a biomass in agriculture industry, RH is becoming a more and more important resource for silica due to its abundance and low cost. The amorphous feature and large surface area of silica derived from RH made it a good raw starting material for silicon based industry application.

CHAPTER 2

Extraction of Lignocellulose and Synthesis of Porous Silica Nanoparticles from Rice Husks - A Comprehensive Utilization of Rice Husk Biomass

2.1. Introduction

Rice husks (RHs) are a tough and bulky biomass with a high silica content from rice production.[1, 3, 11, 13] It contributes ca. 20-25 wt% of the dry weight of paddy rice.[1] The anticipated world rice production in 2012 is 489.1 million tons,[207] which means approximately 122-163 million tons of RH biomass will be generated globally in 2012. The density of an individual RH is ca. 735 kg/m^3, whereas the bulk density of piled RHs is approximately 100~122 kg/m^3.[7-8] Studies have shown that RH contains ca. 15~28 wt% of silica depending on the variety, origin, climate, and geographic location[11, 68] and about 72~85 wt% of lignocellulose (LC),[9, 208] including cellulose (ca. 35-40 wt%), hemicellulose (ca. 15-20 wt%), and lignin (ca. 20-25 wt%).[1, 208] In addition to the two main components, RH also contains a trace amount of other substances such as metal ions, chlorides, phosphates, etc.[13, 209] The application of RHs has been limited because of their tough nature, low nutritional value, and great bulk.[13] Currently, the two most common RHs disposal methods are open field burning and land filling, which result in waste of energy, greenhouse gas emission, air pollution, and huge landfill space occupancy due to their low bulk density.[9, 30] To address those issues, researchers have been investigating for decades to explore more economical ways to make full use of RHs.[68, 210-213] Conventional applications of RHs include producing agriculture compost,[214] making construction materials (e.g., bricks, insulation fillers, etc.),[215] generating electricity (controlled burning).[216] In addition, methods to derive higher values

from RHs have also been explored, such as deriving various silicon based materials,[11, 13, 217] which have attracted high attention in the past decades.

Lignocellulose (LC), a major component in RHs, is an abundant renewable carbohydrate resource that can produce sustainable energy and chemicals. Making full use of LC can help reduce CO_2 emissions and atmospheric pollution.[218] However, during the previous explorations to prepare silicon based materials from RHs, the LC in RHs was largely ignored. They were typically burnt and thus wasted. The major challenge lies in the fact that there was no effective method to separate lignocellulose from RH. This situation has changed since the revolutionary work conducted by Rogers and coworkers[219] on the dissolution of lignocellulose by ionic liquids (ILs).[220-223] It has been shown that several ILs can dissolve the lignocellulose in RHs.[224-225]

In addition to lignocellulose, RH also contains a high concentration of silica. The silicon element enters rice plants via their root in a soluble form, probably as a silicate or monosilicic acid, which undergoes bio-mineralization to form a lignocellulose and silica connected network in rice plant.[226] It is widely agreed that the silica in RHs is predominantly in inorganic linkages. A small portion of the silica might be covalently bonded to the organic compounds.[226] This portion of the silica cannot be dissolved in alkali and can withstand very high temperatures.[226] Studies have shown that the silica in rice plant is mainly localized in the tough external layer (epidermis) of RHs and it also fills in the space between the epidermal cells.[13] Harvesting silicon based materials has been the major research focus on RHs, since silicon based materials have widespread application in auto industry, information technology, fine chemistry, and material science.[20-21] So far, various silicon based materials have been derived from RHs,[13]

including silica,[30] silicon carbide,[103] silicon nitride,[181] silicon tetrachloride,[189] zeolite,[153] and silicon.[119, 195]

It is of great environmental and economical importance to utilize both the lignocellulose and the silica in RHs. In this paper, to our best knowledge, for the first time, a comprehensive approach to make full use of RHs by deriving both lignocellulose and silica from RHs is reported. We firstly used 1-butyl-3-methylimidazolium chloride (BMIMCl), an ionic liquid, to dissolve and isolate LC from RHs. The dissolved LC in BMIMCl could be easily regenerated and is ready for applications in various fields, such as paper pulp, biofuel, etc.[227] After IL extraction, the RH residue can be readily thermally treated to yield high purity, amorphous and porous silica. Through this method, both of the two major components in RHs could be utilized to yield value-added products. In addition, the IL used in this method can be recycled efficiently and be used as a solvent to extract LC from RHs multiple times, which would facilitate the commercialization of this technology.

2.2. Experimental

The RHs used in this study were obtained from Three H's LLC (Arkansas, USA). 1-Butyl-3-methylimidazolium chloride (BMIMCl, Sigma-Aldrich) and concentrated hydrochloric acid (VWR) were used as received without further purification.

RHs were first washed by deionized (DI) water three times to remove dirt and then dried in an oven at 90 °C overnight. The water rinsed and dried RHs (RH-H_2O) were chopped into powders using a regular countertop blender prior to the IL treatment to increase the surface area of RHs. The grounded RH powders were mixed with a pre-

determined amount of IL to extract lignocellulose. The weight ratio of IL to RHs was maintained at 15 to 1. The mixture of IL and RHs was stirred by a magnetic stirrer in an oil bath at a set temperature for a period of time (see Table 2.1). Immediately after the dissolution, the product mixture was centrifuged to separate the insoluble portion of RHs (namely RH residue) when the mixture was still hot to take advantage of its low viscosity. The supernatant was collected and mixed with DI water to precipitate the dissolved lignocellulose in IL. The precipitated LC was collected, washed with DI water three times, and then dried in an oven at 90°C overnight. A small portion of LC was bleached by 5 wt% H_2O_2 for 2 hours at 100 °C, and then the bleached LC was filtered and rinsed with DI water three times for demonstration purpose. The LC after bleaching was dried in an oven at 90 °C overnight.

The separated RH residue was washed by DI water to remove the small amount of absorbed IL, and then re-centrifuged. This process was repeated three times to fully remove the absorbed IL, and then the RH residue was dried in an oven at 90 °C overnight. All the above solutions containing IL were collected and purified following a reported procedure: they were firstly evaporated under vacuum in a rotary evaporator (IKA-RV10) at 90 °C to remove the water as much as possible, and then the recycled IL was dried in a vacuum oven (VWR S/P Model 1430) for 24 hours at 90 °C.[228] The recycled IL was used to extract LC in RHs following the same procedures as described above.

The degree of extraction of LC was calculated according to Equation 1, where w_i is the initial weight of RHs used, w_{re} is the weight of RH residue (insoluble portion) after

IL extraction. LC content was set to be 81.7 wt% in RHs in this article based on the TGA measurement, which will be discussed below.

$$\text{degree of extraction of LC } (wt\%) = \frac{w_i - w_{re}}{81.7\% \times w_i} \times 100\% \qquad (1)$$

In order to compare the effectiveness of IL treatment on the removal of metal cations for the synthesis of silica, acid treated RHs were also prepared and used as a control. Acid treatment was carried out based on the water rinsed and dried RHs, which were directly refluxed in 5.0 wt% HCl in a round bottom flask for 1 hour. After that, the RHs were rinsed with DI water three times before dried in an oven at 90 °C overnight.

Both the RH residue after IL extraction and the acid treated RHs were pyrolyzed at 700 °C for 2 hours to prepare silica nanoparticles.

Scanning electron microscopy images were acquired on a LEO 1530 VP field emission scanning electron microscope (FE-SEM). All Samples were sputter coated with a thin layer (ca. 3 nm) of Au/Pd prior to SEM imaging. The purity of silica was measured on a PANalytical AXIOS X-Ray Fluorescence (XRF) Spectrometer. The surface area of silica nanoparticles was measured on a TriStar II 3020 Surface Area and Porosity System. The samples for surface area measurement were dried at 250 °C over 8 hours prior to the measurement. X-ray diffraction (XRD) patterns were recorded using a Bruker D8 diffractometer with Bragg-Brentano θ-2θ geometry (40 kV and 30 mA), using a graphite monochromator with Cu K_α (λ=0.1540 nm) radiation. Thermogravimetric analysis (TGA) was conducted on a TA Q50 analyzer (TA Instruments) at a heating rate of 10 °C/min in air atmosphere.

2.3. Results and discussion

RHs are mainly composed of lignocellulose (cellulose, hemicellulose, and lignin), hydrated silica, and a trace amount of various metal ions, chlorides, and phosphates.[13, 209] Researchers have managed to synthesize various silicon based materials from RHs[13] while silica has been the major product. Earlier research has proved that metal cations, particularly potassium ions, in RHs are responsible for the melting of silica nanoparticles at relatively low temperatures during pyrolysis,[30, 46, 53, 229-231] which leads to the aggregation of silica nanoparticles and increase of crystallinity. Studies have shown that acid treatment is an effective way to remove the K^+ ions in RHs. Pyrolysis of acid treated RHs yielded silica nanoparticles with high purity and surface area, and low crystallinity.[30, 35, 232] However, acid leaching is demanding on reaction equipment, and may generate potential pollution issues, thus highly undesirable for commercial production. Moreover, few of the approaches to prepare silicon based materials reported so far have taken the lignocellulose into consideration. During the conventional processes, the lignocellulose in RHs was simply burned and wasted, which also leads to severe CO_2 emission and potential pollutions.

ILs have been found to be a group of effective and green solvent for dissolving LC.[220] It has also been reported that LC can be used in renewable energy,[233] paper industry,[234-235] and be converted into biofuel (particularly ethanol).[211-212] Therefore, using IL to extract LC from RHs before harvesting silica (or other silicon based materials) would lead to a comprehensive utilization of the two major valuable components in RHs. At the same time, during the IL extraction of LC, it is expected that the metal impurities, particularly potassium which is typically soluble in water, can be effectively removed

simultaneously, which can bring synergistic benefits for the later stage of harvesting silicon based materials. In our study, the characterization results support this hypothesis, which will be discussed below. The detailed conditions for IL extraction are listed in Table 2.1. These conditions (temperature, time and weight ratio of RHs to IL) for IL extraction of LC were chosen since they are representative and were most typically used in the previous research.[221, 225, 228] The results showed that either a higher extraction temperature or a longer duration is needed to improve the degree of extraction. At 130 °C, ca. 51.1% of LC was extracted after 36 hours of reaction. This extraction rate is comparable to the previous reports which is approximately 30~50 wt%. [225, 228]

Table 2.1 Results on ionic liquid (IL) extraction of lignocellulose (LC). The weight ratio of IL to RH was 15 to 1 for all the samples.

Sample ID	Temperature (°C)	Time (hr)	Degree of Extraction of LC (%)	IL Recovered (%)
RH-IL-1	100	12	21.4	98.9
RH-IL-2	150	12	46.6	97.9
RH-IL-3	130	36	51.0	96.8

The used IL can be easily recovered by a rotary evaporator (Table 2.1), and the IL dissolution efficiency after recycling was also studied. Table 2.2 shows that after 3 times of recycle of IL, the dissolution rate of LC under the same condition decreased from ca. 51.0 to ca. 37.2 percent. The decrease in IL efficiency is probably caused by several reasons. Firstly, a small portion of the IL was decomposed during the RH extracting. Li et al. revealed that during the extraction, part of IL (as high as 15%) would undergo degradation depending on the temperature and duration.[228] Secondly, there is always residual water remained in the recycled IL after recovery and water is a poor solvent for

LC.[228] Since hydrophilic BMIMCl and water molecules could form weak interactions with each other,[236] it is hard to completely remove the water content during recycling. Thirdly, after the LC regeneration, there is always a tiny amount of LC remaining in the IL. The residual LC will interact with IL and this interaction would negatively affect the recycled IL to accommodate new LC from RHs, and thus affect the performance of the recycled IL in the new cycle of extraction.[228] Li et al. studied this phenomenon and based on the color of the recycled IL and ^{13}C NMR results, they found that a low concentration of LC, presumably the ones with low molecular weights could still remain dissolved during the LC regeneration process.[228] Nevertheless, based on our study, even after 3 times of recycling, the IL still remains to be efficient in terms of isolating LC from RHs with a dissolution rate of 37.2 wt%. Overall, the IL efficiency data on LC extraction are in good agreement with earlier reports.[99, 228]

Table 2.2 Effect of BMIMCl recycling on the degree of extraction efficiency.

Sample ID	Temperature (°C)	Degree of Extraction (wt%)	IL Recovered (wt%)	IL Recycled times
RH-IL-3	130	51.0	96.8	0
RH-IL-4	130	44.2	97.1	1
RH-IL-5	130	40.0	98.5	2
RH-IL-6	130	37.2	97.9	3

Note: the weight ratio of RH and IL was 1:15 for all samples and the extraction time were kept at 36 hours.

The collected LC from RH is shown in Figure 2.1. The LC can readily be used in various applications such as renewable energy, biofuel, etc.[211-212, 227, 233] After bleaching, the LC exhibits white color, thus potential for paper industry applications. It was reported

that the LC after IL extraction typically possesses a lower crystallinity compared to the original LC in plants and such LC with a lower crystallinity is a better candidate for widespread application.[237]

Figure 2.1 Regenerated Lignocellulose from RH before (left) and after bleaching (right).

Figure 2.2 shows the TGA results for the water rinsed RH (RH-H_2O), HCl treated RHs (RH-HCl), and RH residue after IL extraction (RH-IL) (which is RH-IL-3 in Table 2.1). Based on Figure 2.2, the RH-H_2O used for this study contains ca. 18.3 wt% RH ash (RHA), most of which is silica. The ash content for RH-HCl and RH-IL is 24.8 and 33.4 wt%, respectively. This shows that after either HCl or IL treatment, the silica content in RH residue was increased. For RH residue after IL treatment, the increase of silica content is simply owing to the partial dissolution of LC in RHs by BMIMCl. For the HCl treated RHs, the increase of silica content can be explained by the fact that the HCl treatment can help hydrolyze the organic components in RHs, especially hemicellulose.[211, 238] Hemicellulose is hydrogen-bonded to the surface of cellulose micro-fibrils. Under acid pretreatment, part of hemicellulose could be depolymerized by acid

assisted hydrolysis and this will also release some lignin which is indirectly associated with cellulose via linkage to xylan.[238]

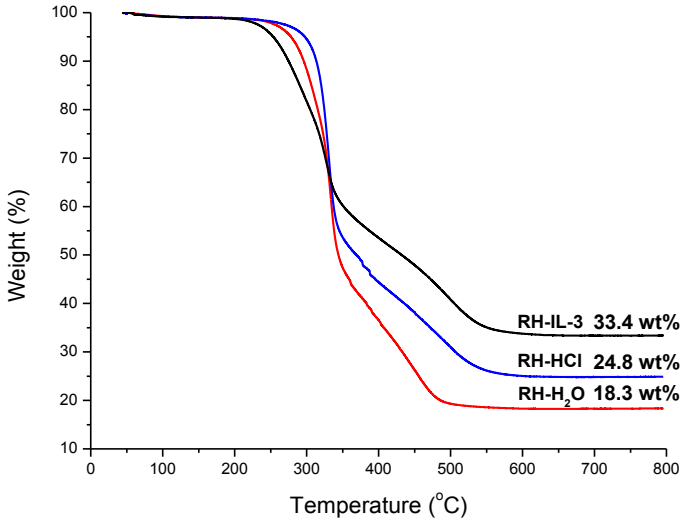

Figure 2.2 TGA study of various rice husks. Samples were water treated RHs (RH-H_2O), acid treated RH (RH-HCl), and RH residue after 1-butyl-3-methylimidazolium chloride (BMIMCl) extraction (RH-IL-3).

Previous work has shown that in order to prepare high quality silica nanoparticles from RH, metal cations, particularly K^+ cations, must be removed. Acid treatment has proved to be effective to remove metal cations.[35, 46] In this work, it is expected that metal cations, particularly the ones soluble in water, can be removed during IL extraction, and achieve a similar effect as HCl treatment. To compare the metal removing effect, the silica samples prepared from both the RH residue after IL extraction and HCl treated RHs are systematically evaluated.

Table 2.3 shows the XRF results of the silica samples from the water, IL, and HCl treated RHs. Among the three samples, the silica from the HCl treated RHs exhibits the

highest purity of 99.80 wt%; the silica from the IL treated RHs exhibits a slightly lower purity of 99.52 wt%; while the silica from the H_2O treated RHs possesses a much lower purity of 96.91 wt% compared to the above two. Overall, the XRF results support that the IL treatment is much more effective than the water rinse and is comparable to the HCl treatment in terms of metal and non-mental impurities removal. This is probably because during the dissolution of LC, the impurities in the dissolved LC were removed together with this portion of LC. Meanwhile, the partial dissolution of RHs disrupted the overall structure of RHs, allowing for better contact between the ILs and the RH residue, which helps further remove the impurities in RH residue via an ion exchange process. In particular, IL treatment can effectively remove potassium cations, whose absence has proved to be very critical for the synthesis of high quality silica nanoparticles from RHs.[35, 46] This in turn is consistent with the high purity silica samples from the HCl and IL treated RHs, which will be discussed in detail below. As such, the results support our initial expectation that the IL treatment, whose major purpose is to extract LC, can lead to a synergistic effect to remove critical metal cations, facilitating the subsequent synthesis of silica nanoparticles from RH residue.

The XRD patterns of the silica samples from HCl and IL treated RHs are shown in Figure 2.3. The two patterns are very close to each other, and suggest that the silica samples are amorphous. This again suggests that the IL extraction process has effectively removed K^+ cations, which is consistent with the above XRF results.

Table 2.3 XRF data of the silica made from the pyrolysis of RHs at 700 °C for 2 hours. The RHs were treated by H_2O, IL, and HCl, respectively.

Compound	Silica from RH-H_2O (wt%)	Silica from RH-IL-3 (wt%)	Silica from RH-HCl (wt%)
SiO_2	96.89	99.52	99.80
CaO	1.22	0.05	--
Cr_2O_3	0.61	--	--
P_2O_5	0.31	0.02	0.03
MgO	0.25	--	--
SO_3	0.19	0.04	0.06
Fe_2O_3	0.18	0.30	0.06
K_2O	0.11	--	--
MnO	0.10	--	--
ZnO	0.08	--	--
NiO	0.04	0.05	0.03
CuO	0.02	0.02	0.02

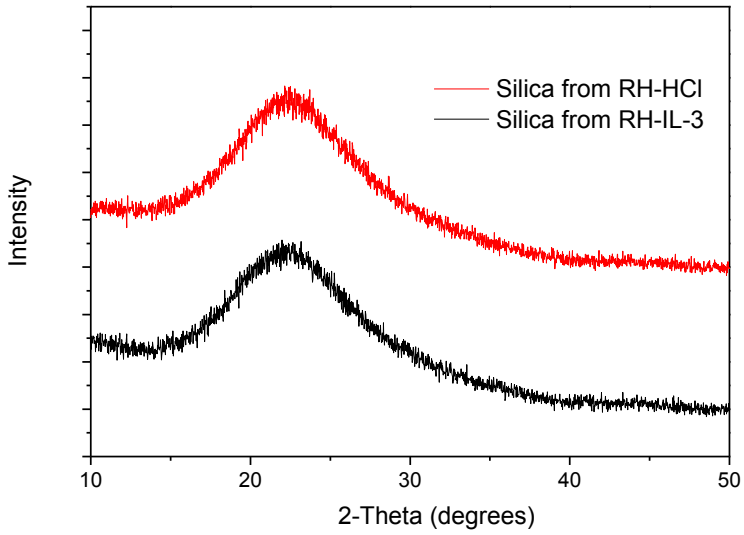

Figure 2.3 XRD patterns of two silica samples. Samples were prepared from RH-HCl (up curve) and RH-IL-3(down curve), respectively.

Figure 2.4 shows the SEM images of the silica samples from the pyrolysis of HCl and IL treated RHs. The SEM images show that the diameter of the silica nanoparticles from the HCl leached RHs is ca. 50 nm, which is slightly lower than that of the silica nanoparticles (ca. 70 nm) from the IL treated RHs (RH-IL-3). Such a minor dimensional difference might be owing to the slightly higher concentration of metal cations in the IL treated RHs, particularly Ca^{2+} and Fe^{3+}. It has been reported that Ca^{2+} can promote the melting of silica, although its promoting effect is much less significant compared to K^{+} cations.[239-240] In addition, both silica nanoparticle samples exhibit a narrow particle size distribution, which is very valuable for their future applications.

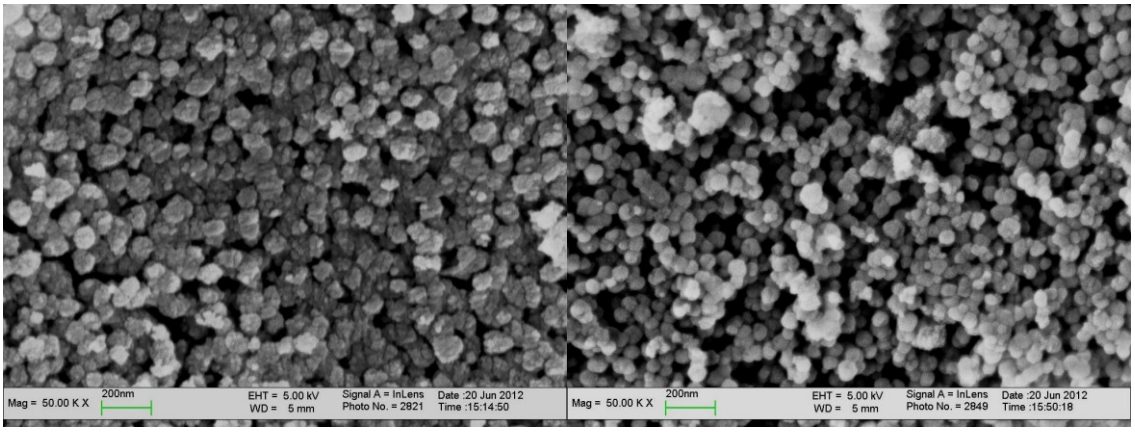

Figure 2.4 SEM images of silica nanoparticles from RH. Left: silica nanoparticles from the pyrolysis (2 hr @ 700 °C) of the IL treated RHs (RH-IL-3); Right: silica nanoparticles from the pyrolysis (2 hr @ 700 °C) of the HCl treated RHs (RH-HCl).

While the two silica samples differ slightly in particle size, both of them exhibit a porous structure. The surface area of the silica nanoparticles from the HCl treated RHs is 283.3 m^2/g according to the BET characterization, which is slightly higher than that of the silica nanoparticles from the IL treated RHs (241.1 m^2/g). Assuming all the particles are solid (nonporous) and perfectly spherical, and the density of silica is 2.22 g/m^3 then

based on the particle size of the two samples in Figure 2.4 (~50 nm and ~70 nm),[46] their specific surface areas should be ca. 54.1 and 38.6 m^2/g, respectively. Thus, the BET surface area measurement showed that those silica nanoparticles were actually porous. The porous structure is probably because the silica retained its cellular skeleton structure in RHs,[241] which is originated from the loose aggregation of primary silica nanoparticles. The porous silica structures observed here are consistent with our previous work.[46]

While this work focuses on silica, other silicon based materials can also be synthesized after IL extraction. On the other hand, this comprehensive utilization approach can be applied to other biomass containing silica such as wheat, sorghum, etc. or other valuable inorganic materials which cannot be dissolved in ILs.[3]

2.4. Conclusions

Our study has shown that ionic liquid BMIMCl is an effective solvent to extract lignocellulose in RHs. The LC in RHs can be easily isolated and collected. The degree of extraction of LC by using BMIMCl reached 51.0 wt%, and the BMIMCl can be collected and reused for the extraction of LC. The IL treatment of RHs leads to a synergistic effect to effectively remove K^+ cations, which has been conventionally achieved by HCl leaching of RH. Amorphous silica nanoparticles with a high purity, high surface area, and narrow particle size distribution were synthesized by the pyrolysis of RH residue after IL extraction. This work represents a fine first example of comprehensive application of RHs, which is expected to promote effective utilization of RH biomass globally in the near future.

CHAPTER 3

Synthesis of Lithium Aluminum Silicate Based on Different Sources of Silica via Sol-Gel Method

3.1. Introduction

Lithium aluminum silicate (LAS) glass-ceramic is widely known for its low and even negative thermal expansion coefficient (TEC).[198, 242-247] Two well-known brands of glass-ceramic are Zerodur® and Sitall® which can be commonly found on telescope mirrors.[248-249] The TEC of Zerodur® and Sitall® is about $\pm 1 \times 10^{-7}$/K, and $\pm 1.5 \times 10^{-7}$/K, respectively. Glass-ceramic possesses other attractive properties including low heat conduction coefficient, good resistance to mechanical and thermal shock, and excellent chemical durability.[242-243] There are variety of glass-ceramic systems which usually are denoted according to their chemical compositions, such as MAS-system ($MgO\text{-}Al_2O_3\text{-}nSiO_2$), ZAS-system ($ZnO\text{-}Al_2O_3\text{-}nSiO_2$), $Cu_2O\text{-}Al_2O_3\text{-}SiO_2$, and $CaO\text{-}MgO\text{-}Al_2O_3\text{-}SiO_2$ system etc.[243, 250] Originally, glass-ceramic was developed for use in the mirrors and mirror mounts of astronomical telescopes.[248-249] However, its use in cooktops, cookware, bakeware, and high performance reflectors for digital projectors, has made glass-ceramic an important commercial product.[251]

LAS has been one of the most important glass ceramic system because of its low and even negative thermal expansion coefficient as well as excellent thermal and chemical durability. According to the previous studies,[198, 252] either β-eucryptite ($Li_2O\text{-}Al_2O_3\text{-}2SiO_2$) phase or β-spodumene ($Li_2O\text{-}Al_2O_3\text{-}4SiO_2$) phase can be the dominant crystalline phase in LAS glass-ceramic system. Quite a few approaches have been developed to synthesize LAS powders. For instance, commercial β-spodumene is

normally prepared by the recrystallization of solidified glass melt, in which a sintering agent is usually needed.[198] The incorporation of a sintering agent will result in a large thermal expansion coefficient for the final products .[253] Thus, preparation of homogeneous and fine β-spodumene without sintering agent is important. Sol-gel methods do not require sintering agents to synthesize glasses and ceramic composites. And the method has the advantages of low sintering temperature, high degree of product homogeneity, high purity and yield, short processing time, low cost, as well as being environment friendly.[252]

In Chapter 1, it has been discussed that Rice husk (RH) is an abundant biomass with high silica content. RH can be used as a sustainable and renewable feedstock if treated properly.[197] As has been discovered, RH contains ca. 15~28 wt % of silica depending on the variety, origin, climate, and geographic location. It would be beneficial if this silica could be harvested and utilized as a sustainable and renewable feedstock for the preparation of LAS glass-ceramic because the silica is of low cost and of very high purity.[30, 254] Actually, researchers did try to use the silica from RH in to synthesize LAS through a sol-gel method.[198, 252] The adopted silica was from non-treated RH, i.e., rice husk ash (RHA) from RH burning in air. RHA is a low purity, and partially crystallized silica. It has been found that the reactivity of RHA from non-treated RH was low and had poor results in preparing LAS glass-ceramics powders when compared with other sources of silica such as fumed silica.[198, 252] Our study confirmed that RHA has low reactivity but on the other hand, we found that the silica from treated RH showed high reactivity which is comparable to that of fumed silica. Fumed silica is usually produced through burning of chlorosilane in air. And the process normally involves multiple reactions, high energy

input, and toxic reactants and byproducts. Thus the cost of the fumed silica is high. Based on the current market prices of fumed silica, we have estimated that the cost of producing fumed silica is about $1200/t, while the cost of silica from treated RH is about $400/t. That is to say, the silica from treated RH could be an ideal substitute for fumed silica in the synthesis of LAS glass-ceramics since their reactivity is similar but the cost is much lower for silica from treated RH than that of fumed silica.

3.2. Experimental

Aluminum nitrate nonahydrate ($Al(NO_3)_3 \cdot 9H_2O$, 97+%), lithium nitrate anhydrous ($LiNO_3$, 99%), ammonium hydroxide ($NH_3 \cdot H_2O$, 28%), concentrated hydrochloric acid (HCl, 37%), potassium bromide (KBr, 99+%) were purchased at VWR and used as received.

Fumed silica used in this study is provided by Evonik Industries Corp. (Aerosil® 155). Silica from RH (RHA) without any treatment is from Guangzhou, China. Silica from HCl treated RH (RH-HCl-Silica) is prepared according to the method previously reported.[30] Raw RH was first rinsed with deionized water three times at room temperature to remove dusts and then dried at 100 °C for 24 h. The dried RH was then refluxed in 5.0 wt% HCl solution in a round bottom flask for 2 hours. Then, the RHs were rinsed with DI water three times before dried in an oven at 100 °C for 24 h. Calcination of this HCl treated dry RH at 700 °C for 2 hours yields the RH-HCl-Silica.

Scheme 3.1 illustrates the procedures of preparation of lithium aluminum silicate (LAS) powders from different sources of silica, i.e., fumed silica, silica from HCl treated RH (RH-HCl-Silica), and silica from non-treated RH (RHA). Overall, the procedure can be divided into two major steps. The first step is to prepare the sol of Lithia-Alumina

with their stoichiometric compositions. The second step is to prepare the sol of Lithia-Alumina-Silica with their stoichiometric compositions by adding certain amount of various silica sources to the sol prepared in the first step.

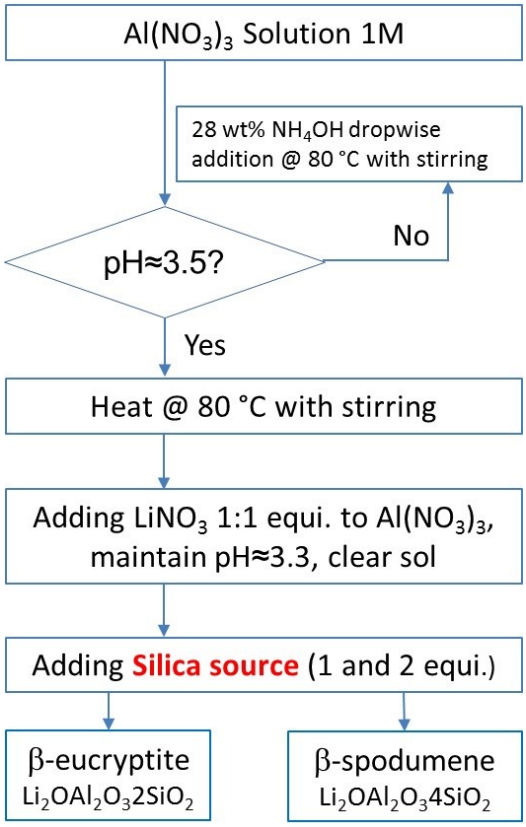

Scheme 3.1 Schematic illustration of synthesizing LAS. Sol-gel method and different silica sources were used. Note: equi.: equivalent amount.

As shown in Scheme 3.1, the first step was to add the concentrated ammonia solution dropwise to the prepared $Al(NO_3)_3 \cdot 9H_2O$ solution (1M), until the pH of the solution becomes approximately 3.5 (measured by a pH meter). The mixture is under stirring and is kept at 80 °C while adding the ammonia solution. Keep heating the solution for 4 to 5 hours to allow adequate polymerization of the $[Al(H_2O)_6^{3+}]$ which indicated by the final solution becoming slightly white and opaque. Then to

the above semi-transparent solution, stoichiometry amount of $LiNO_3$ to $Al(NO_3)\cdot 9H_2O$ (1:1 mole ratio of Li to Al) was added under stirring, then the proper amount of ammonia solution to maintain the pH at about 3.3 was added. The sol of Lithia-Alumina is thus prepared for the second step reaction which in brief involves the addition of various silica sources at room temperature to form the sol of Lithia-Alumina-Silica. Note that both the RH-HCl-Silica and RHA were thoroughly ground to increase the surface area of the silica before adding into the solution at the second step. For different stoichiometric composition of Li_2O-Al_2O_3-SiO_2, two series of sol, namely LAS-1 (Li_2O-Al_2O_3-$2SiO_2$) and LAS-2 (Li_2O-Al_2O_3-$4SiO_2$) were prepared for each source of silica. All the final sols were continuously heated at 80 °C under stirring to get the corresponding gel powder. The agglomerated gels were ground thoroughly and then were subjected to calcination in air at various temperatures, i.e., 400 °C, 600 °C, 800 °C, 1000 °C respectively in a box furnace for 2 h to obtain the final LAS oxide powders.

Scanning electron microscopy images were characterized on a LEO 1530 VP field emission scanning electron microscope (FE-SEM). The SEM samples were sputter coated with a thin layer (ca. 3 nm) of Au/Pd prior to imaging. X-ray diffraction (XRD) patterns were recorded using a Bruker D8 diffractometer with Bragg-Brentano θ-2θ geometry (40 kV and 30 mA), using a graphite monochromator with Cu K_α (λ=0.1540 nm) radiation. FT-IR spectra were collected using a Nicolet 730 FT-IR spectrometer. KBr was used to make the pellet of FTIR samples.

3.3. Results and Discussion

LAS prepared from various sources of silica were characterized by XRD to study their crystallization behavior as a function of reaction temperature. XRD patterns of the LAS powders are shown in Figure 3.1 to Figure 3.3. Each Figure corresponds to two series samples (LAS-1 and LAS-2) made from fumed silica, RH-HCl-Silica, and RHA respectively. The calcination temperatures were individually at 400, 600, 800, and 1000 °C. In Figure 3.1, it can be seen that at 400 °C, both the samples in LAS-1 and LAS-2 are in amorphous phase. The crystallization phase of β-eucryptite and β-spodumene start to appear at 600 °C. The peaks and base lines of samples made at 600, 800, and 1000 °C in Figure 3.1 are sharp and smooth, indicating the crystalline phase in those samples are dominant.

For the sample series of LAS-1 and LAS-2 prepared from RH-HCl-Silica (Figure 3.2), the overall crystallization behavior is similar to that in fumed silica series (Figure 3.1). At 400 °C, both the samples in LAS-1 and LAS-2 are in amorphous phase. It can be seen that starting from 600 °C, the crystallization of both β-eucryptite and β-spodumene phases appeared. We noticed that, the base lines and peaks of both samples (LAS-1 and LAS-2) made at 600 °C is less smooth and sharp than that in Figure 3.1, which indicates that the degree of crystalline in RH-HCl-Silica series made at 600 °C is lower than that in fumed silica series made at 600 °C. However, the base lines and the peaks becomes similarly smooth and sharp starting from 800 °C to that of the corresponding temperatures in Figure 3.1, indicating that content of crystalline phase of samples made from RH-HCl-Silica becomes comparable to that of fumed silica series.

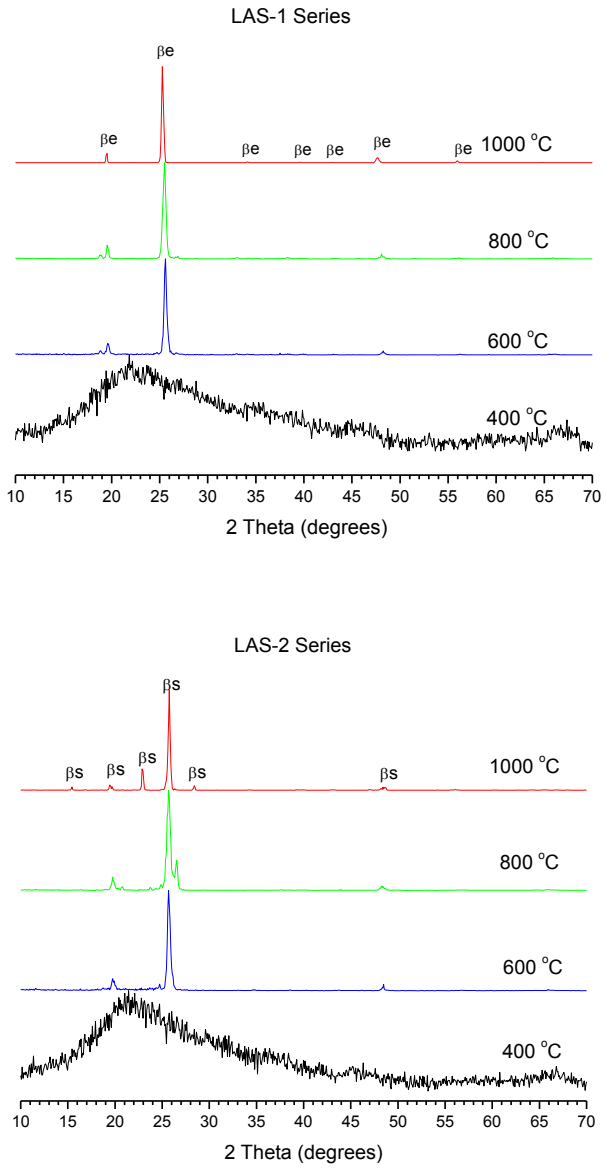

Figure 3.1 XRD patterns of LAS samples based on fumed silica at various temperatures; 2 hours calcination time at each temperature. βe: β-eucryptite; βs: β-spodumene.

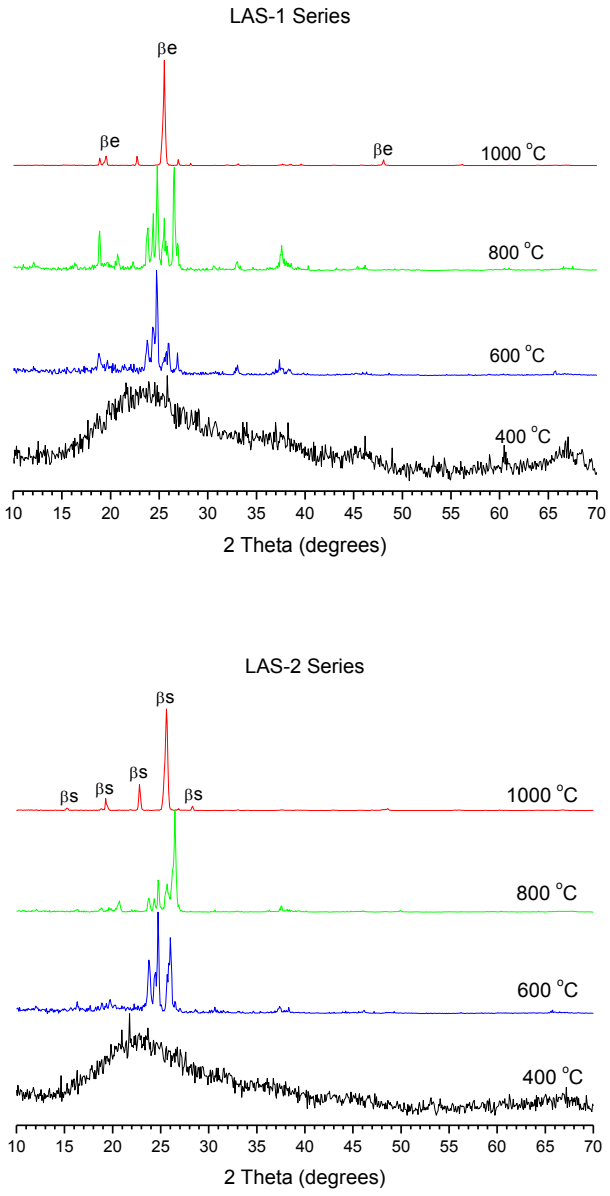

Figure 3.2 XRD patterns of LAS samples based on silica from HCl treated rice husk. 2 hours calcination time at each temperature. βe: β-eucryptite; βs: β-spodumene.

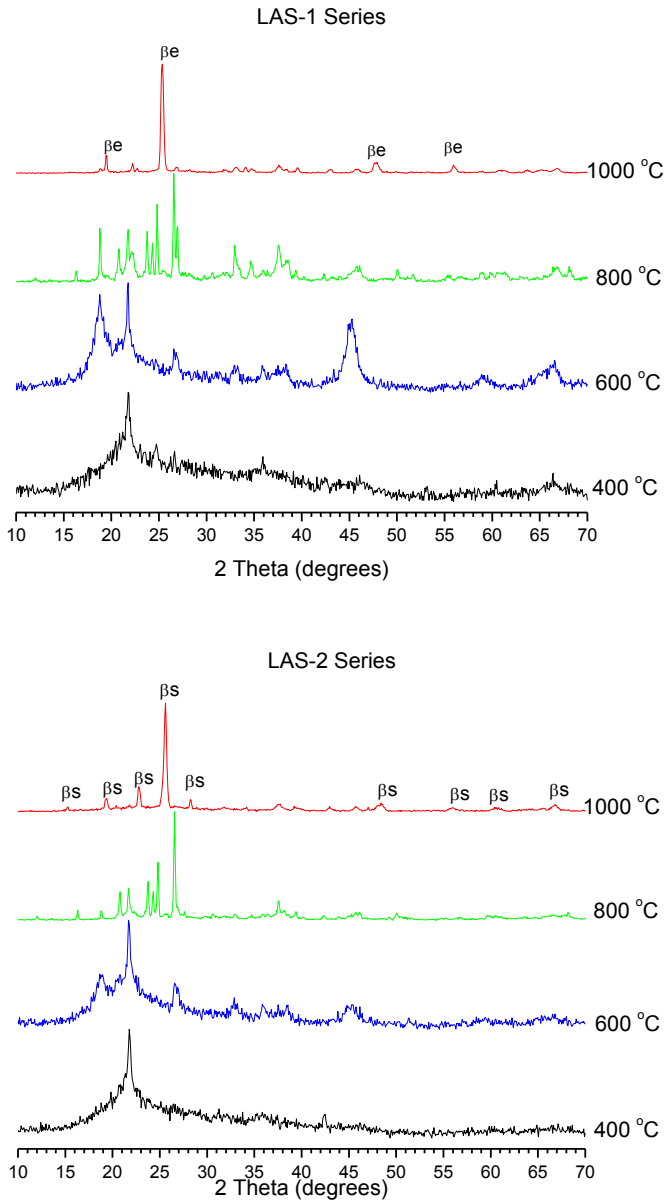

Figure 3.3 XRD patterns of LAS samples based on silica from non-treated rice husk. 2 hours calcination time at each temperature. βe: β-eucryptite; βs: β-spodumene.

For the sample series of LAS-1 and LAS-2 made from RHA (Figure 3.3), it is obvious that starting at 800 °C, the crystalline phase was developed according to the base line and peak shape of the spectra. At 400 and 600 °C, the amorphous phase appears to be

dominant. At 1000 °C, the base line of the XRD spectrum becomes flat and smooth, more characteristic peaks appeared and the intensity increased, indicating the crystalline phase became well developed. For all the samples made from the three sources of silica, LAS-2 series (β-spodumene) appeared be better developed than that of LAS-1 ones according to the number of characteristic peaks and peak intensity formed at 1000 °C.

From the discussion above, it can be concluded that the apparent reactivity of the three different sources of silica in the LAS synthesis decreased from the fumed silica to the silica from non-treated RH (RHA). RH-HCl-Silica is in the middle and its apparent reactivity is comparable to that of fumed silica. This conclusion is a little different from previous studies.[198, 252] In those studies, it was observed that through the similar sol-gel method, even for fumed silica, at 600 °C, no crystalline phases were developed according to their XRD results.[198] In their fumed silica series, the calcination time of the LAS synthesis was 1 h at each temperature. In this study the difference in calcinations time might be the reason why crystalline phases were not observed starting at 600 °C even for fumed silica which supposed to have higher apparent reactivity in both investigations. When comparing with RHA, they found that the RHA based LAS synthesis only gives crystalline phase starting at 800 °C. The observation is consistent with our current study (see Figure 3.3). Moreover, in our current study, the silica from treated RH (RH-HCl-Silica) was used for comparison together with fumed silica and RHA. And we have found that RH-HCl-Silica has higher apparent reactivity than that of RHA, and is comparable to that of fumed silica (see Figure 3.1 and 3.2). Both of the LAS samples made from fumed silica and RH-HCl-Silica begin to crystallize at 600 °C.

It has been studied that the high chemical reactivity of silica from RH is largely due to its high surface area and low crystallinity.[255] This is easy to understand because the contact area between the reactants should be proportional to the reaction rate. The surface area of a reactant will directly affect the contact area between the reactants. On the other hand, the degree of crystallinity of a reactant would also affect the reactant's reactivity. Crystallinity is closely related to activation energy of a reaction. For instance, the crystal lattice energy has to be overcome as the additional activation energy for a specific reaction to start. In our previous study, we found that silica from treated RH can have the surface area up to 280 m^2/g, and silica from non-treated RH usually have the surface area around 2.1 m^2/g.[12, 255] Also, it has been shown that the silica from non-treated RH has higher degree of crystallinity (Figure 3.4). The different apparent reactivity from the three sources of silica in the LAS synthesis presumably has to do with their surface area and crystallinity. Figure 3.4 is the XRD pattern of the three silica sources. It can be seen that the fumed silica has the lowest crystallinity among the three and the RHA has the highest crystallinity. The crystallinity of the three different sources of silica is consistent with their apparent reactivity based on Figure 3.4.

Regarding the difference in silica reactivity, it may also directly relate to its intrinsic structure. It has been discovered that, there are mainly three forms of silica exist in rice husk namely Q4 [$*Si(OSi)_4$], Q3 [$(OH)*Si(OSi)_3$], and Q2 [$(OH)_2*Si(OSi)_2$], all of which are different in form and affect crystallinity.[81] In brief, an increase in the amount of the Q4 form of silica, increases the silica's crystallinity, which is shown by NMR and XRD results in the same paper.[81] That is to say, higher crystallinity of silica contains greater amounts of Q4 silica; and lower crystallinity of silica contains lesser

amounts of Q4 silica (more Q3 and Q2 consequently). Considering that in the synthesis of LAS powder (and other silica related chemical reactions), the Q4 form of silica would be much less reactive than that of Q3 and Q2 silica. Thus it is reasonable to say that for the silica from RH, the low crystallinity samples would contains lower amount of Q4 silica (more Q3 and Q2 consequently) so the reactivity would be higher. On the contrary, the higher crystallinity silica from RH would contains higher amount of Q4 silica (less Q3 and Q2 consequently) so the reactivity would be lower, In this sense, based on Figure 3.1 to 3.4, it can be concluded that there should be a relation between the silica crystallinity and their apparent reactivity. That is to say, the higher the crystallinity is, the lower the apparent reactivity would be. This could be confirmed by ^{29}Si solid NMR results, but we did not investigate this claim due to instrumentation limitation.

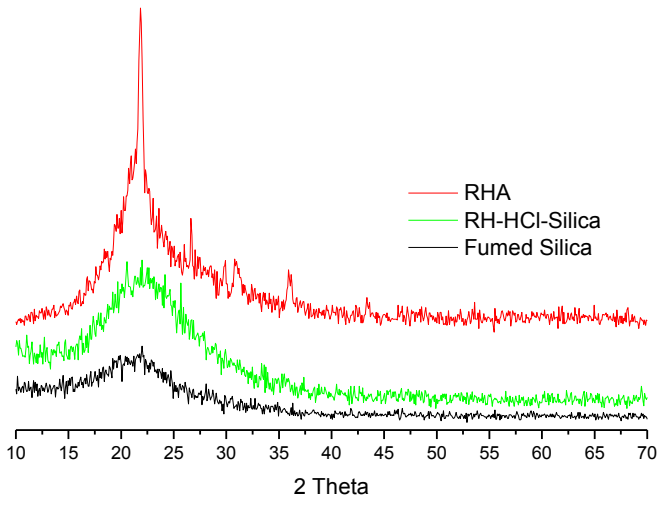

Figure 3.4 XRD patterns of RHA, RH-HCl-Silica, and fumed silica respectively. The pattern indicates that the degree of crystallinity increased from fumed silica, silica-RH-HCl, to RHA respectively.

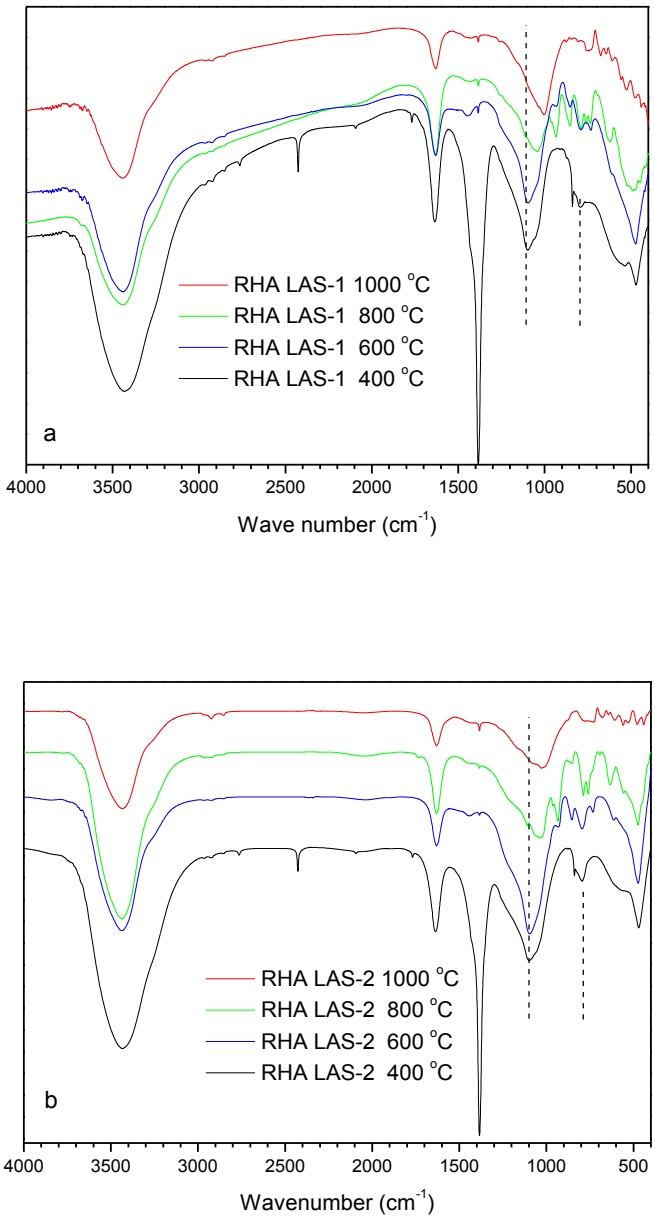

Figure 3.5 FTIR spectra of LAS samples prepared from RHA at various temperatures.

FTIR was conducted in order to investigate the structure change in the synthesis of LAS when calcined at different temperatures (Figure 3.5). FTIR was conducted using KBr pellets for RHA series as representative of the rest LAS samples. For both RHA

based LAS-1 and LAS-2 samples, there are strong broad bands between 1100-1000 cm^{-1}. Notice that the band shifted to a lower wave number region with increase of the calcination temperature from 400 °C to 1000 °C. This was attributed to the higher substitution of AlO_4 tetrahedra in SiO_4 tetrahedra unit.[256] Therefore, the characteristics band for Si-O-Si vibration changed to Si-O-Al^{IV} vibration with increase in temperatures. The results are consistent with earlier studies.[198, 257]

The medium strong bands between 800 cm^{-1} and 950 cm^{-1} are attributed to the characteristic absorption bands for AlO_6 octahedra with nonbridging oxygens.[252, 258] This band can be found in both the samples LAS-1 and LAS-2 that were calcined at 400–800 °C (Figure 3.5) while such bands were found missing in both the samples calcined at 1000 °C. This could be explained that at higher temperatures, AlO_6 octahedra changed to AlO_4 tetrahedra structure.[198]

The absorption between 720–780 cm^{-1} indicated the characteristic vibration of Al–O covalent bond in AlO_4 tetrahedra[256, 259-260] in β-eucryptite phase and β-spodumene phase of LAS-1 and LAS 2 respectively. The absorption band at around 675 cm^{-1} in LAS-1 was the characteristic band for β-eucryptite.[258] At around 420–480 cm^{-1}, the absorption band found in all the spectra was the characteristic band of Si–O–Si bending vibration in SiO_4 tetrahedra.[258-259] The characteristic absorption bands of β-eucryptite were found at around 670–685 cm^{-1} for the sample LAS-1 and the band at 565 cm^{-1} was due to the presence of β-spodumene. For sample LAS-2 calcined at 800–1000 °C, the characteristic absorption bands of β-spodumene was observed at 552 cm^{-1} accompanying with the characteristic band of eucryptite at 685 cm^{-1} (Figure 3.5b). The strong bands at 3300 cm^{-1} and 1640 cm^{-1} were attributed to hydroxyl group bending bands of water.[244] The band at

1385 cm^{-1} was due to the characteristic band of NH_4^+ for ammonium nitrate. This band was attributed to fact that during the sol preparation, Ammonium hydroxide was used to adjust pH value of the sol.[261] The above FTIR results are consistent with the crystallization results obtained from XRD characterization.

The microstructure properties of LAS-2 samples prepared from different sources of silica at 1000 °C were characterized by SEM since the crystalline phase were relatively better developed according to the XRD spectra (Figure 3.1−3.3). The SEM results are shown in Figure 3.6−3.8. The SEM images showed that the β-spodumene powders (as observed from XRD) were cobble-stone like morphology with multiple particle size distribution. From the SEM images of Figure 3.6−3.8, no distinguishable morphologies were observed for the three β-spodumene samples.

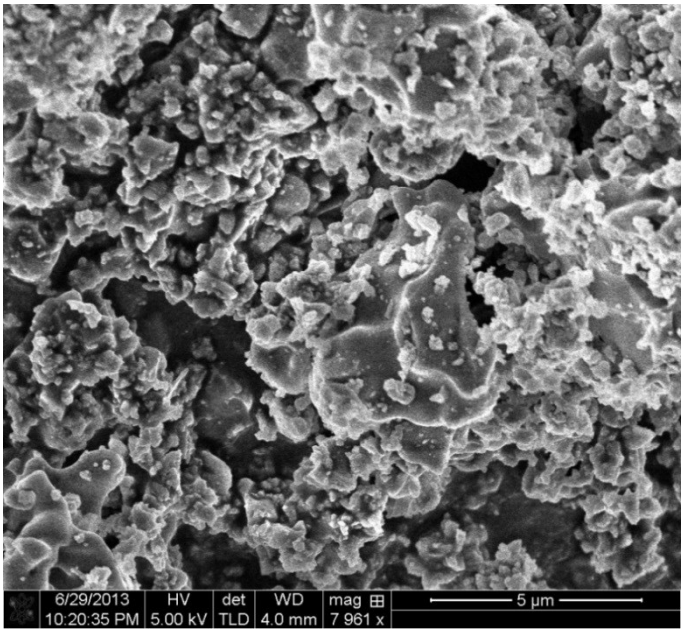

Figure 3.6 SEM image of LAS samples based on fumed silica. Sample (β-spodumene, $Li_2O•Al_2O_3•4SiO_2$) was prepared from calcination at 1000 °C for 2h.

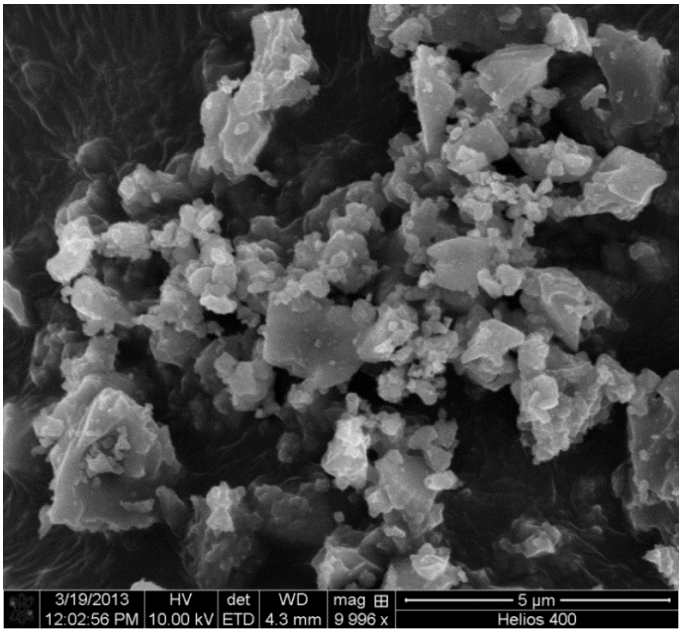

Figure 3.7 SEM images of LAS sample based on RH-HCl-Silica. Sample (β-spodumene, $Li_2O•Al_2O_3•4SiO_2$) was prepared from calcination at 1000 °C for 2h.

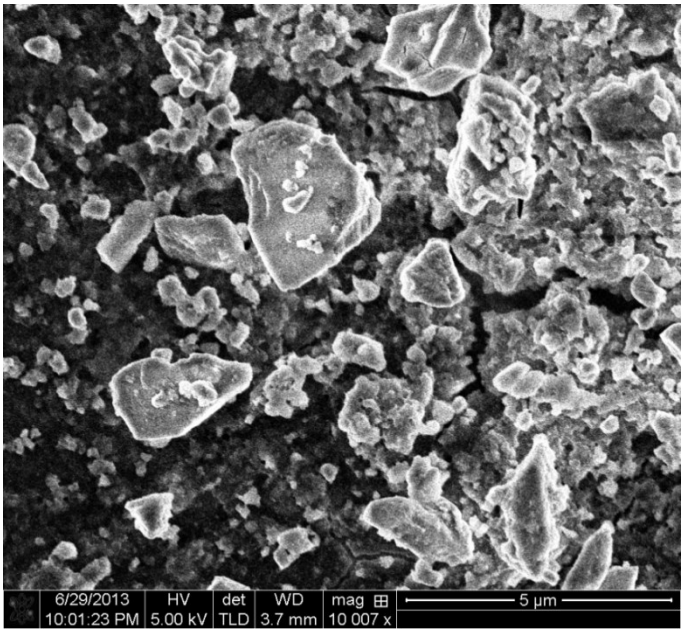

Figure 3.8 SEM images of LAS sample based on RHA. Sample (β-spodumene, $Li_2O•Al_2O_3•4SiO_2$) was prepared from calcination at 1000 °C for 2h.

3.4. Conclusions

In this study, LAS glass-ceramic powders were successfully synthesized from three different sources of silica namely fumed silica, RH-HCl-Silica, and RHA respectively. It has been shown that silica from HCl treated RH can be a good substituent material for fumed silica, which is more expensive in the synthesis of LAS powders through sol-gel method. Based on XRD characterization, silica from HCl treated RHs shows similar reactivity as that of fumed silica in LAS samples synthesis. When the reaction temperature is equal or higher than 600 °C, both series (fumed silica and RH-HCl-Silica) yield significant amounts of crystalline structure. On the contrary, RHA series shows the lowest reactivity among the three silica sources investigated in this study. For RHA series, LAS crystalline structure forms when temperature is higher than 800 °C. The apparent reactivity of the three different sources of silica is dependent on their surface area and crystallinity. According to the discussion on the different forms (Q4, Q3, and Q2) that existed in the silica derived from RH, the reactivity of the different silica could also be related to their crystallinity characterized by XRD, i.e., the higher degree of silica crystallinity will presumably result in the lower reactivity in the LAS synthesis.

CHAPTER 4

Platinum Nanoparticles Supported by Nanostructured Silica Derived from Rice Husks for Heterogeneous Catalysis Applications

4.1. Introduction

Noble metal nanoparticles that are immobilized on a substrate to serve as catalyst have been intensively studied for decades.[262-265] Researchers agree that the substrates of the noble metal nanoparticles play an important role in catalyst performance such as selectivity, stability, and activity.[266-268] For choosing proper substrates, two properties should be considered. First, is the chemical and thermal stability of the substrate during the catalysis reaction; second, is whether or not the substrate can accommodate the guest noble metal nanoparticles enough to allow formation of well dispersed and easily accessible catalytically active sites.[265-266] Various substrates for supporting noble metal nanoparticles, such as organic polymeric materials,[269] inorganic materials,[266] and organic/inorganic hybrid materials have been studied.[270] Among the previously mentioned supporting substrates, nano sized silica appear to be a good candidate, due to its thermal and chemical stability, high surface area, easy tunability and low cost.[265, 271]

Rice husk (RH) is a byproduct of rice milling. Currently, applications of RH have been very limited due to their tough nature and low nutritional value.[6-8] Thus RH is often considered as a biowaste. So far the most common methods of RH disposal are open field burning,[9, 12] which result in waste of energy, air pollution, and greenhouse gas emission. Therefore, a more economically benefiting and energy efficient use for RH is needed.

RH is mainly composed of lignocellulose (72-85%) and silica (15-28%).[12] According to our previous research, through a simple treatment, RH can be easily

converted to high purity, amorphous, and porous silica.[30, 46] Therefore, silica derived from RH has irregular morphology and rough surface. The surface area can be up to 280 m^2/g and the particles sizes can be around 50 nm. These properties make it a suitable substrate for novel metal nanoparticles based on the discussion above. In this study, our research goal is to utilize silica derived from acid treated RH which is thermally and chemically stable, has a rough surface and high surface area, amorphous and low cast to produce efficient catalysts for various chemical reactions.

As mentioned above, silica has been used to support metal nanoparticles to prevent agglomeration of the nanoparticles and maintain a high surface area of the catalytically active sites. Without silica as a support, the nanoparticles aggregate, which decreases their effectiveness as a catalyst.[266] So the ideal silica candidate should have a rough surface where the metal nanoparticles can settle well. Most silica in nature exists either in the form of quartz or quartz fragments (e.g. sand). Settling any type of metal nanoparticles on quartz would be difficult because of the perfect crystal structure of quartz, which results in very low specific surface areas on which a metal nanoparticle could stick. As a result, naturally occurring silica is not ideal for catalyst applications. A common method of producing silica nanoparticles in lab is through Stöber method using organosilane such as tetraethyl orthosilicate (TEOS).[272-273] However, the silica nanoparticles produced from TEOS are nearly perfectly spheres with a smooth surface, which in theory would be less ideal as a support for a metal nanoparticle catalyst, since a smooth surface would be less accommodative than that of rough one. In contrast, the silica nanoparticles produced from RH are imperfectly shaped and have many crevices where the metal nanoparticles can settle. As a result, it is hypothesized that the silica

derived from RH will be more effective than the TEOS silica in terms of supporting metal nanoparticles. This hypothesis was later supported in this work through a model reaction of 4-nitrophenol reduced by sodium borohydride into 4-aminophenol.

In order to use silica as a substrate for noble metal nanoparticles, one thing that needs to be considered is the relatively weak interaction between metal nanoparticles/metal precursor and silica surface, which makes it difficult to immobilize the metal nanoparticles on bare silica surface. Often the silica surface is functionalized with appropriate ligand, such as thiol, or amino group and then the guest noble metal nanoparticles get immobilized.[266, 274-275] In this study, the silica was surface modified by a coupling agent (3-aminopropyl)triethoxysilane (APTES) to introduce amino group on the surface, and then the platinum nanoparticles will be grown on the surface. Platinum was selected because of its excellent performances exhibited in various reactions.[266] It is worth mentioning that the platinum nanoparticles supported by nanostructured silica derived from rice husks for heterogeneous catalysis applications have not been previously reported. Confirmation of the hypotheses discussed above would increase the applications of rice husks.

4.2. Experimental

4.2.1. Materials & Methods

The raw RHs used in this study were obtained from Three H's LLC (Arkansas, USA). Concentrated hydrochloric acid (HCl, 37%), dihydrogen hexachloroplatinate(IV) hexahydrate ($H_2PtCl_6 \cdot 6H_2O$, 99.9%), 4-nitrophenol (4-Nph), sodium borohydride ($NaBH_4$), tetraethyl orthosilicate (TEOS), absolute ethanol, and ammonium hydroxide

(28%) were purchased from VWR. (3-Aminopropyl)triethoxysilane (APTES) was obtained from Sigma-Aldrich. All of the above chemicals were used as received.

4.2.2. Synthesis of silica from RH

RH Silica was synthesized according to the procedures developed in our previous research.[30, 46] In brief, RHs were first washed by deionized (DI) water to remove dirt and then dried in an oven at 90 °C overnight. The dried RHs were boiled in 5 wt % HCl solution for 2 hours followed by washing by DI water and drying in an oven at 90 °C overnight. RH silica was obtained by heating HCl-treated RHs in a box furnace at 700 °C for 2 hours in air. The yield silica was grinded in an agate mortar and pestle before surface modification.

4.2.3. Synthesis of silica from tetraethyl tetraethyl orthosilicate (TEOS)

As a control, another kind of silica nanoparticles were synthesized by hydrolysis of TEOS with aqueous ammonia, according to the reported Stöber method.[272-273] In a typical synthesis, 2.9 mL of TEOS, 3.8 mL of ammonium hydroxide (28%), 80 mL of ethanol, and 1.4 mL DI water were mixed under stirring in a 200 mL flask for 10 hours at room temperature. The solution was then centrifuged to separate the yield silica nanoparticles from the rest chemical mixture. The silica nanoparticles were washed and separated in about 10 mL ethanol three times. After washing the silica was redispersed in 7.5 mL of ethanol before surface modification.

4.2.4. Surface modification of silica

The silica prepared from RH and TEOS were both modified by (3-aminopropyl)triethoxysilane (APTES) in order to introduce the amino functional groups on their surface. In a typical modification, 2.0 mL of APTES and 0.1g of RH silica (or

1.0 mL of TEOS silica dispersion prepared in previous step) were added into 10.0 mL of ethanol and stirred for 12 hours at room temperature. The resulting APTES-modified silica was washed by ethanol and separated by centrifugation three times. At last, the APTES-modified silica was dispersed in 9.0 mL DI water for future use.

4.2.5. Synthesis of platinum nanoparticles (Pt-NPs) supported by silica

The APTES-modified silica were used as a supporting material for Pt-NPs. In a typical synthesis, 800 μL of 0.1M H_2PtCl_6 water solution was added to the dispersions of modified silica prepared from the previous step from both RH and TEOS respectively. Both samples were stirred for 24 hours at room temperature. After 24 hours of stirring, the solutions were centrifuged one more time to remove the excessive H_2PtCl_6 and the separated silica was then redispersed in 9.0 mL DI water to which 1.0 mL of 50 mg/mL $NaBH_4$ ethanol solutions were added (respectively). The mixture was stirred for another 24 hours at room temperature. The Pt-NPs supported by RH silica and TEOS silica were obtained by collecting the silica through centrifugation. The final products were stored in 10.0 mL DI water for future use.

4.2.6. Characterization

Transmission electron microscopy (TEM) images were taken on a JEOL 1200 EXII. Samples were prepared by depositing a drop of dispersion of nanoparticles on a copper grid. Scanning electron microscopy (SEM) images were acquired on a Leo 1530 VP field emission scanning electron microscope (FE-SEM). All Samples were sputter coated with a thin layer (ca. 3 nm) of Au/Pd prior to SEM imaging. X-ray diffraction (XRD) patterns were recorded using a Bruker D8 diffractometer with Bragg-Brentano

θ−2θ geometry (40 kV and 30 mA), using a graphite monochromator with Cu K_α (λ=0.1540 nm) radiation.

4.2.7. Catalytic reaction of reduction of 4-Nitrophenol

The reduction of 4-Nph by NaBH4 was chosen as a model reaction and UV-Vis was used to test the catalytic activity of the Pt-NP since this reaction has been previously studied and the UV behavior of the reaction has been well established.[269, 276-281] In a typical reaction formula, 51.0 mg of $NaBH_4$ dissolved in 3.3 mL DI water were added into 23 mL of 0.12 mmol/L 4-Nph solution. After mixing, the given amount of catalysts was added to facilitate the reaction. UV-Vis spectra were recorded at 1 min intervals to monitor the kinetic of the reaction. The absorption spectra of the solution were measured at the range of 250-550 nm. The rate constants of the reduction process were determined through measuring the change in absorbance at 400 nm as a function of time. The reaction process could also be conveniently visually observed as the 4-nitrophenol will slowly change color from bright yellow to colorless as the reaction goes on. In the absence of the catalyst, this reaction takes several hours or even days, but the reaction can be completed within a few minutes by using this catalyst. At the end of the reaction, the catalyst can be recovered for repeated use by centrifuging the reaction mixture.

4.3. Results and Discussion

Scheme 4.1 shows the overall procedure for the fabrication of the Pt-NPs supported by RH silica. The detailed procedures were described in the experimental section. Briefly, silica nanoparticles were prepared by calcining HCl treated RHs. Then the silica was surface modified by APTES to introduce amino group in order to improve the interactions between the metal precursors and the surface of RH silica. The silica-NH_2

functionality exhibits good capability not only for adsorption of platinum precursor H_2PtCl_6 onto the silica surface but also for immobilization of small Pt-NPs later on yielded. The surface modified RH silica was impregnated in the solution of platinum precursor H_2PtCl_6, followed by reduction by $NaBH_4$. Thus Pt-NPs supported by RH silica was prepared.

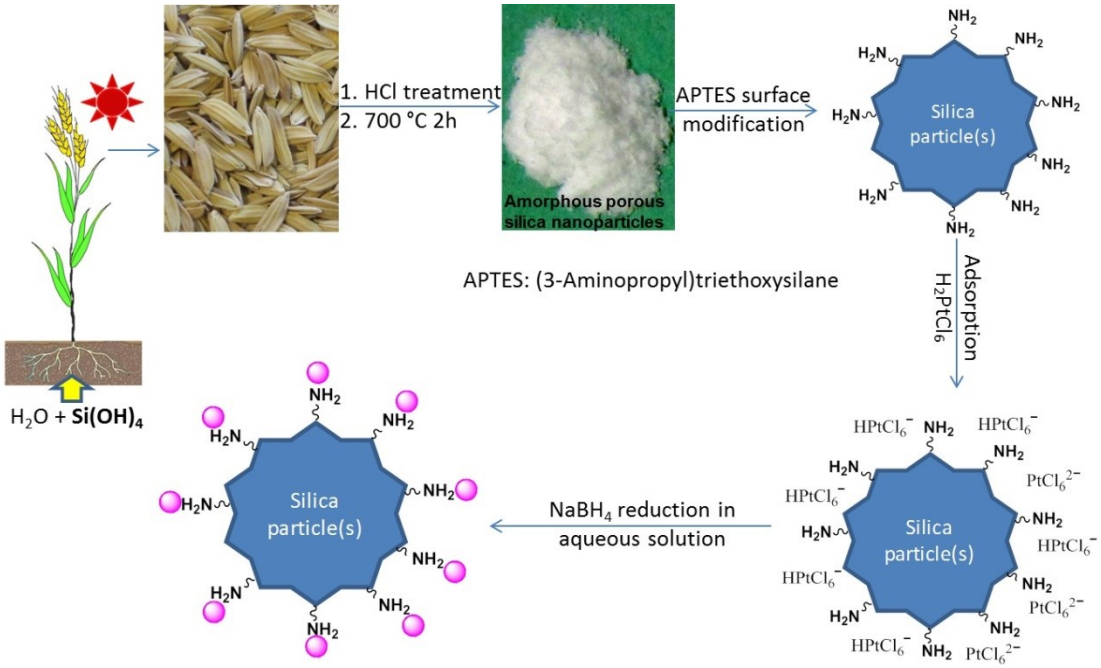

Scheme 4.1 Schematic illustration of synthetic procedure of Pt-NPs. Silica derived from RHs was used as substrate.

Silica nanoparticles and Pt-NPs supported by RH silica and TEOS silica were observed under the SEM and TEM. From the SEM images, it was easy to observe that the TEOS silica particles were uniform and spherical (Figure 4.1). In contrast, the RH silica particles were very randomly configured and lacked uniformity. This is consistent with our previous observations that RH silica particles were rough and had an irregular shape. These "perfect" TEOS silica particles are similar to that of other literature.[265, 276] The

images from the TEM also showed that the RH silica particles possessed very irregular geometries (Figure 4.2), and the TEOS silica particles were spherical and have a smooth surface (Figure 4.3). TEM images also showed that the platinum nanoparticles had grown on the silica (Figure 4.2, 4.3). Platinum is identified as small darker dots at 1-2 nm in diameter when viewed under the TEM. On images of the platinum catalyst supported on RH silica (Figure 4.2), many small dots with a diameter of 1-2 nm were individually present on the rough and irregular shape of the RH silica. That is to say, Pt-NPs are homogeneously distributed on the silica surface derived from RH. However, on the images of platinum catalyst supported on TEOS silica, less platinum particles were able to be clearly identified (Figure 4.3). Therefore, the platinum particles settled better on the RH-silica surface, due to the Pt-NPs morphological quality of TEOS and RH silica (Figure 4.2−4.3).

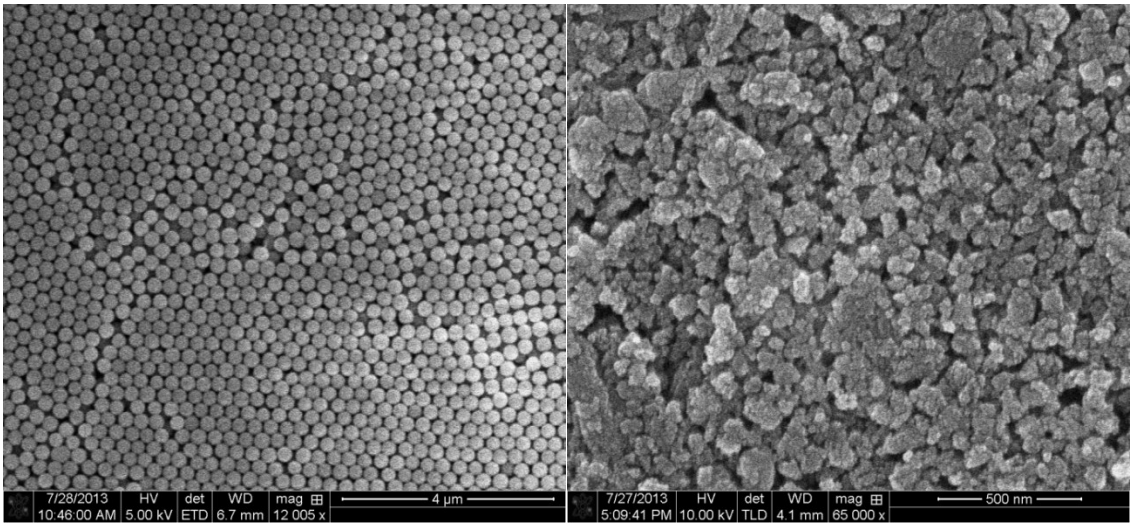

Figure 4.1 SEM images of TEOS silica (left) and silica from HCl treated RHs (right).

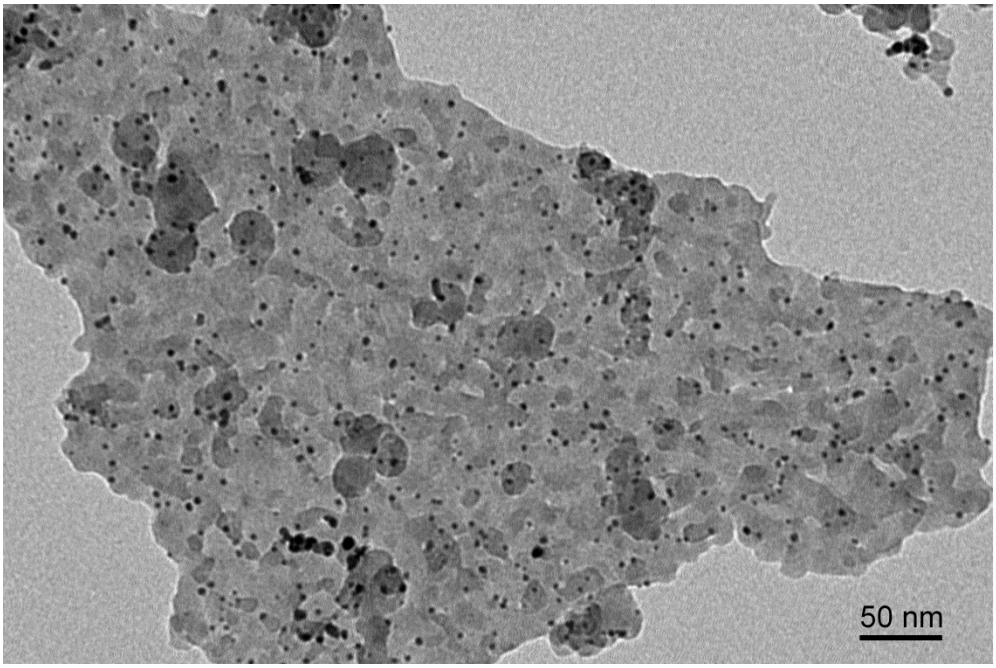

Figure 4.2 TEM image of Pt-NPs catalyst supported by APTES modified RH silica.

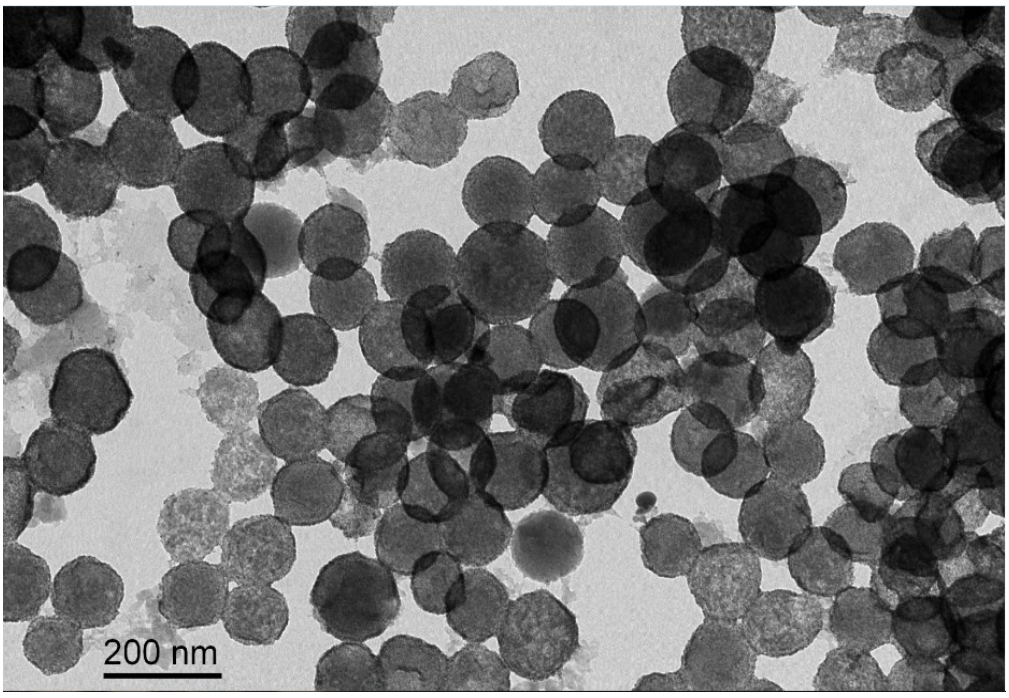

Figure 4.3 TEM image of Pt-NPs catalyst supported by APTES modified TEOS silica.

4.3.1. Reduction of 4-Nitrophenol (4-Nph) with sodium borohydride

Pt-NPs supported by RH and TEOS silica were tested as a catalyst for the reduction of 4-Nph by reducing agent $NaBH_4$. As shown in (Figure 4.4), an aqueous solution of 4-nitrophenol has a maximum absorption at 317 nm. The peak shifted immediately from 317 nm to 400 nm upon addition of $NaBH_4$, indicating the formation of 4-nitrophenolate ions.[279-281] This peak remains unaltered for hours without the present of the catalyst, which suggests that the reduction proceeds very slow in the absence of catalyst as reported in the literature.[277-281] After addition of Pt-NPs supported by RH silica, the absorption intensity of 4-Nph at 400 nm decreases gradually over time, meanwhile a new peak appears at ca. 300 nm, which is attributed to the absorption of 4-aminophenol (4-Aph) (Figure 4.5). Since the concentration of $NaBH_4$ added in the system is much higher (more than 22 equivalent times higher) than that of 4-nitrophenol, and it remains constant during the reaction, it is reasonable that the reduction rate can be assumed to be independent of $NaBH_4$ concentration. Thus, pseudo-first-order kinetics were used to evaluate the kinetic reaction rate of the current catalytic reaction. The ratio of C_t and C_0 was determined by the relative intensity of each absorbance A_t/A_0. Here C_t and C_0 are 4-nitrophenol concentrations at time t and 0, respectively; A_t and A_0 represent the absorbance at the time t and 0 of 4-nitrophenolate ion. Under above assumption and according to Arrhenius equation (not shown here), if the reaction temperature is kept the same, the plot of $\ln(C_t/C_0)$ vs. t (time) should be linear for pseudo-first-order kinetics. As expected, the linear relationships between and reaction time are observed, as shown in Figure 4.6. The rate constant (k) was estimated by using the slopes of straight lines

(Table 4.1). The rate constants observed in this work are similar to previously reported constants which are usually between 10^{-3} s^{-1} to 10^{-4} s^{-1}.[278, 280-281]

The effect of the amount of catalyst on the rate of the reaction was also investigated. As shown in Figure 4.6, the reduction of 4-nitrophenol exhibits a faster rate with an increasing amount of catalyst used. The rate constant increases linearly with the amount of catalyst, which is consistent to the results reported in the literature.[278, 281]

The reduction reaction can also be visualized by the color change of the solution. In order to compare the catalytic performance of RH silica and TEOS silica supported Pt-NPs catalyst, a simple demonstration has been conducted as the following: two disposable plastic cuvettes were each filled with 3.0 mL of 50 mg/mL sodium borohydride and 0.1 mL 0.01 M 4-nitrophenol, which was sufficient to show the distinctive bright yellow color. Then 0.1 mL of Pt-NPs catalyst supported by TEOS silica was added to one cuvette, while 0.1 mL of Pt-NPs catalyst supported by RH silica was added to the other. Pictures of both cuvettes were taken at time 0, 5, 10, and 15 min. From the images, it was easy to see that the reduction of 4-nitrophenol occurred much faster in the cuvette with Pt-NPs catalyst supported by RH silica, while the cuvette with Pt-NPs catalyst supported by TEOS silica showed slower change in color (Figures 4.7). This observation is consistent with the hypothesis that the silica derived from RH will be more effective than the TEOS silica in terms of accommodating metal nanoparticles.

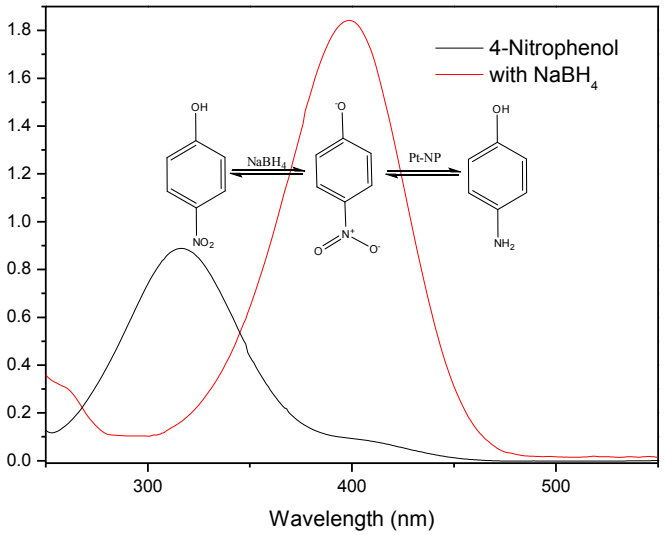

Figure 4.4 UV-Vis spectra for 4-nitrophenol in aqueous solution (left curve). The right curve was 4-nitrophenol mixed with NaBH4 solution.[278]

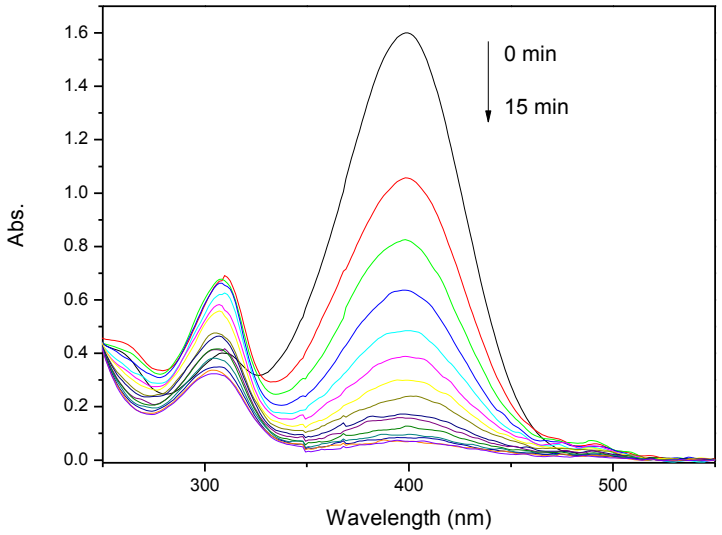

Figure 4.5 UV-Vis spectra of 4-nitrophenol and $NaBH_4$ mixture after adding Pt-NPs.

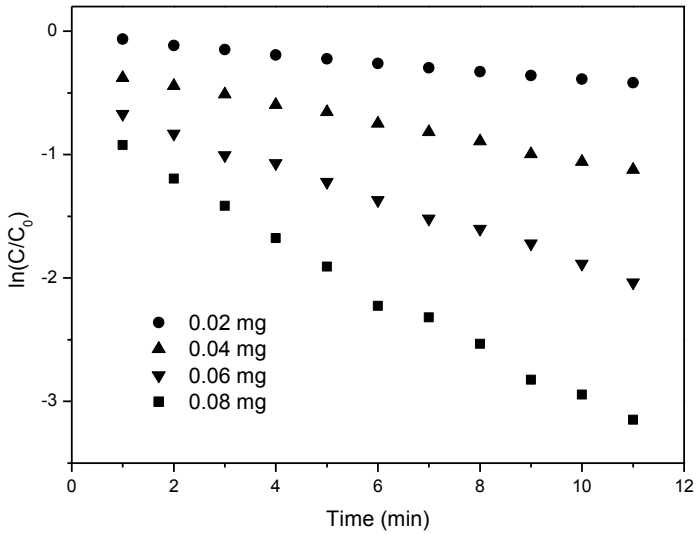

Figure 4.6 $Ln(C_t/C_0)$ vs. time for the reduction of 4-nitrophenol. Curves corresponding different amount of added Pt-NPs catalyst.

Table 4.1 Rate constant of the reduction reaction calculated from Figure 4.6.

Catalyst amount(mg)	0.02	0.04	0.06	0.08
Rate constant (s^{-1})	$5.8x10^{-4}$	$1.3x10^{-3}$	$2.2x10^{-3}$	$3.7x10^{-3}$

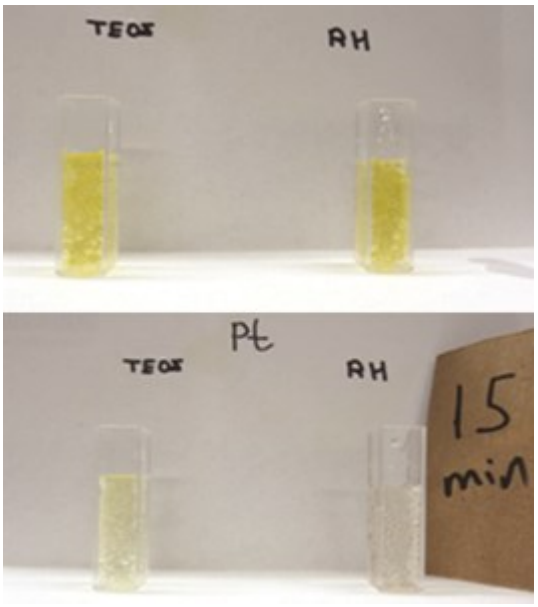

Figure 4.7 Reduction of 4-nitrophenol by $NaBH_4$, with Pt catalyst. TEOS silica and RH silica as Pt-NP substrate respectively; 0.06 mg Pt-NPs catalyst was used.

High resolution transmission electron microscopy (HRTEM) studies were conducted to further investigate the structure of the Pt-NPs catalyst supported on RH silica (Figure 4.8). HRTEM clearly shows that the Pt-NPs have been attached on the silica surface. Based on the image, a lattice constant was calculated. The results are consistent with that of platinum theoretical lattice constants.

Electron diffraction pattern of Pt catalyst supported with APTES modified RH silica was shown in Figure 4.9. The pattern shows that the majority of the matter is not crystalline phase. The Pt-NPs themselves remained their nature crystal property. XRD pattern (Figure 4.10) of the Pt-NPs supported by silica derived from RHs showed that after the attachment of Pt-NPs on the silica surface, the majority of the material is still in amorphous phase, which indicating that the metal portion was very low relative to the amorphous silica.

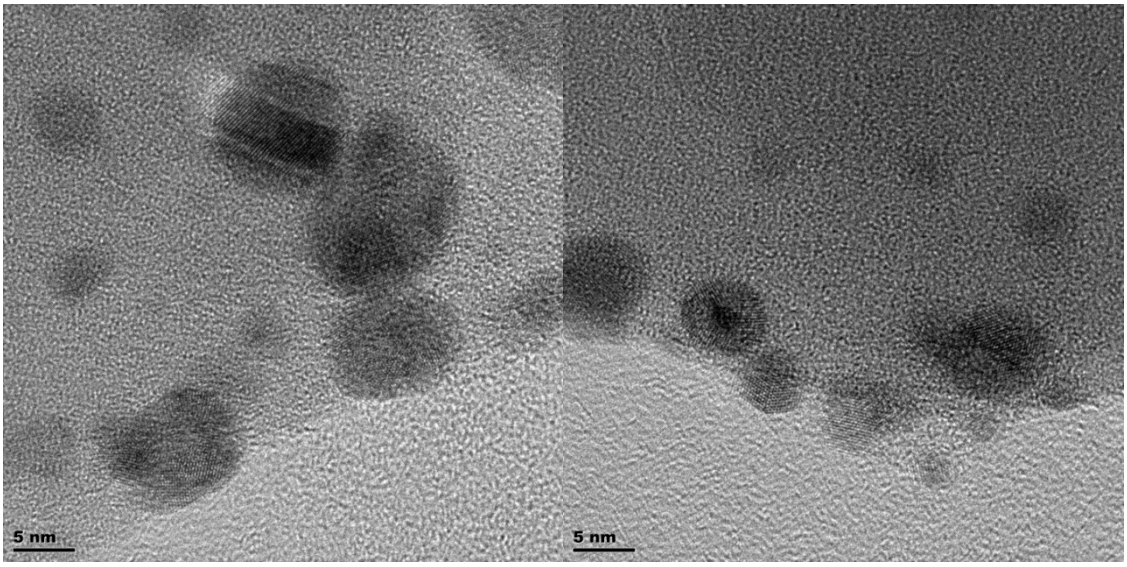

Figure 4.8 HR-TEM image of Pt-NPs catalyst. The Pt-NPs were supported by APTES modified RH silica.

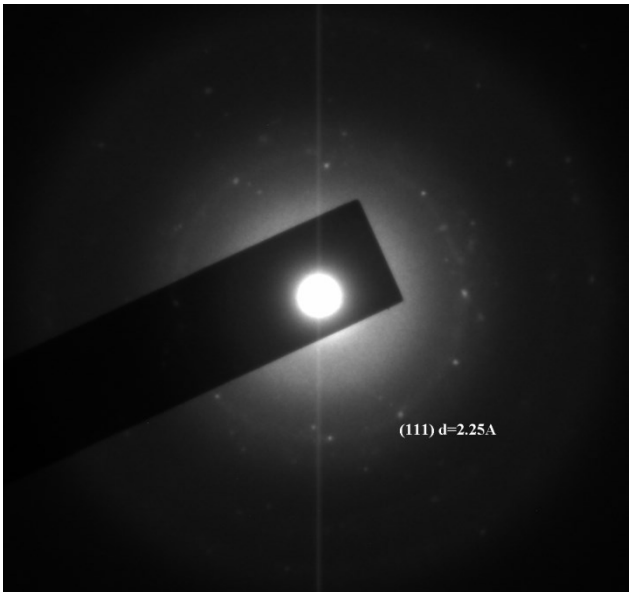

Figure 4.9 Electron diffraction pattern of Pt-NPs catalyst. The Pt-NPs were supported by APTES modified RH silica.

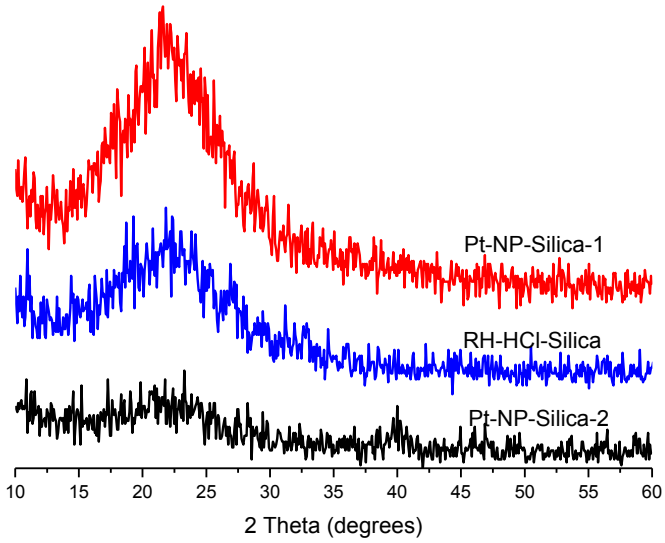

Figure 4.10 XRD patterns of the RH silica and RH silica supported Pt-NPs. Pt-NPs-Silica-2 has higher concentration of metal precursor (H_2PtCl_6) than Pt-NPs-Silica-1 in Pt-NPs preparing reaction.

4.4. Conclusions

In this study, Platinum nanoparticles (Pt-NPs) were attached on the surface of silica derived from HCl treated RHs by a facile method. The thus synthesized Pt-NPs have relatively narrow particles size distribution. The Pt-NPs size are about 2-5 nm range according to HRTEM image. The prepared RH silica supported Pt-NPs showed excellent catalytic performance in the reduction of 4-nitrophenol, which is much more effective than Pt-NPs supported on TEOS silica in the model reaction. It seems the modification of silica surface using APTES helped in the synthesis of Pt-NPs on RH silica surface. The work that we completed has made important advancements in the study for the use of rice husks, and may create a new field in the development of Pt-NPs heterogeneous catalysts by using RH silica as a support.

In brief, our work has clearly demonstrated that rice husks, a biowaste, can have unique applications in catalysis and replace expensive silica nanoparticles derived from TEOS. Such a process would allow us to convert a waste into a valuable material at a very low cost.

CHAPTER 5

Photoluminescent Silica Derived from Rice Husk Biomass

5.1. Introduction

In the past decades, silica based photoluminescent materials have inspired tremendous research efforts.[282-283] Silica based luminescent materials have widespread applications such as use in bioanalytical assays, labeling, chemical sensing, lighting, and drug delivery etc.[282-285] Sailor et al pioneered work in defect-related silica luminescent materials and their mechanisms.[286] The majority of luminescent silica materials have been chemically synthesized from alkoxysilanes.[283] Typically, metal activators or dyes are involved during the synthesis of luminescent silica as fluorescence sites.[282] Recently, fluorescent silica derived from rice husk (RH) has drawn some attention, because it can potentially be used as a sustainable, renewable energy source.[287-289] The fluorescent silica emits white photoluminescence (PL) under UV light irradiation at room temperature (RT). Such materials could be used as metal-free fluorescent materials, which have the advantage of being environmentally benign, chemically inert, and thermally stable, because they are essentially just silica networks.[287-291]

Rice husks are considered a biowaste of rice production. Globally, millions of tons of rice husk are produced every year.[207] Evidently the applications of RH have been very limited due to their tough nature and low nutritional value.[7-8] The most common disposal method so far is still open filed burning according to the study did by Manan et al.[9] The open field burning inevitably results in waste of energy, air pollution, and greenhouse gas emission.[12] If utilized properly, RH could be a good candidate of feedstock for silica based materials because of its high silica content (15−28 wt %) and

large availability.[12, 207] It is of great economical and environmental importance to find more beneficial and energy efficient uses for RHs. The development of carbon-incorporated luminescent silica from RH utilized both the silica and the carbon component. This direct method of preparing luminescent silica has the advantage of a simpler and faster procedure, and being free of toxic chemicals, when compared to the chemical method of preparing luminescent silica based materials.

Ishikawa et al. reported that white PL silica can be derived from thermally treated rice husk.[287-291] They found that the silica prepared from rice husk emitted strong white PL at RT under UV light irradiation. The PL spectrum of the luminescent silica derived from RH covers the entire visible wavelength range, and the PL curve shape is similar to that of sunlight. The PL spectrum is continuous with no separate sharp peaks on the curve. The rice husk used in their study had no pretreatment by any means. Several types of mineral impurities exist within silica; thus, the PL property of silica derived from RH may be affected, which complicated subsequent investigations and arguments in their reports.

To address this issue, we conducted a similar study, in which silica was prepared from RH. A series of silica samples were prepared from hydrochloric acid (5 wt %) pretreatment rice husk at the temperature of 550 °C for 2 hours in various flow rate of air. The study was intended to provide a better understanding of the mechanisms of the fluorescent silica derived from HCl treated rice husk. Microstructure, crystallinity, composition, and bonding state of the samples were investigated and characterized by various instruments. We observed a new phenomenon which is that on the PL spectra of the silica derived from acid treated RH, several prominent sharp peaks appeared which

presumably correspond to different defects structure in silica. The defect structures could be carbon substitutional defect,[286] oxygen deficiencies,[292] radical carbonyl defects,[292] chemical bond cleavage and resultant carbon formation etc.[293] That is to say, in silica derived from acid treated RH, contain more than one type of defect structures which are responsible for its overall luminescent property.

Overall, carbon-incorporated silica which is derived from rich husks is very likely to be a promising metal-free, low cost, and safe fluorescent material. Therefore, it is highly desirable to gain a better understanding the structure property relationship of the silica from RH to achieve optimal photoluminescence.

5.2. Experimental

The RHs used in this study were obtained from Three H's LLC (Arkansas, USA). Hydrochloric acid (37 wt %), phosphoric acid (85%), sodium dodecyl sulfate (SDS) were purchased from VWR and used as received.

The thermal treatment of rice husk involves two processes: pretreatment by hydrochloric acid and calcination in MTI OTF-1200X-III three zone tube furnace. An alumina crucible was used as the container during the thermal treatment. Typically the water-rinsed (to remove adhering soil and dust) rice husk, was mixed with a hydrochloric acid solution (5 wt %) and boiled for 2 hours to remove mineral impurities.Then, rice husks were dried at 90 °C for 24h and rinsed with deionized water 3 times. While in the calcination process, pretreated and dried rice husks were heated at 550 °C for 2 hours. The temperature raising rate was set to 10K/min until the temperature reached 550 °C, which is the best temperature for preparing fluorescence silica from RH according to our previous studies. The acid treatment was applied because of the concerns of the

possibility that PL may be influenced by the impurities such as K, Ca, S, Fe, Mn etc metal elements.[49, 288] In the meanwhile, acid treatment could help to preserve the amorphous feature of the silica in RH which means no silica phase transitions will happen. Different air flow was used, because the carbon residue in silica can be greatly affected by the calcination atmosphere.[46] Therefore, we collected various samples that contains different amount of carbon residues. Beside the air flow applied, the position of the crucible in tube would also affect the quality of silica product (Figure 5.1). Through practice, the air flow rate and the crucible position were carefully adjusted so that RH silica with different levels of carbon residue content could be prepared in a repeatable and controllable manner. Using this method, enough RH silica was collected for multiple preparations of PL silica. Due to the tube diameter limitation, only a small amount of RH silica can be made each time for one sample. Besides the tube furnace, a box furnace was also used to prepare luminescent silica samples.

PL measurements were performed at 365 nm UV light excitation at room temperature. The microstructural properties and compositions of samples were observed on a LEO 1530 VP field emission scanning electron microscope (FE-SEM) equipped with Energy-dispersive spectroscopy (EDS). X-ray diffraction (XRD) were recorded using a Bruker D8 diffractometer with Bragg-Brentano θ-2θ geometry (40 kV and 30 mA), using a graphite monochromator with Cu Kα (λ=0.1540 nm) radiation. The bonding state was estimated by X-ray photoelectron spectroscopy (XPS).

5.3. Results and Discussion

In order to investigate how carbon content is affecting the PL property of the silica from RH. A series of silica samples that contain different levels of carbon are

desired. Considering that oxygen content during the thermal treatment of RH could greatly affect the silica appearance, more specifically the unburned carbon residue in silica, we carefully designed a method that produced a series of silica samples that contain different levels of carbon residue which can be easily seen by the naked eye. This method is a combination of air flow rate and sample sitting position in the tube furnace during the treatment (Figure 5.1). Generally, the higher the air flow rate, the less carbon residue the sample will have. An exception is that, higher air flow will result in lower sample surface temperature, so it is possible that with a lower air flow rate, the sample carbon residue level is lower than that of higher rate air flow due to the latter will bring down the sample actual temperature, thus affected the calcination process. Another general rule about the sample preparation is that the further the sample sits from the air source, the greater the amount of carbon residue will be in the sample.

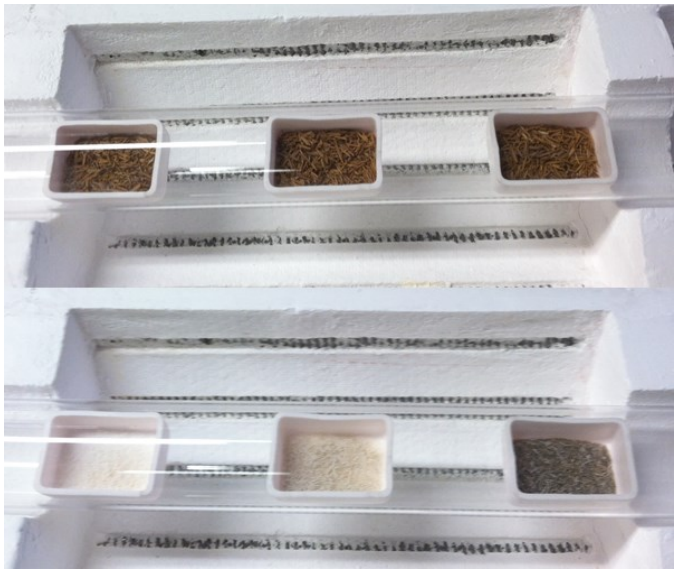

Figure 5.1 Silica samples preparation set-up under different air flow. Upper image is showing loaded RH sitting in the furnace; lower one is showing the appearance of the silica product after thermal treatment. Note that the sample which is further from the air source in the tube appears darker from higher carbon residue content.

Figure 5.2 to 5.6 presented the visual appearance of various samples under day light and UV light (365 nm) irradiation. Based on Figure 5.2 to 5.6 observations, it seems that the apparent fluorescence intensities under UV (365) mainly have to do with their carbon residue content in the silica samples, since except carbon residue, other impurities would have little difference in all the silica samples because the acid pretreatment could remove most of the mineral impurities in RHs.[30, 46] For instance, in Figure 5.2, all the samples were calcined in the batch same condition in a box furnace. According to the amount of the starting RHs, it can be roughly estimated that increasing the amount of starting RH will increase the carbon residue in the sample, given the assumption that the air is static during the calcination. The final product appearance verified the above estimation. In Figure 5.2, upper row showing that the 4g RH silica is darker than the 1g RH silica, indicating 4g RHs silica contains higher carbon residue. While under UV (365 nm), it clearly showed that 4g RH silica gives the highest fluorescence intensity, and the rest fluorescence intensity goes 3g>2g>1g. In Figure 5.3 and 5.4, the starting RHs amounts were all set to be 1 g. All the sample were put in furnace at the sample time at 550 °C, then the individual crucibles were taken out at a preset time. We predicted that the longer the calcination time, the lower the carbon residue. The final product appearance in Figure 5.3 and 5.4 were consistent with the prediction. In Figure 5.3, the apparent fluorescence intensity of each RH silica goes 0.5h<1.0h<1.5h<2.0h. In Figure 5.4, the apparent fluorescence intensity of each RH silica goes 2.0h>2.5h>3.0h>3.5h. Based on Figure 5.2, 5.3 and 5.4, we concluded that too much or too little carbon residue content in RH silica will both decrease the sample fluorescence intensity. There should be

an optimized carbon residue level in RH silica under which the RH silica will give the strongest fluorescence intensity.

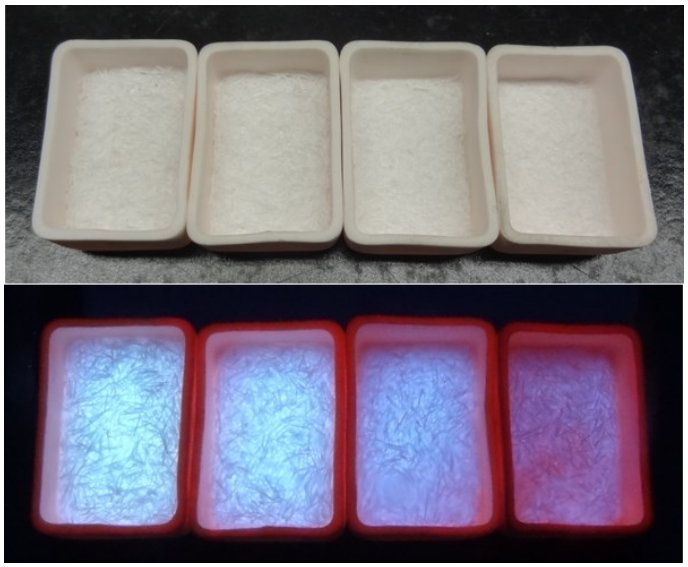

Figure 5.2 Silica prepared from acid treated RH at 550 °C for 6h in box furnace. Starting RH loading from left to right: 4g, 3g, 2g, 1g; Upper row was showing the appearance of silica product under day light; lower row was showing the apparent fluorescence intensity under UV (365 nm) The red color was from the crucibles.

Figure 5.3 Silica prepared from acid treated RH at 550 °C in box furnace. Each crucible had 1g starting RH; calcination time from left to right, 2.0 h, 1.5 h, 1.0 h, 0.5 h; upper row was showing the appearance of silica product under day light; lower row was showing the apparent fluorescence intensity with UV (365 nm) The red color was from the crucibles.

Figure 5.4 Silica prepared from acid treated RH at 550 °C in the box furnace. Each crucible had 1g of RH; calcination time from left to right, 2 h, 2.5 h, 3 h, 3.5 h; upper row shows the appearance of the silica product under day light; lower row shows the apparent fluorescence intensity with UV (365 nm) The red color was from the crucibles.

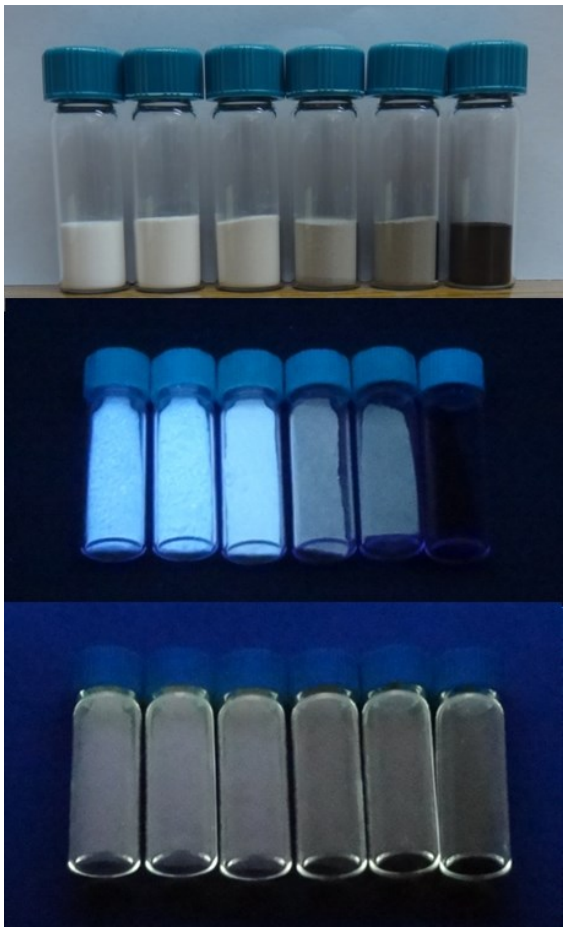

Figure 5.5 Silica prepared from acid treated RH at 550 °C in tube furnace. Middle row showing the PL properties of RH silicas with 365 nm UV; bottom row was with 254 nm UV.

Note that the samples in Figure 5.5 were prepared in a tube furnace so that the air flow rate can be carefully tuned to have the carbon residue content in final RH silica to be reliable between different batches of operation. The other conditions like starting RH amount, calcination temperature and time are same to all samples in Figure 5.5. As shown in the photo, the six samples appear gradually darker from left to right indicating a gradually increase of the carbon residue levels. In order to make the discussion easy to follow, those samples were labeled at RH-Silica-C1 to RH-Silica-C6. The code C1 refers to the least carbon residue content sample, it appears to be the whitest sample (the most left RH silica in the top row Figure 5.5). The code C6 refers to the highest carbon residue content sample and corresponding to the darkest RH silica (the sample farthest to the right in the top row of Figure 5.5). Figure 5.5 shows that all samples emit a similar intensity light when excited under 254 nm UV (bottom row). The fluorescence was much stronger under 365 nm UV (middle row). The PL properties were quantitatively measured by PL spectrometer for RH-Silica-C1 to RH-Silica-C6 samples (Figure 5.7).

Figure 5.7 shows that the fluorescence intensity under UV (365 nm) is decreasing with the increasing of carbon residue content (in a sequence of RH-Silica-C1 to RH-Silica-C6). Another feature of the PL spectra curves are the small prominent sharp peaks located at 400 nm, 500 nm, 600 nm, and 700 nm respectively. This feature may indicate that in RH silica, there are different types of structures (centers and defects).[283, 286, 289, 294-295] This is to say, more than one type of defect or mechanism might exist simultaneously in the RH silica. Multiple defects or mechanisms that co-exist can be regarded as intrinsic features that only exist in RH silicas. Also, it is possible that this feature also has to do

with the RH types itself. This phenomenon has never been reported before to our knowledge.

X-ray photoelectron spectroscopy (XPS) is a surface-sensitive quantitative spectroscopic technique that can measure elemental composition, empirical formula, chemical state, and electronic state of an element that exists in a material. For better understanding of the fluorescence mechanism, XPS measurements focusing on carbon elements are needed. The XPS tests are being collected by one of our collaborators in Shanghai, China. XRD results shows there are little differences among this series of samples, i.e., all the samples are amorphous silica, and the degree of crystallinity is similar, see Figure 5.8.

During the investigation of this work, two side experiments were carried out to explore the PL properties of different RH silicas. First, we found the PL intensity of RH silica was significantly enhanced after used H_3PO_4 to soak HCl treated RH for 24 h before preparing the RH silica (Figure 5.6). Second, we found the PL intensity of RH silica was enhanced by simply mixing RH silica with a small amount of SDS (16 wt %) in aqueous dispersion and then dried (data not shown here). This is very interesting since they may indicate new mechanisms that have never been report before either. We did not further investigate this trend, due to the time frame of this study.

Figure 5.6 Silica prepared from HCl and H3PO4 treated RH at 550 °C. Calcination time was 2 h; from left to right, each 1g HCl treated RH was soaked by 8 M, 0.8M, 0.08M, 0 M H_3PO_4 for 24 h; Upper row shows the appearance of silica product under day light; lower row shows the apparent fluorescence intensity with UV (365 nm) The red color was from the crucibles.

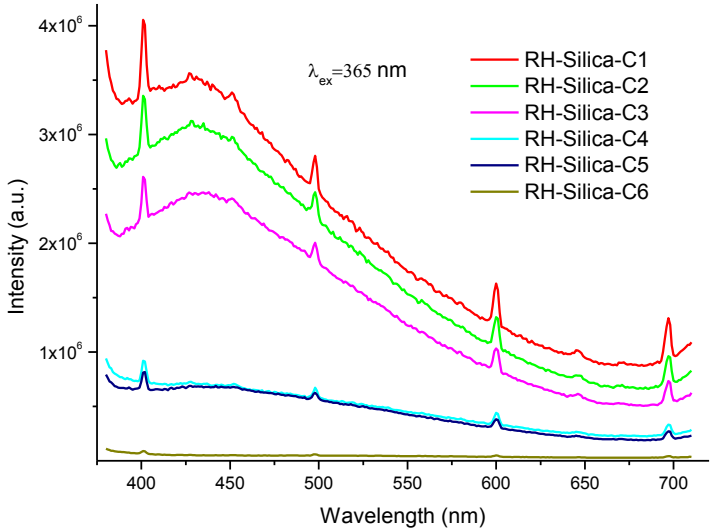

Figure 5.7 PL spectra of silica prepared from acid treated RH in a tube furnace. Samples were calcined at 550 °C for 2 h.

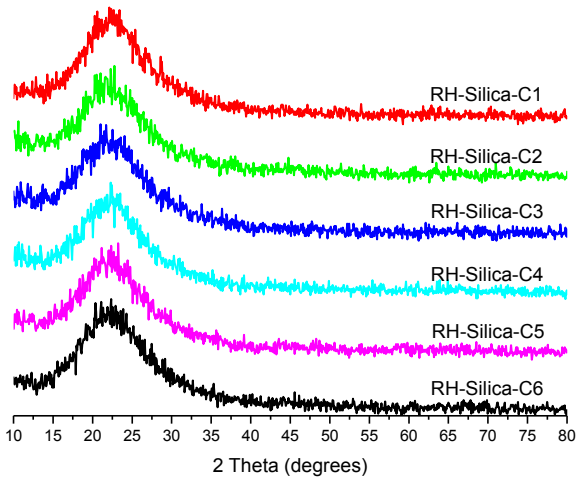

Figure 5.8 XRD pattern of the silica prepared from acid treated RH in a tube furnace. Samples were calcined at 550 °C for 2 h.

More studies showed that the position of the prominent sharp discrete peaks on RH silica PL spectra shift as a function of excitation wavelength. Figure 5.9 and 5.10 clearly showed that when the excitation wavelengths increase, the small peaks at emission PL spectra shift to higher wavelengths. More experiments are needed to fully understand this phenomenon.

Figure 5.11 includes more PL spectra results showing that the carbon residue content are relating to the PL intensity. The letters A, B, and C in sample id indicate their position in tube furnace, i.e., A, B, C corresponding to the three samples in Figure 5.1 bottom image, from left to right. The numbers in sample id indicate the air (or nitrogen) flow rate, and the letter N means thermal treated in nitrogen. For example, A50 means sample A was made under 50 ml/min air flow rate. A50N means the sample A50 was thermal treated again in nitrogen under 50 ml/min flow rate. From Figure 5.11, it can be

concluded that after the RH silica sample is prepared, further thermal treatment with nitrogen did not change the PL properties of those silicas significantly.

SEM images are shown in Figure 5.12 for three RH silica samples prepared from acid treated RHs under different conditions. No substantial morphology difference was observed among the three fluorescent RH silica samples. The particles sizes are in the range of 50 nm to 400 nm.

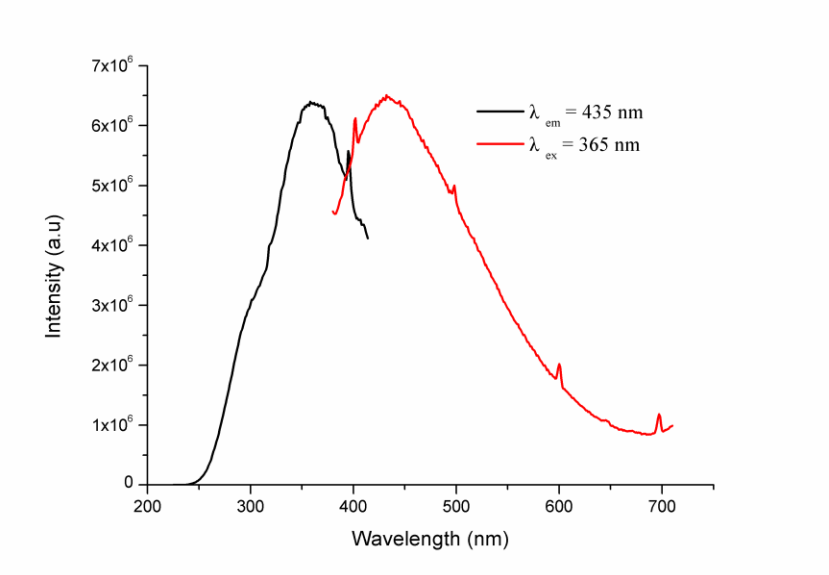

Figure 5.9 PL spectra of silica prepared from acid treated RH. Samples were calcined at 550 °C for 6 h in a tube furnace.

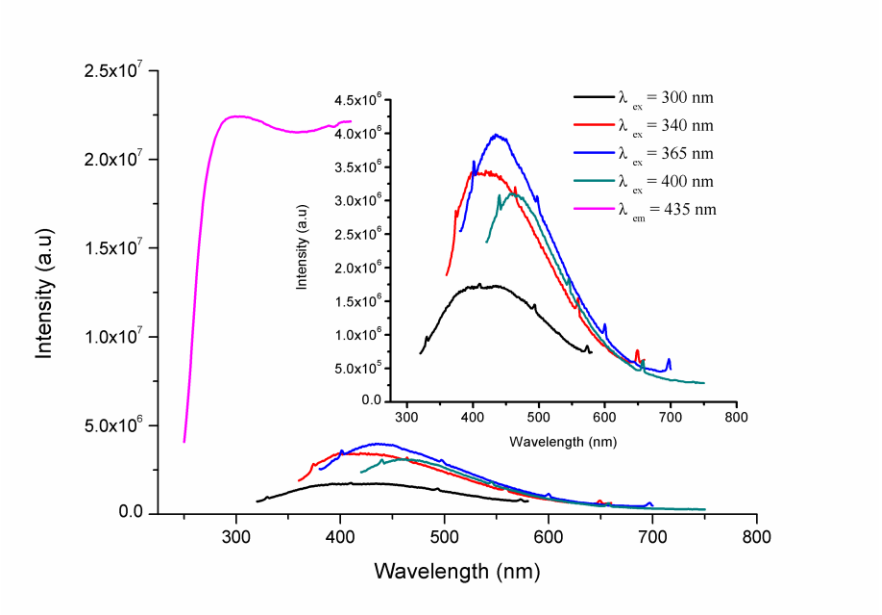

Figure 5.10 PL spectra of silica prepared from acid treated RH. Samples were calcined at 550 °C for 6 h in a tube furnace.

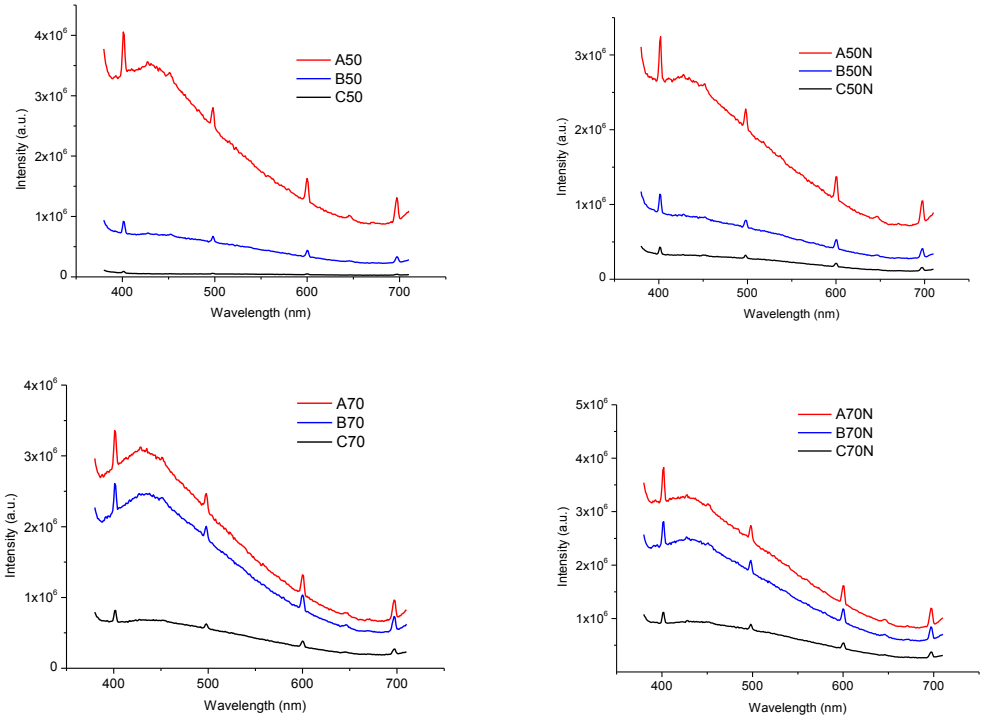

Figure 5.11 PL spectra of silica derived from HCl treated RHs. Left column, silica derived at different air flow; right column is treated with nitrogen atmosphere after the silica preparation. Note: The meaning of samples id is defined at page 123.

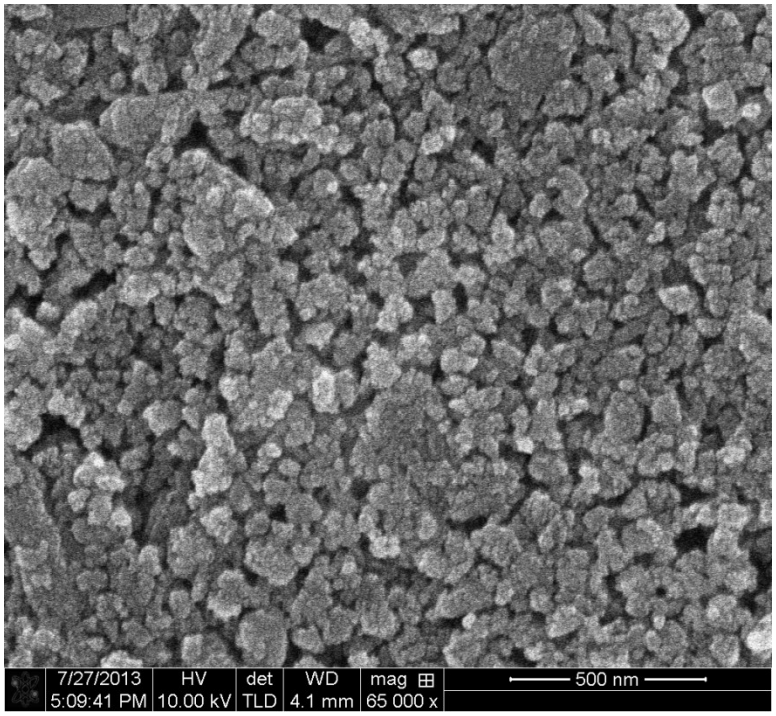

a) SEM image of RH-700-2 silica

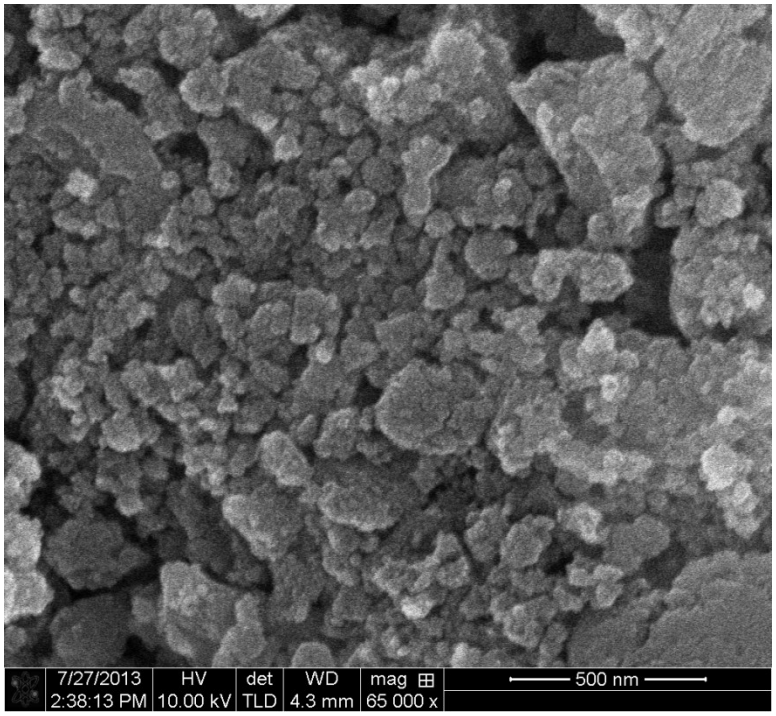

b) SEM image of RH-Silica-C1

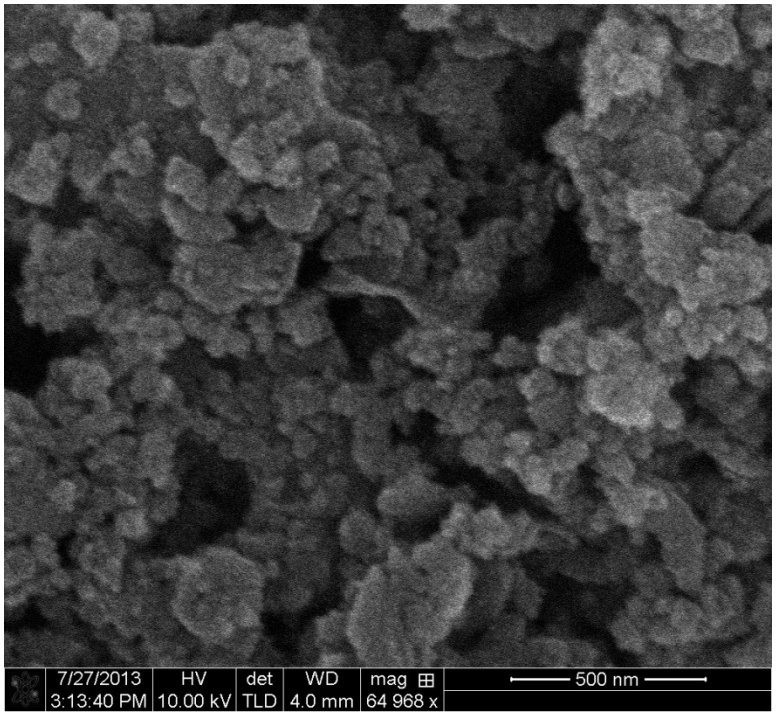

c) SEM image of RH-Silica-C6

Figure 5.12 SEM images of various RH silicas prepared from acid treated RHs.

5.4. Conclusion

Photoluminescent silica derived from HCl treated rice husks has been prepared at various conditions. The Photoluminescence properties of the silica were investigated by PL spectrometer, XRD, and SEM. XPS and elemental analysis are being collected by one of our collaborator in Shanghai, China. The intensities of some of the specific samples were strong enough to be viewed by naked eye in daylight under 365 nm UV light excitation at room temperature. More than one mechanism for PL (centers or defective structures) in this strained carbon doped silica network exists according to the characterization results in this study. It is believed that the PL correlates with the strained

silica that changes the energy gap and could cause the PL shift from the UV-blue range to the visible range.

Our study may provide rice husk with another promising application: being a raw photoluminescence material. The photoluminescent silica could be applied for wall materials, cosmetics, and tooth bleaching, because the silica is a low-cost and stable material and contains no toxic materials. More studies are needed to better understand the structure properties relationship of the luminescent silica derived from acid treated RHs.

CHAPTER 6

Ceramic Pigment Synthesis Based on Silica Derived from Rice Husk

6.1. Introduction

The global milled rice production in 2012 is estimated to be 489.1 million tons (>700 million tons for paddy rice).[207] As a byproduct of rice milling, there was ca. 160 million tons of RH was generated solely from the production of paddy rice in 2012. Evidently the applications of RH have been extremely limited due to their tough structure and low nutritional value.[7-8] The most common disposal method so far is open field burning, according the study by Manan and coworkers.[9] Open field burning of RH results in waste of energy, air pollution, and greenhouse gas emission.[12] RH could be a suitable candidate of feedstock for silica based materials because of its high silica content (15−28 wt %) and large availability.[12, 207] There have been reports on utilizing and converting RH biomass into useful materials. Wang et al. harvested high purity and amorphous silica through the calcination of acid treated RH under various conditions.[30, 46] Sun and coworkers studied the comprehensive utilization of RH by extracting lignocellulose from RH by Ionic liquid (IL) and preparing high quality silica from the RH residue after IL extrication.[12]

Ceramic pigments are important industrial materials that can be used to introduce color into ceramic materials and glazes. Both natural and synthetic pigments are manufactured and marketed to be used as a colorant in decorative and protective coatings. Generally pigment powders used for coloring ceramics require thermal and chemical stability at high temperature and must be inert to molten glass etc.[296] In order to reduce the cost of pigment production, research efforts have been conducted and new

technology, such as rotative furnaces, and new raw materials have been discovered.[296-297] A lot of industrial wastes were also evaluated by researchers to be used as raw materials to prepare ceramic pigments, such as the metal-ions containing sludge, chromium-rich tannery waste, and titania-rich slag etc.[298-300] The utilization of those waste materials satisfied the sustainable development and environmental demand which is becoming increasingly important.[296] Besides industrial waste, Bondioli et al. utilized agro-waste to prepare ceramic pigment.[301] Rice husk ash (RHA), which is a byproduct of calcination of non-treated RH, is utilized as the silica precursor in order to prepared yellow Pr-$ZrSiO_4$ pigment. Inspired by Bondioli's pioneer work, various ceramic pigments have been prepared by using RHA as a silica precursor, such as vanadium doped $ZrSiO_4$ (blue and green),[197] Praseodymium doped ZrSiO4 (yellow),[302] iron doped ZrSiO4 (red/coral),[296] and $Ca_3Cr_2Si_3O_{12}$ (victoria green)[303] ceramic pigments. However, each of the three groups listed above were using RHA instead of silica from acid treated RH as precursor to prepare ceramic pigments. No other work has used this method, since the five papers published by three different groups. It is worth mentioning that silica derived from acid treated RH has never been used in the ceramic pigment preparation so far.

There are issues associated with using RHA as a silica precursor in ceramic pigment preparation. The most important issue is that the final pigment prepared from RHA, can have unexpected color (details see session 6.3). Due to the lack of pretreatment, the quality of RHA is always low in terms of appearance and purity. RHA usually appears grey, because it contains carbon residue. The pigment color will be affected by the grey color of RHA or by impurities in RHA. RH silica quality has been intensively discussed in our previous works.[30, 46] Due to the partial crystallization of

RHA, there is little to no advantage of having larger surface area and reducing the energy consumption in pigment production compared to natural silica. In order to address this issue, the following experiment was conducted.

The high purity, amorphous silica derived from acid treated RH has a wider range of application than the crystalline quartz in naturally occurring silica.[13] In chapter three we discussed that amorphous silica has a similar reactivity to that of fumed silica and can be an ideal substituent for fumed silica in lithium aluminum silicate synthesis. Therefore, it is also worth trying to use silica derived from acid treated RH in the synthesis of ceramic pigments. Our goal is to determine whether there are substantial advantages to using silica from acid treated RH in pigment synthesis. As the control, quartz silica and fumed silica were used in this study. To our knowledge, this is the first attempt to use the silica derived from acid treated RH in ceramic pigment preparation.

Three zirconia silicate based pigment (total four colors) were prepared in this studied, because they were first commercially introduced and they are the most classical and widely used ceramic pigments since their discovery in 1960s.[197, 304]

6.2. Experimental

Zirconium (IV) oxide (ZrO_2), vanadium(V) oxide (V_2O_5, 98+%), sodium fluoride (NaF, 99%), sodium chloride (NaCl), praseodymium (III,IV) oxide (Pr_6O_{11}), silicon(IV) oxide (SiO_2, 99.5%) in crystalline form, hydrochloric acid (37 wt %) were all purchased from VWR and used as received. Fumed silica was obtained from Evonik Industries Corp. (Aerosil®155).

Silica from acid treated RH was prepared according to the procedure descried in our previous work.[30, 46] DI water rinsed RH was dried in an oven at 90 °C for 24 hours

and then refluxed in a round bottom flask with 5 wt % hydrochloride acid solution for 2 hours. Then, the acid treat RH was rinsed with DI water and dried at 90 °C in oven. The silica was derived from calcination of the dried acid treated RH in a box furnace in static air at 700 °C for 2h. The silica yield by this method had very high purity, which was up to 99.80% pure.[12]

Ceramic pigments were produced by following established formula in the literature[197, 301, 305] and were concluded in Table 6.1 and 6.2. Table 6.1 applies to all of the color formulations. Table 6.2 applies to each color pigment formulation. After measuring proper amounts of chemicals, the raw reactants were mixed together with a small amount of acetone (1−2mL) and grinded thoroughly in an agate mortar and pestle. Next, the grinded pigment mixture was placed in a crucible with lid and placed in a box furnace for thermal treatment. Furnace temperature raising rate was set to be 10 °C/min. The calcination time was 5h for all samples. Calcination temperature was set to 1050 °C, 950 °C, and 850 °C respectively in order to study the temperature effect on pigment formation. After calcination, the product was grinded and used for various characterizations. Fumed silica and crystalline quartz were also used as silica precursor as control groups to prepare ceramic pigments.

X-ray diffraction (XRD) characterizations were recorded using a Bruker D8 diffractometer with Bragg-Brentano θ-2θ geometry (40 kV and 30 mA), using a graphite monochromator with Cu Kα (λ=0.1540 nm) radiation. The microstructures properties and compositions of samples were observed on a LEO 1530 VP field emission scanning electron microscope (FE-SEM)) equipped with energy-dispersive spectroscopy (EDS).

6.3. Results and Discussion

Figure 6.1 shows an illustration of various ceramic pigment preparation processes. The photos on left side show the reactants mixture after grinding in agate mortar and pestle. The chemicals in the middle refer to the components in the formula. The photos on the right side show the ground pigment products. In this study, a total of four colors were prepared and studied which are yellow, blue, green, and red/coral as seen in Figure 6.1 right side.

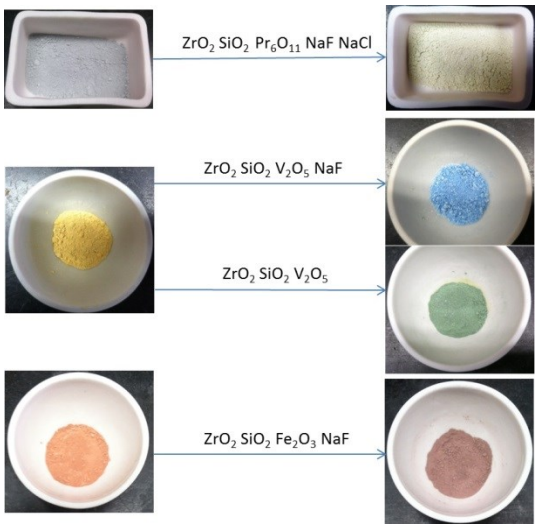

Figure 6.1 Photo illustration of various ceramic pigment preparations. All the samples were calcined at 950 °C for 5h in a box furnace in static air; photos on the left side show the ground reactants mixture; the chemicals in the middle refer to the components in the formula; photos on the right side show the ground pigment products.

Table 6.1 Pigment main components content.

Chemical	ZrO_2	SiO_2
Weight (g)	0.3075	0.1800

Table 6.2 Other components of the pigment according to each color.

Color	Green	Blue		Red		Yellow		
Chemical	V_2O_5	V_2O_5	NaF	Fe_2O_3	NaCl	Pr_6O_{11}	NaF	NaCl
weight (g)	0.01950	0.01950	0.0229	0.0500	0.0370	0.0410	0.0211	0.0370

Figure 6.2 shows the vanadium doped green pigments prepared from using RHA and RHS-700-2h as silica precursor respectively. It is shown that not only was the color of the reactant mixtures different, but the color of the final product pigments were different when using various silica precursors. Figure 6.2 and Figure 6.3 indicate that using RHA as starting material in pigment preparation, can results in an unexpected product color. Though unexpectedness is not necessarily a bad thing in research, it could be a disaster in the manufacturing of ceramic pigments. RHS-700-2 and RHA are essentially the same cost, but could results in completely different products (qualified vs. defect).

Figure 6.3 shows the images of the actual samples of RHS-700-2 and RHA, (left) and pigments prepare from calcination at 1050 °C for 5h using RHA and RHS-700-2 as precursor. The middle four pigments supposed to be blue, red, yellow, and green which can be seen in the right image contains pigments started from RHS-700-2. Due to the quality of RHA, none of the four colors turned out as expected.

Figure 6.4 shows images of the four color pigments prepared from calcination at 1050 °C, 950 °C, 850 °C for 5 hours using RHS-700-2 silica precursor. The best color quality was developed when the reaction temperature was 1050 °C for each silica precursor which can be seen in the photo on the left in Figure 6.4.

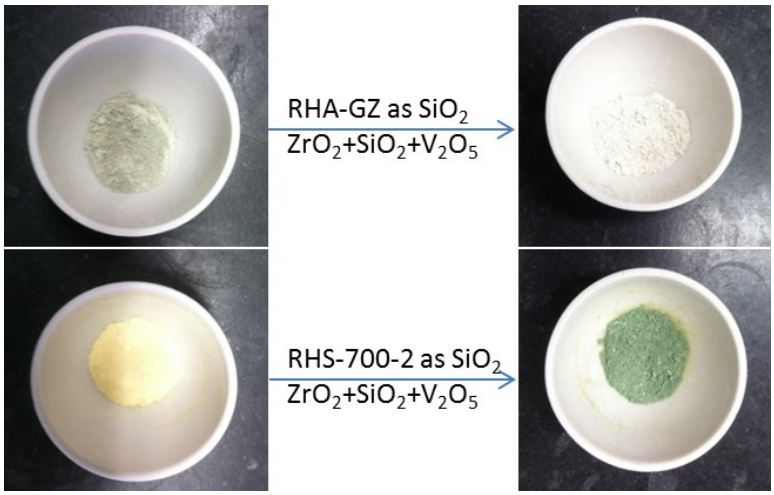

Figure 6.2 Photo illustration of green pigment from RHA and RHS-700-2 silica. The two samples were calcined at 950 °C for 5h in a box furnace in static air; left side photos show the ground reactants mixture; the chemicals in the middle refer to the components in the formula; photos on the right side show the ground pigment products. Note: RHA-GZ silica is grey in color while RHS-700-2 is pure white.

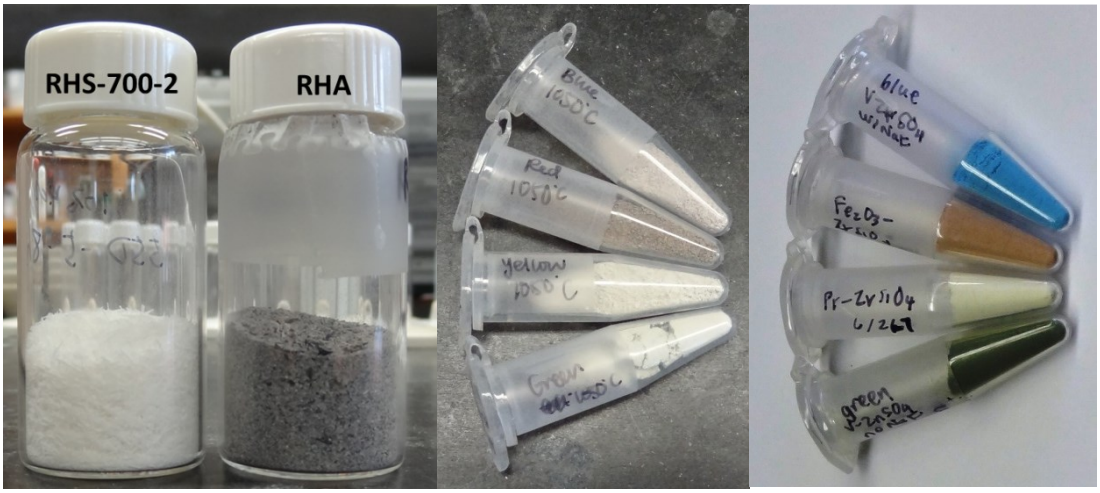

Figure 6.3 Photo images of RHS-700-2 vs. RHA and corresponding ceramic pigments. Ceramic pigments were made from RHA (middle four tubes), and RHS-700-2 (right four tubes). All pigments prepared at 1050 °C for 5h using corresponding silica precursor.

Figure 6.4 Photo image of ceramic pigments prepared from RHS-700-2. Samples were made at 1050 °C, 950 °C, 850 °C (left to right) for 5h using RHS-700-2 as the silica precursor.

As discussed in chapter 3, the crystallinity of the silica may affect their reactivity, thus we concluded that the apparent reactivity of silica derived from acid treated RH is similar to that of fumed silica and the silica from acid treated RH can be an ideal substituent for fumed silica in lithium aluminum silicate synthesis. To study the ceramic pigment preparation using different silica sources, a series of samples were prepared at different temperature. The silica source was commercial crystalline quartz, silica from acid treated RH (RHS-700-2h), and fumed silica (Aerosil®155). RHA was not chosen for reasons discussed in introduction section. Figure 6.5 shows the XRD pattern of commercial quartz and silica derived from acid treated RH. It is clear that the RHS-700-2 is amorphous and the degree of crystallinity can be ignored relative to crystalline silica. Figure 6.6 is the standard XRD pattern for quartz and zirconia silica respectively. Figure 6.6 is used to help to identify the crystalline phase in the final pigment products. For instance, in Figure 6.7, for the sample that was prepared at 1050 °C 5h using fumed

silica, the crystalline phase was identified as zirconia silicates (majority), baddeleyite (minor), monoclinic ZrO_2 (minor) and cristobalite (minor) according to Figure 6.6 and literature.[197, 306-307] Figure 6.8 is XRD pattern comparison of various pigments prepared from calcination at 950 °C for 5h. All the peaks were nominalized based on each sample's most intensive peak. Yellow and red/coral pigments prepared at 950 °C were not sufficient to convert the reactants into zirconia silicate according to the intensity of two ZrO_2 peak located at 2 theta 28 and 31 degrees. For blue and green color, the $ZrSiO_4$ crystalline phase was dominant indicating that the temperature was enough for both reactions to happen.

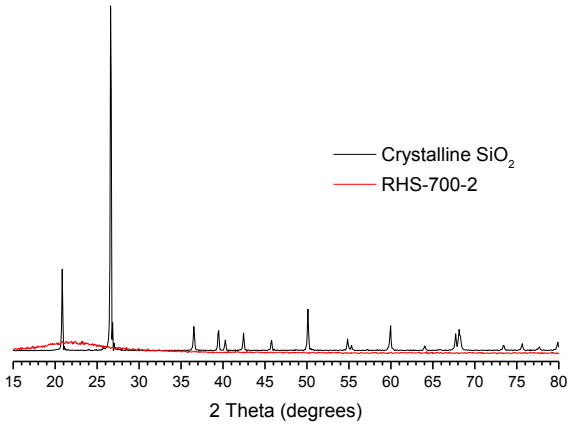

Figure 6.5 XRD pattern comparison of RHS-700-2 and commercial crystalline SiO_2.

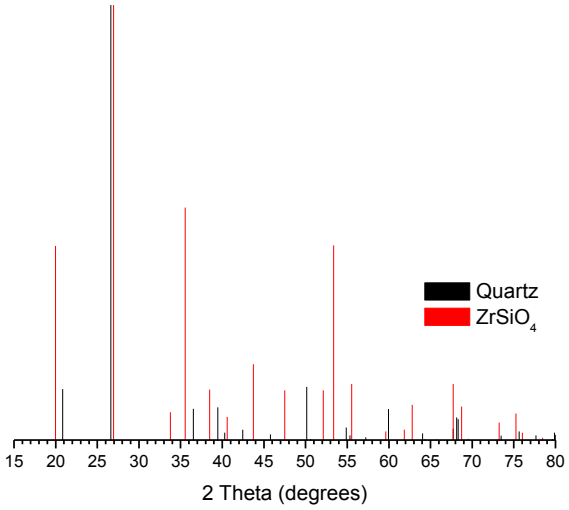

Figure 6.6 Standard XRD pattern of Quartz (PDF#85-0798) and ZrSiO4 (PDF#71-0991)

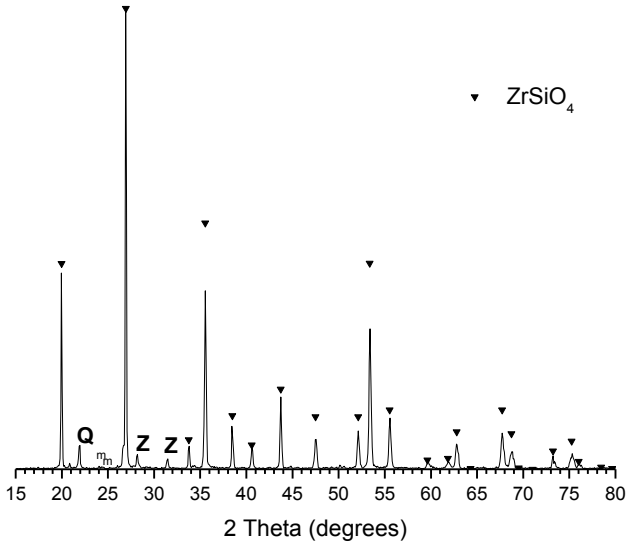

Figure 6.7 XRD analysis for fumed silica based V-ZrSiO4 (green) sample. Sample was prepared at 1050 °C for 5 h; Z, baddeleyite (ZrO_2), m, monoclinic ZrO_2; Q, cristobalite (SiO_2).[197, 306]

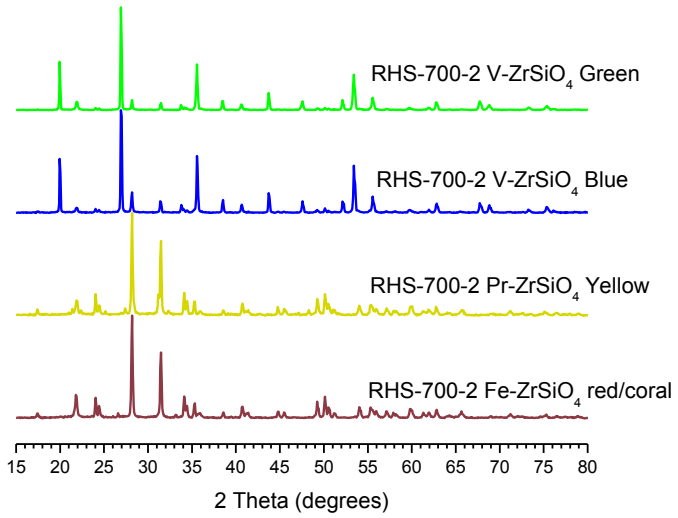

Figure 6.8 XRD patterns of different color pigments. Samples were prepared at 950 °C for 5h.

Figure 6.9, 6.10, and 6.11 are XRD patterns of vanadium doped blue pigment prepared using fumed silica, RHS-700-2, and quartz silica as precursor from the calcination at 1050 °C, 950 °C, and 850 °C for 5h respectively. All the peaks were nominalized based on each sample's most intensive peak. Based on the relative peak intensity of the cristobalite, monoclinic ZrO2, baddeleyite, and as well as the $ZrSiO_4$ major peaks (2 theta degrees at 20, 27, 35.5), it can be concluded that, the apparent reactivity of fumed silica is the highest; the RHS-700-2 has similar reactivity to the fumed silica; both apparent reactivity of fumed silica and RHS-700-2 are higher than that of quartz silica. The different apparent reactivity from the three sources of silica in this pigment synthesis presumably has to do with their surface area and crystallinity. For fumed silica and silica from acid treated RH, the surface areas are in hundreds of square meters per gram, but the crystallized quartz silica has a surface area of less than ten square meters per gram.[12, 255] As discussed in previous literature,[255] the contacting area

between reactants is proportional to the reactivity, and reactants' surface area will directly affect the contacting area between them. So the higher the reactant's surface area, the higher the reactivity would be. The results in Figure 6.9, 6.10, and 6.11 support this statement. Also, it has been shown that the silica from acid treated RH has higher degree of crystallinity than fumed silica (Figure 3.4), and both have much lower crystallinity than commercial crystalline quartz (Figure 6.5). The crystallinity of silica could affect its reactivity, because lattice energy has to overcome as additional activation energy in a reaction compared to the amorphous silica. So the higher the crystallinity the silica is, the lower the reactivity will be. The results in Figure 6.9, 6.10, and 6.11 support this statement.

Regarding the difference in silica reactivity, it may also directly relate to its intrinsic structure. It has been discovered that, there are mainly three forms of silica exist in RH, namely Q4 [$*Si(OSi)_4$], Q3 [$(OH)*Si(OSi)_3$], and Q2 [$(OH)_2*Si(OSi)_2$], all of which can affect crystallinity.[81] That is to say, an increase in the portion of the Q4 form of silica, increases the silica's crystallinity, which is shown by NMR and XRD results in the same paper.[81] Thus, higher crystallinity of silica contains greater portion of Q4 silica; and lower crystallinity of silica contains less portion of Q4 silica (more Q3 and Q2 consequently). Considering that in the synthesis of pigments, the Q4 form of silica would be much less reactive than that of Q3 and Q2 forms silica. Therefore, it can be concluded that silica that has high crystallinity, would contain greater amounts of Q4 silica (less Q3 and Q2 consequently) and the reactivity would be lower. On the contrary, the lower crystallinity silica contains less portion of Q4 silica (more Q3 and Q2 consequently), which would increase reactivity. In this sense, based on Figure 6.9, 6.10, and 6.11, it can

be concluded that there should be a relation between the silica crystallinity and their apparent reactivity. That is to say, the higher the crystallinity is, the lower the apparent reactivity would be. This could be confirmed by ^{29}Si solid NMR results, but we did not investigate this claim due to instrumentation limitation.

It was concluded that for blue V-$ZrSiO_4$ pigment, the reaction temperature lower than 950 °C would be insufficient in terms of $ZrSiO_4$ conversion for the reaction. Figure 6.11 indicates that the dominant crystalline phase was still ZrO_2.

Based on the XRD characterization, some reactions were not fully completed in terms of $ZrSiO_4$ crystals forming which means to call the final product as $ZrSiO_4$ would not be appropriate. But for convenience, in this chapter, the name of $ZrSiO_4$ was used simply to describe the final product, not necessary mean the final product is $ZrSiO_4$.

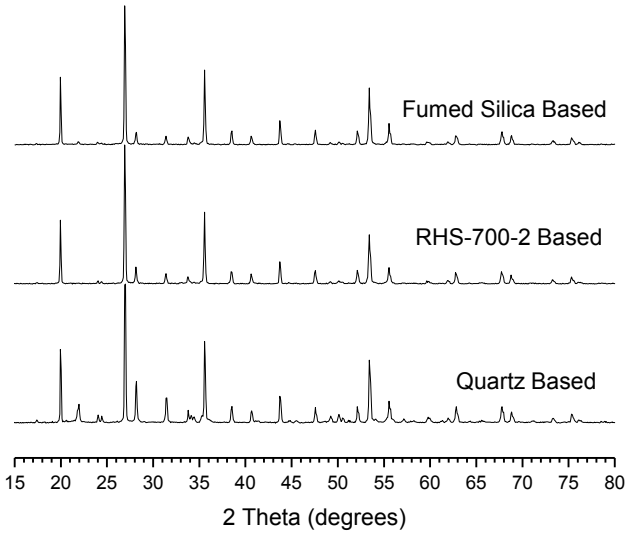

Figure 6.9 XRD patterns of blue pigment prepared at 1050 °C. Calcination time was 5h. Fumed silica, RHS-700-2, and Quartz were used as the silica precursor.

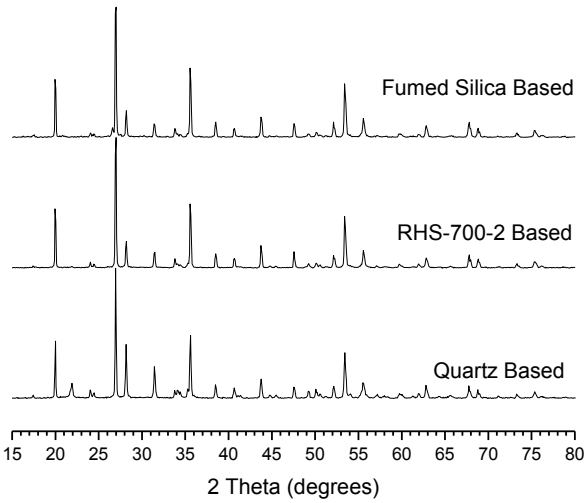

Figure 6.10 XRD patterns of blue pigment prepared at 950 °C. Calcination time was 5h. Fumed silica, RHS-700-2, and Quartz were used as the silica precursor.

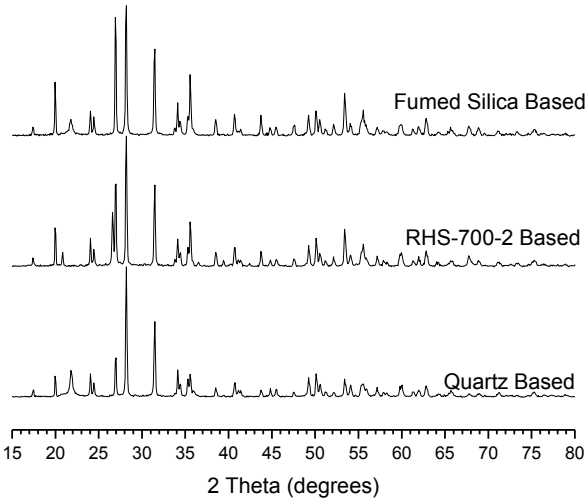

Figure 6.11 XRD patterns of blue pigment prepared at 850 °C. Calcination time was 5h. Fumed silica, RHS-700-2, and Quartz were used as the silica precursor.

Figure 6.12, 6.13, and 6.14 are XRD patterns of vanadium doped, green pigments prepared from fumed silica, RHS-700-2, and quartz silica as a precursor calcined at 1050 °C, 950 °C, and 850 °C for 5h respectively. All the peaks were nominalized based on each sample's most intensive peak. The results in Figure 6.12, 6.13, and 6.14 support the above discussion of apparent reactivity. For the reaction temperature it was concluded that for green V-$ZrSiO_4$ pigments, the reaction temperature is sufficient even at 850 °C in terms of $ZrSiO_4$ conversion. Figure 6.12 indicates that the dominant crystalline phase was $ZrSiO_4$.

For apparent reactivity of different silica precursors, the results in Figure 6.15, 6.16, 6.17 and Figure 6.18, 6.19, 6.20 still consistent with the discussions for the Figure 6.9, 6.10, and 6.11. Regarding the reaction temperature, it seems that for yellow Pr-$ZrSiO_4$ pigment, 1050 °C was not high enough in terms of $ZrSiO_4$ conversion. Figure 6.15 shows that even for the sample using a fumed silica precursor, no significant crystalline of $ZrSiO_4$ was detected. For the red/coral Fe-$ZrSO_4$ pigments, temperatures lower than 1050 °C would be insufficient for all silica precursors in terms of $ZrSiO_4$ conversion for the reaction. Figure 6.18 shows that for fumed silica and silica from acid treated RH precursor, 1050 °C was enough for the conversion of $ZrSiO_4$, but was not enough for quartz silica.

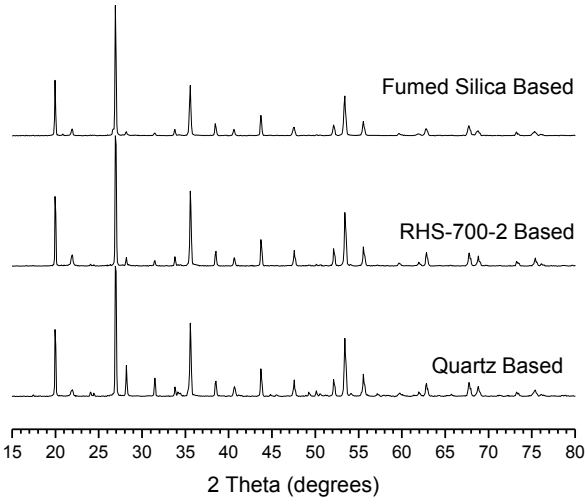

Figure 6.12 XRD patterns of green pigments prepared at 1050 °C. Calcination time was 5h. Fumed silica, RHS-700-2, and Quartz were used as the silica precursor.

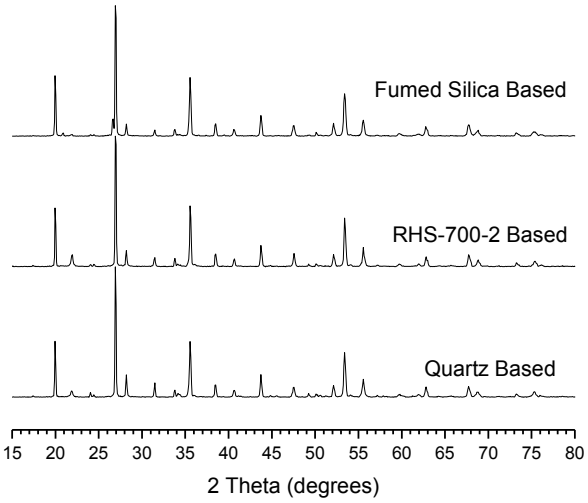

Figure 6.13 XRD patterns of green pigments prepared at 950 °C. Calcination time was 5h. Fumed silica, RHS-700-2, and Quartz were used as the silica precursor.

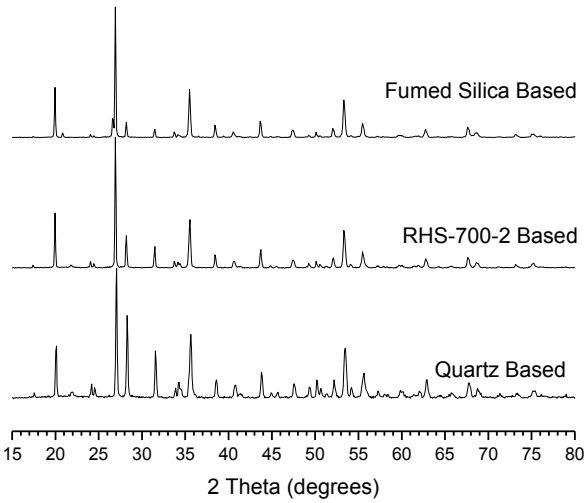

Figure 6.14 XRD patterns of green pigments prepared at 850 °C. Calcination time was 5h. Fumed silica, RHS-700-2, and Quartz were used as the silica precursor.

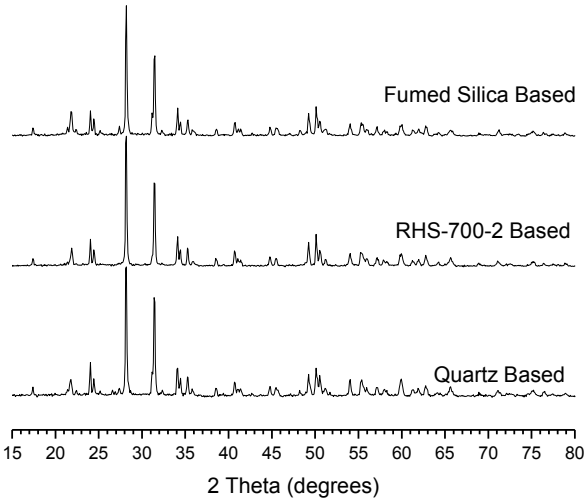

Figure 6.15 XRD patterns of yellow pigments prepared at 1050 °C. Calcination time was 5h. Fumed silica, RHS-700-2, and Quartz were used as the silica precursor.

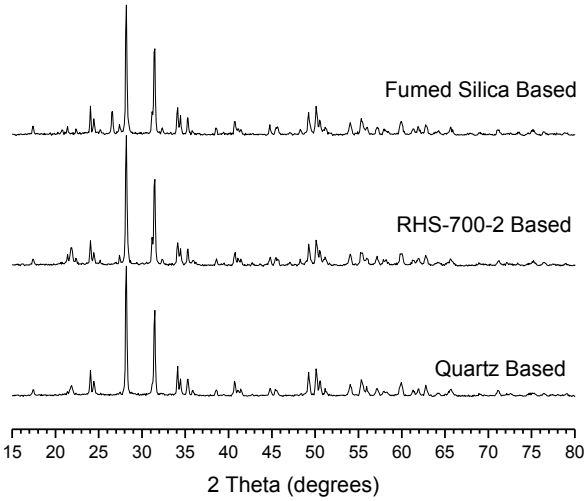

Figure 6.16 XRD patterns of yellow pigments prepared at 950 °C. Calcination time was 5h. Fumed silica, RHS-700-2, and Quartz were used as the silica precursor.

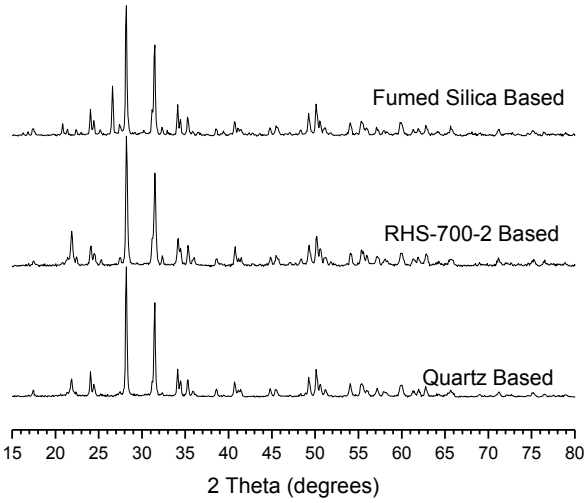

Figure 6.17 XRD patterns of yellow pigments prepared at 850 °C. Calcination time was 5h. Fumed silica, RHS-700-2, and Quartz were used as the silica precursor.

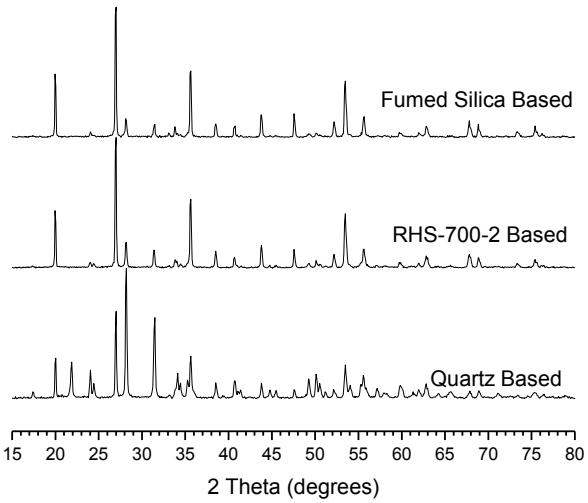

Figure 6.18 XRD patterns of red/coral pigments prepared at 1050 °C. Calcination time was 5h. Fumed silica, RHS-700-2, and Quartz were used as the silica precursor.

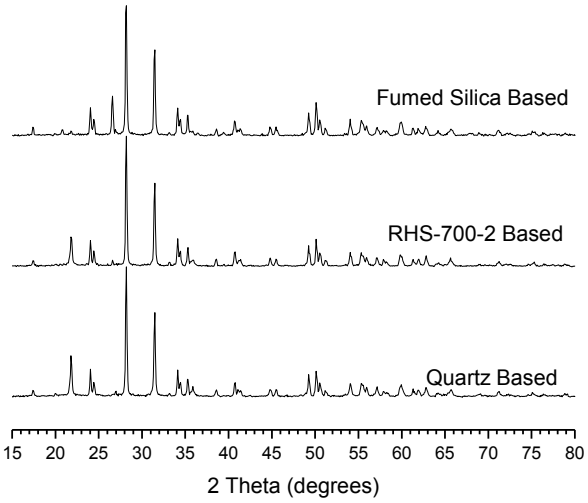

Figure 6.19 XRD patterns of red/coral pigments prepared at 950 °C. Calcination time was 5h. Fumed silica, RHS-700-2, and Quartz were used as the silica precursor.

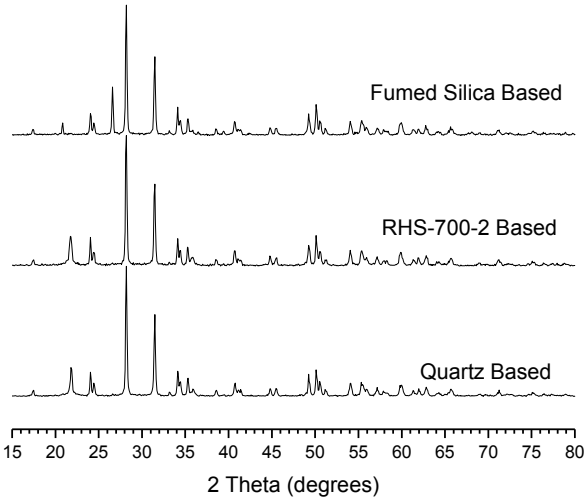

Figure 6.20 XRD patterns of red/coral pigments prepared at 850 °C. Calcination time was 5h. Fumed silica, RHS-700-2, and Quartz were used as the silica precursor.

The results of SEM characterization are shown in Figure 6.21 to 6.24. The images in turn correspond to green, blue, yellow, and red/coral pigment prepared using RHS-700-2 as silica precursor in this report. In Figure 6.21, the red arrows are referring to $ZrSiO_4$ rhombohedrical crystals according to the study Bondioli et al. together with EDS results (not shown here).[301] In accordance with XRD results in Figure 6.9 (RHS-700-2 based) the majority of the crystals are $ZrSiO_4$, and very little raw material crystals were observed. Figure 6.22 had similar crystals as Figure 6.21, and the morphology is also in accordance with the XRD pattern in Figure 6.9 (RHS-700-2 based), most crystals are $ZrSiO_4$, and little raw materials crystal were observed. Figure 6.23 is for yellow pigment. Based on XRD pattern (Figure 6.15), 1050 °C, not much $ZrSiO_4$ yield was produced. Almost no big rhombohedrical $ZrSiO_4$ crystals are seen On SEM image Figure 6.23.

Morphology in Figure 6.24 is similar to the work by Herrera et al.,[304] which are in accordance with the XRD results in Figure 6.18.

For all the pigments we made, we tested the samples color value, only the results of the green and blue pigments were listed in this report (Table 6.3) because XRD results show (Figure 6.9−6.11 and 6.12−6.14), that only two color pigment series yield substantial ZrSiO4 starting from 850 °C. To my knowledge, no similar data (CIE-L*a*b*) for the pigments themselves is available through the literature.

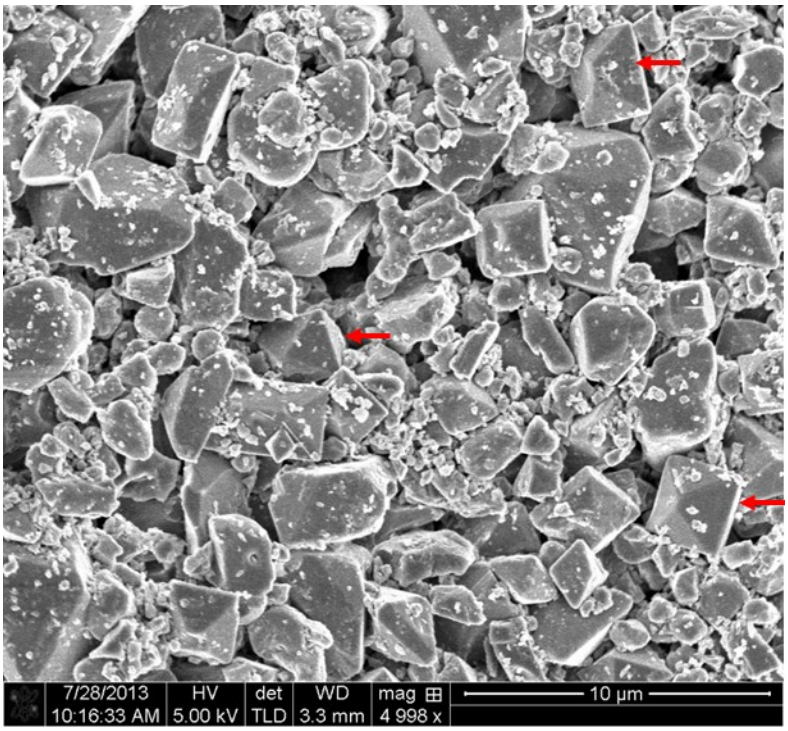

Figure 6.21 SEM image of green pigment prepared at 1050 °C using RHS-700-2. Calcination time was 5h. The red arrows refer to the $ZrSiO_4$ crystal.[301]

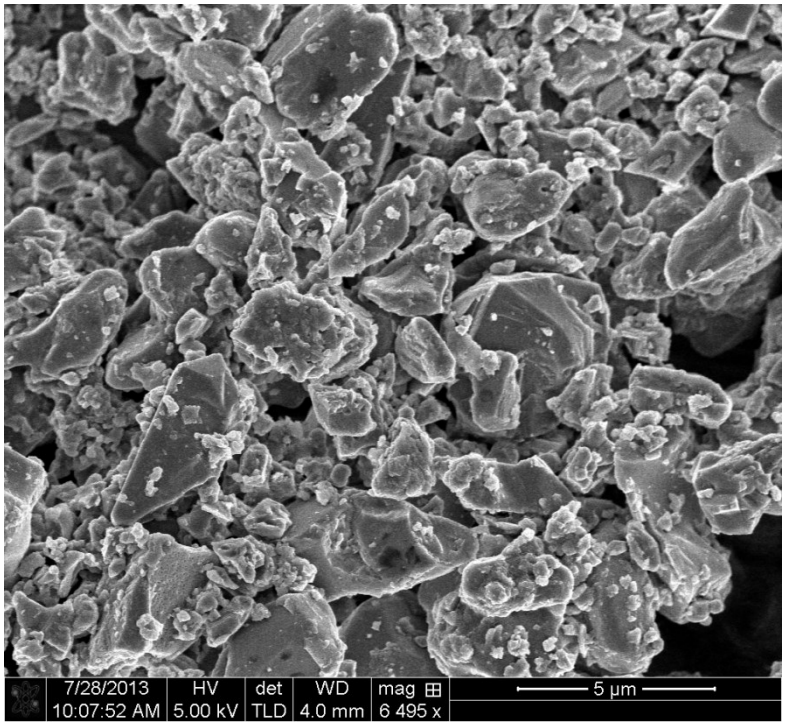

Figure 6.22 SEM image of blue pigment prepared at 1050 °C using RHS-700-2. Calcination time was 5h.

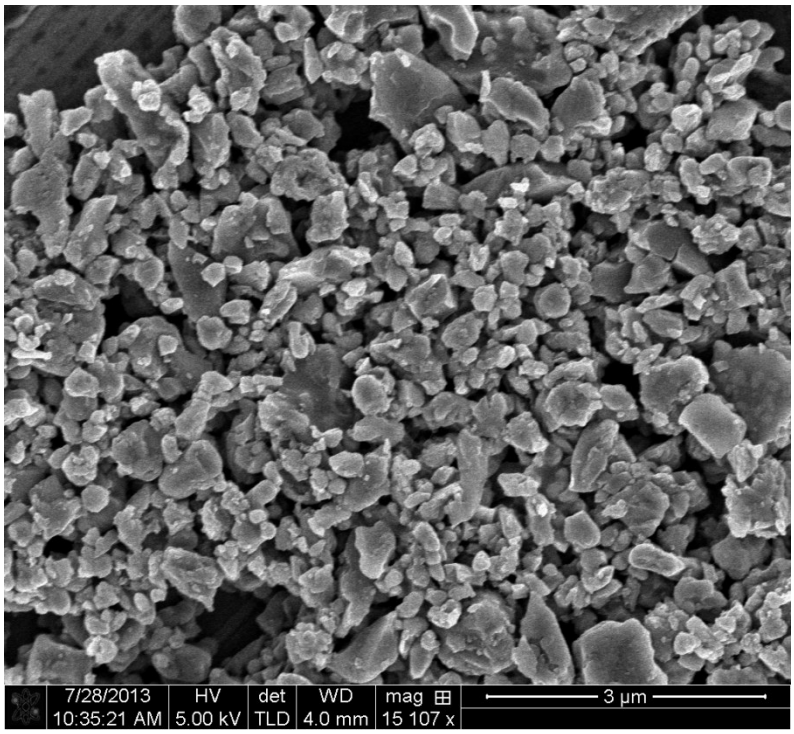

Figure 6.23 SEM image of yellow pigment prepared at 1050 °C using RHS-700-2. Calcination time was 5h.

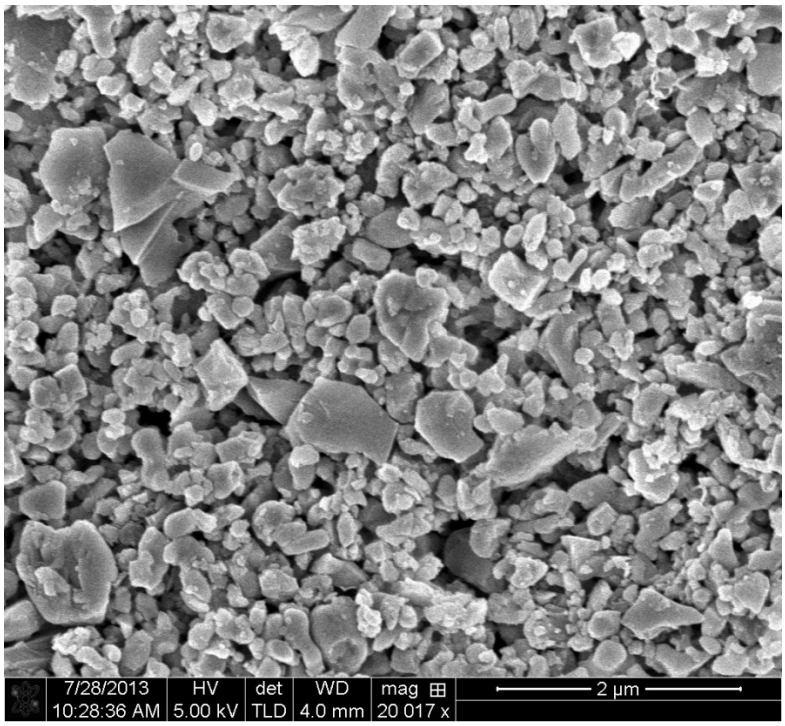

Figure 6.24 SEM image of red/coral pigment prepared at 1050 °C using RHS-700-2. Calcination time was 5h.

Table 6.3 CIE-L*a*b* value for different silica at different temperatures.

Color	Silica Type	850℃			950℃			1050℃		
		L*	a*	b*	L*	a*	b*	L*	a*	b*
green	Fumed silica	57.11	-2.83	12.20	51.75	-2.68	10.08	51.13	-4.76	11.17
	RHS-700-2	49.29	-8.37	7.95	49.14	-7.45	8.87	56.86	-7.55	5.13
	Quartz silica	54.89	-9.92	8.30	57.12	-6.96	7.92	53.06	-4.44	9.71
blue	Fumed silica	81.33	-8.79	-4.54	72.50	-11.69	-15.60	70.72	-11.95	-16.72
	RHS-700-2	79.74	-9.58	-8.38	68.00	-13.08	-20.65	70.61	-12.85	-18.87
	Quartz silica	81.12	-9.46	-8.28	69.93	-13.21	-18.57	65.15	-13.71	-20.71

6.4. Conclusion

Four colored ceramic pigments, namely green, blue, yellow, and red/coral, were prepared and studied in this report. Three different silica precursors, fumed silica, RH-HCl-Silica, and commercial crystalline silica, were used in the preparation of the four

pigments above. Beside silica precursors, three different calcination temperature, 1050 °C, 950 °C, and 850 °C, were also studied. Based on XRD characterization, it has been shown that silica from HCl treated RH has similar apparent reactivity to that of fumed silica and can be a suitable substituent material for the latter in pigment preparation. Among the three silica precursors, commercial crystalline silica possesses the lowest apparent reactivity in terms of $ZrSiO_4$ conversion rate. Silica from non-treated RH (RHA) is not an ideal candidate in pigment synthesis since it could yield unexpected color due to the RHA's low quality. The apparent reactivity of the three silica precursors depends on their surface area and crystallinity. According to the discussion on the silica forms (Q4, Q3, and Q2), the reactivity of the different silica could also be related to their crystallinity characterized by XRD, i.e., higher degree of silica crystallinity will presumably result in the lower reactivity in the pigment synthesis.

CHAPTER 7

Outlook and Summary

Biomass has drawn increasing attention since sustainability efforts became widespread. All the non-renewable energy is eventually going to be depleted. Ultimately sustainable development and renewable energy will become the future of mankind.

Our group has been researching sustainability efforts involving rice husk (RH) for several years. RH is a type of biomass/biowaste (which is referred to as an agro-waste in industry). At the present time, RH is considered as a "true" biowaste. Various biomasses have been studied and utilized to generate useful material or energy for the world. In general, biomasses can be classified into three categories. Category one is food competitor, which means that this kind of biomass can serve as food for living creatures, such as corn. When this kind of biomass is utilized to generate other useful materials or energy, the availability of food will inevitably decrease. Category two is for biomasses that are non-food competitors. But they still have to be purposely grown or harvested prior to utilizing them, such as switch grass. To utilize this kind of biomass, extra resources will be consumed. Category three is "true biowaste", which means they are generated as a byproduct of another useful resource. RH is a "true biowaste"; it is always generated when rice is produced. Compared to the other two categories of biomasses, the "true biowaste" would be the most beneficial to humans if they are used properly since the essential investment on the raw material would be virtually "zero".

Millions of tons of rice husks are produced every year.[207] Evidently the applications of RH have been very limited due to their tough nature and low nutritional value.[7-8] The most common disposal method so far is open field burning according to the

study by Manan et al.[9] The open field burning inevitably results in waste of energy, air pollution, and greenhouse gas emission.[12] If utilized properly, RH could be a suitable candidate of feedstock for silica based materials because of its high silica content (15−28 wt %) and large availability. Moreover, the silica in RH is pure and in amorphous form, which is extremely valuable as discussed in the first chapter. The problem now is how we could efficiently harvest RH without changing its purity, morphology, and crystallinity.

Presently, amorphous silica can be harvested, but the morphology control requires further research. At the present time the yielded silica tend to agglomerate with each other, which typically results in larger particles, and thus limited its application.

Luminescent silica material preparation is also an interesting topic. The procedure is simple, because no other raw materials are needed to prepare luminescent silica from RH. If the luminescence of the silica from RH can be sufficiently strong and efficient, we could potentially replace the toxic materials currently in use in fluorescent light bulbs. The mechanism of luminescent silica from RH is still under debating. More research is needed in this area.

All in all, RH biomass is worthy of extensive investigation and exploration, because it has great potential to benefit the world's sustainability efforts.

REFERENCES

1. Yu, J.; Zhang, J. B.; He, J.; Liu, Z. D.; Yu, Z. N., Combinations of mild physical or chemical pretreatment with biological pretreatment for enzymatic hydrolysis of rice hull. *Bioresource Technology* **2009,** *100* (2), 903-908.

2. Cabane, E.; Zhang, X.; Langowska, K.; Palivan, C. G.; Meier, W., Stimuli-responsive polymers and their applications in nanomedicine. *Biointerphases* **2012,** *7* (1-4), 9-9.

3. Balamurugan, M.; Saravanan, S., Producing nanosilica from Sorghum vulgare seed heads. *Powder Technology* **2012,** *224*, 345-350.

4. Chang, F. W.; Tsay, M. T.; Kuo, M. S., Effect of thermal treatments on catalyst reducibility and activity in nickel supported on RHA-Al_2O_3 systems. *Thermochimica Acta* **2002,** *386* (2), 161-172.

5. Zhang, X.; Shen, Y.; Yu, X.-y.; Liu, X.-j., Dissipation of chlorpyrifos and residue analysis in rice, soil and water under paddy field conditions. *Ecotoxicology and Environmental Safety* **2012,** *78*, 276-280.

6. Houston, D. F., Rice: Chemistry and Technologh. *American Association of Cereal Chemists, Inc.: St Paul, MN* **1972**.

7. Fang, M.; Yang, L.; Chen, G.; Shi, Z.; Luo, Z.; Cen, K., Experimental study on rice husk combustion in a circulating fluidized bed. *Fuel Processing Technology* **2004,** *85* (11), 1273-1282.

8. Efremova, S. V., Rice hull as a renewable raw material and its processing routes. *Russian Journal of General Chemistry* **2012,** *82* (5), 999-1005.

9. Lim, J. S.; Manan, Z. A.; Alwi, S. R. W.; Hashim, H., A review on utilisation of biomass from rice industry as a source of renewable energy. *Renewable & Sustainable Energy Reviews* **2012,** *16* (5), 3084-3094.

10. Martin, J. I., MS thesis. *Louisiana State University, USA* **1938**.

11. Chiew, Y. L.; Cheong, K. Y., A review on the synthesis of SiC from plant-based biomasses. *Materials Science and Engineering B-Advanced Functional Solid-State Materials* **2011,** *176* (13), 951-964.

12. Chen, H. R.; Wang, W. X.; Martin, J. C.; Oliphant, A. J.; Doerr, P. A.; Xu, J. F.; DeBorn, K. M.; Chen, C. X.; Sun, L. Y., Extraction of Lignocellulose and Synthesis of Porous Silica Nanoparticles from Rice Husks: A Comprehensive Utilization of Rice Husk Biomass. *Acs Sustainable Chemistry & Engineering* **2013,** *1* (2), 254-259.

13. Sun, L. Y.; Gong, K. C., Silicon-based materials from rice husks and their applications. *Industrial & Engineering Chemistry Research* **2001,** *40* (25), 5861-5877.

14. Suraporniboon, P.; Julsrigival, S.; Senthong, C.; Karladee, D., Genetics of silicon content in upland rice under drought condition. *Sabrao Journal of Breeding and Genetics* **2008,** *40* (1), 27-35.

15. Bryant, R.; Proctor, A.; Hawkridge, M.; Jackson, A.; Yeater, K.; Counce, P.; Yan, W.; McClung, A.; Fjellstrom, R., Genetic variation and association mapping of silica concentration in rice hulls using a germplasm collection. *Genetica* **2011,** *139* (11-12), 1383-1398.

16. Zemnukhova, L. A.; Nikolenko, Y. M., Study by X-ray photoelectron spectroscopy of rice husk and the products of its processing. *Russian Journal of General Chemistry* **2011,** *81* (4), 694-700.

17. Chen, X. G.; Lv, S. S.; Zhang, P. P.; Zhang, L.; Ye, Y., Thermal destruction of rice hull in air and nitrogen. *Journal of Thermal Analysis and Calorimetry* **2011,** *104* (3), 1055-1062.

18. Park, B. D.; Wi, S. G.; Lee, K. H.; Singh, A. P.; Yoon, T. H.; Kim, Y. S., Characterization of anatomical features and silica distribution in rice husk using microscopic and micro-analytical techniques. *Biomass & Bioenergy* **2003,** *25* (3), 319-327.

19. Shim, M. S.; Kwon, Y. J., Stimuli-responsive polymers and nanomaterials for gene delivery and imaging applications. *Advanced Drug Delivery Reviews* **2012,** *64* (11), 1046-1058.

20. Beall, G. H., Industrial applications of silica. *Silica: Physical Behavior, Geochemistry and Materials Applications* **1994,** *29*, 469-505.

21. Martin, K. R., The chemistry of silica and its potential health benefits. *Journal of Nutrition Health & Aging* **2007,** *11* (2), 94-98.

22. Glasser, F. P., silica in Encyclopedia of materials science and engineering. *The MIT Press: Cambridge, Massachusetts.* **1986,** *6*, 4393-4401.

23. Uhrlandt, S., Silica in Kirk-Othmer Encyclopedia of Chemical Technology. *John Wiley & Sons, Inc.: Hoboken, New Jersey* **2006,** *22*, 365-379.

24. Slowing, II; Trewyn, B. G.; Giri, S.; Lin, V. S. Y., Mesoporous silica nanoparticles for drug delivery and biosensing applications. *Advanced Functional Materials* **2007,** *17* (8), 1225-1236.

25. Gurav, J. L.; Jung, I. K.; Park, H. H.; Kang, E. S.; Nadargi, D. Y., Silica Aerogel: Synthesis and Applications. *Journal of Nanomaterials* **2010**.

26. Rösch, L.; John, P.; Reitmeier, R., Silicon Compounds, Organic. In *Ullmann's Encyclopedia of Industrial Chemistry*, Wiley-VCH Verlag GmbH & Co. KGaA: 2000.

27. Shen, J. F.; Liu, X. Z.; Zhu, S. G.; Zhang, H. L.; Tan, J. J., Effects of calcination parameters on the silica phase of original and leached rice husk ash. *Materials Letters* **2011,** *65* (8), 1179-1183.

28. Abo-El-Enein, S. A.; Eissa, M. A.; Diafullah, A. A.; Rizk, M. A.; Mohamed, F. M., Removal of some heavy metals ions from wastewater by copolymer of iron and aluminum impregnated with active silica derived from rice husk ash. *Journal of Hazardous Materials* **2009,** *172* (2-3), 574-579.

29. Jang, H. T.; Park, Y.; Ko, Y. S.; Lee, J. Y.; Margandan, B., Highly siliceous MCM-48 from rice husk ash for CO(2) adsorption. *International Journal of Greenhouse Gas Control* **2009,** *3* (5), 545-549.

30. Wang, W.; Martin, J. C.; Zhang, N.; Ma, C.; Han, A.; Sun, L., Harvesting silica nanoparticles from rice husks. *Journal of Nanoparticle Research* **2011,** *13* (12), 6981-6990.

31. Adam, F.; Chua, J. H., The adsorption of palmytic acid on rice husk ash chemically modified with Al(III) ion using the sol-gel technique. *Journal of Colloid and Interface Science* **2004,** *280* (1), 55-61.

32. Chandrasekhar, S.; Pramada, P. N.; Praveen, L., Effect of organic acid treatment on the properties of rice husk silica. *Journal of Materials Science* **2005,** *40* (24), 6535-6544.

33. Markovska, I. G.; Lyubchev, L. A., A Study on the thermal destruction of rice husk in air and nitrogen atmosphere. *Journal of Thermal Analysis and Calorimetry* **2007,** *89* (3), 809-814.

34. Umeda, J.; Kondoh, K.; Michiura, Y., Process parameters optimization in preparing high-purity amorphous silica originated from rice husks. *Materials Transactions* **2007,** *48* (12), 3095-3100.

35. Umeda, J.; Kondoh, K., High-purification of amorphous silica originated from rice husks by combination of polysaccharide hydrolysis and metallic impurities removal. *Industrial Crops and Products* **2010,** *32* (3), 539-544.

36. Shinde, A. B.; Shrigadi, N. B.; Samant, S. D., Development of Fe-, Sb-, Bi- and Al-impregnated silica catalysts using rice husk silica as a support for Friedel-Crafts

benzylation of arenes. *Journal of Chemical Technology and Biotechnology* **2003,** *78* (12), 1234-1238.

37. Radhika, T.; Sugunan, S., Influence of surface and acid properties of vanadia supported on ceria promoted with rice husk silica on cyclohexanol decomposition. *Catalysis Communications* **2006,** *7* (8), 528-533.

38. Rafiee, E.; Khodayari, M.; Kahrizi, M.; Tayebee, R., $H_5CoW_{12}O_{40}$ supported on nano silica from rice husk ash: A green bifunctional catalyst for the reaction of alcohols with cyclic and acyclic 1,3-dicarbonyl compounds. *Journal of Molecular Catalysis a-Chemical* **2012,** *358*, 121-128.

39. Rafiee, E.; Khodayari, M.; Shahebrahimi, S.; Joshaghani, M., 12-Tungstophosphoric acid supported on nano silica from rice husk ash as an efficient catalyst for direct benzylation of 1,3-dicarbonyl compounds in solvent-free condition. *Journal of Molecular Catalysis a-Chemical* **2011,** *351*, 204-209.

40. Renu, P.; Radhika, T.; Sugunan, S., Characterization and catalytic activity of vanadia supported on rice husk silica promoted samaria. *Catalysis Communications* **2008,** *9* (5), 584-589.

41. Zemnukhova, L. A.; Egorov, A. G.; Fedorishcheva, G. A.; Barinov, N. N.; Sokol'nitskaya, T. A.; Botsul, A. O., Properties of amorphous silica produced from rice and oat processing waste. *Inorganic Materials* **2006,** *42* (1), 24-29.

42. Tsay, M. T.; Chang, F. W., Characterization of rice husk ash-supported nickel catalysts prepared by ion exchange. *Applied Catalysis a-General* **2000,** *203* (1), 15-22.

43. Chang, F. W.; Tsay, M. T.; Kuo, M. S.; Yang, C. M., Characterization of nickel catalysts on RHA-Al_2O_3 composite oxides prepared by ion exchange. *Applied Catalysis a-General* **2002,** *226* (1-2), 213-224.

44. Chang, F. W.; Kuo, M. S.; Tsay, M. T.; Hsieh, M. C., Hydrogenation of CO_2 over nickel catalysts on rice husk ash-alumina prepared by incipient wetness impregnation. *Applied Catalysis a-General* **2003,** *247* (2), 309-320.

45. Chang, F. W.; Kuo, M. S.; Tsay, M. T.; Hsieh, M. C., Effect of calcination temperature on catalyst reducibility and hydrogenation reactivity in rice husk ash-alumina supported nickel systems. *Journal of Chemical Technology and Biotechnology* **2004,** *79* (7), 691-699.

46. Wang, W. X.; Martin, J. C.; Fan, X. T.; Han, A. J.; Luo, Z. P.; Sun, L. Y., Silica Nanoparticles and Frameworks from Rice Husk Biomass. *Acs Applied Materials & Interfaces* **2012,** *4* (2), 977-981.

47. Yalcin, N.; Sevinc, V., Studies on silica obtained from rice husk. *Ceramics International* **2001,** *27* (2), 219-224.

48. Liou, T. H., Evolution of chemistry and morphology during the carbonization and combustion of rice husk. *Carbon* **2004,** *42* (4), 785-794.

49. Liou, T. H., Preparation and characterization of nano-structured silica from rice husk. *Materials Science and Engineering a-Structural Materials Properties Microstructure and Processing* **2004,** *364* (1-2), 313-323.

50. Liou, T. H.; Wu, S. J., Kinetics Study and Characteristics of Silica Nanoparticles Produced from Biomass-Based Material. *Industrial & Engineering Chemistry Research* **2010,** *49* (18), 8379-8387.

51. Bassett, D. R.; Boucher, E. A.; Zettlemo.Ac, Effect of alkali-halides and silver-nitrate on crystallization of silica powders. *Journal of Materials Science* **1972,** *7* (12), 1379-1382.

52. Real, C.; Alcala, M. D.; Criado, J. M., Preparation of silica from rice husks. *Journal of the American Ceramic Society* **1996,** *79* (8), 2012-2016.

53. Real, C.; Alcala, M. D.; Munoz-Paez, A.; Criado, J. M., XAFS analysis of the potassium-silica interaction in rice husks. *Nuclear Instruments & Methods in Physics Research Section B-Beam Interactions with Materials and Atoms* **1997,** *133* (1-4), 68-72.

54. Adam, F.; Andas, J., Amino benzoic acid modified silica - An improved catalyst for the mono-substituted product in the benzylation of toluene with benzyl chloride. *Journal of Colloid and Interface Science* **2007,** *311* (1), 135-143.

55. Ahmed, A. E.; Adam, F., Indium incorporated silica from rice husk and its catalytic activity. *Microporous and Mesoporous Materials* **2007,** *103* (1-3), 284-295.

56. Adam, F.; Ahmed, A. E.; Min, S. L., Silver modified porous silica from rice husk and its catalytic potential. *Journal of Porous Materials* **2008,** *15* (4), 433-444.

57. Adam, F.; Sugiarmawan, I. A., A porous ruthenium silica catalyst modified with amino benzoic acid for the oxidation of butanol with molecular oxygen. *Journal of Porous Materials* **2009,** *16* (3), 321-329.

58. Adam, F.; Andas, J.; Ab Rahman, I., A study on the oxidation of phenol by heterogeneous iron silica catalyst. *Chemical Engineering Journal* **2010,** *165* (2), 658-667.

59. Adam, F.; Iqbal, A., The oxidation of styrene by chromium-silica heterogeneous catalyst prepared from rice husk. *Chemical Engineering Journal* **2010,** *160* (2), 742-750.

60. Adam, F.; Thankappan, R., Oxidation of benzene over bimetallic Cu-Ce incorporated rice husk silica catalysts. *Chemical Engineering Journal* **2010,** *160* (1), 249-258.

61. Adam, F.; Chew, T. S.; Andas, J., Liquid Phase Oxidation of Acetophenone over Rice Husk Silica Vanadium Catalyst. *Chinese Journal of Catalysis* **2012,** *33* (3), 518-522.

62. Grisdanurak, N.; Chiarakorn, S.; Wittayakun, J., Utilization of mesoporous molecular sieves synthesized from natural source rice husk silica to chlorinated volatile organic compounds (CVOCs) adsorption. *Korean Journal of Chemical Engineering* **2003,** *20* (5), 950-955.

63. Patel, M.; Karera, A.; Prasanna, P., Effect of thermal and chemical treatments on carbon and silica contents in rice husk. *Journal of Materials Science* **1987,** *22* (7), 2457-2464.

64. Umeda, J.; Kondoh, K., High-purity amorphous silica originated in rice husks via carboxylic acid leaching process. *Journal of Materials Science* **2008,** *43* (22), 7084-7090.

65. Markovska, I. G.; Bogdanov, B.; Nedelchev, N. M.; Gurova, K. M.; Zagorcheva, M. H.; Lyubchev, L. A., Study on the Thermochemical and Kinetic Characteristics of Alkali Treated Rice Husk. *Journal of the Chinese Chemical Society* **2010,** *57* (3A), 411-416.

66. Javed, S. H.; Naveed, S.; Ramzan, N.; Feroze, N.; Zafar, M., Characterization of Amorphous Silica Obtained from KMnO4 Treated Rice Husk. *Journal of the Chemical Society of Pakistan* **2010,** *32* (1), 78-82.

67. Zhang, H.; Zhao, X.; Ding, X.; Lei, H.; Chen, X.; An, D.; Li, Y.; Wang, Z., A study on the consecutive preparation of D-xylose and pure superfine silica from rice husk. *Bioresource Technology* **2010,** *101* (4), 1263-1267.

68. Ma, Y.; Zhao, X.; Zhang, H.; Wang, Z., Comprehensive utilization of the hydrolyzed productions from rice hull. *Industrial Crops and Products* **2011,** *33* (2), 403-408.

69. Adam, F.; Kandasamy, K.; Balakrishnan, S., Iron incorporated heterogeneous catalyst from rice husk ash. *Journal of Colloid and Interface Science* **2006,** *304* (1), 137-143.

70. Ubukata, M.; Mitsuhashi, S.; Ueki, A.; Sano, Y.; Iwasa, N.; Fujita, S.; Arai, M., Quality Determination of Nickel-Loaded Silica Prepared from Poaceous Biomass. *Journal of Agricultural and Food Chemistry* **2010,** *58* (10), 6312-6317.

71. Adam, F.; Hello, K. M.; Ben Aisha, M. R., The synthesis of heterogeneous 7-amino-1-naphthalene sulfonic acid immobilized silica nano particles and its catalytic activity. *Journal of the Taiwan Institute of Chemical Engineers* **2011,** *42* (5), 843-851.

72. Kalapathy, U.; Proctor, A.; Shultz, J., An improved method for production of silica from rice hull ash. *Bioresource Technology* **2002,** *85* (3), 285-289.

73. Kalapathy, U.; Proctor, A.; Shultz, J., A simple method for production of pure silica from rice hull ash. *Bioresource Technology* **2000,** *73* (3), 257-262.

74. Kalapathy, U.; Proctor, A.; Shultz, J., Silica xerogels from rice hull ash: structure, density and mechanical strength as affected by gelation pH and silica concentration. *Journal of Chemical Technology and Biotechnology* **2000,** *75* (6), 464-468.

75. Tang, Q.; Wang, T., Preparation of silica aerogel from rice hull ash by supercritical carbon dioxide drying. *Journal of Supercritical Fluids* **2005,** *35* (1), 91-94.

76. Li, T.; Wang, T., Preparation of silica aerogel from rice hull ash by drying at atmospheric pressure. *Materials Chemistry and Physics* **2008,** *112* (2), 398-401.

77. Berlin, M.; Allen, J.; Kailasam, V.; Rosenberg, D.; Rosenberg, E., Nanoporous silica polyamine composites for metal ion capture from rice hull ash. *Applied Organometallic Chemistry* **2011,** *25* (7), 530-536.

78. Nayak, J. P.; Bera, J., Preparation of Silica Aerogel by Ambient Pressure Drying Process using Rice Husk Ash as Raw Material. *Transactions of the Indian Ceramic Society* **2009,** *68* (2), 91-94.

79. Bhagiyalakshmi, M.; Yun, L. J.; Anuradha, R.; Jang, H. T., Utilization of rice husk ash as silica source for the synthesis of mesoporous silicas and their application to CO_2 adsorption through TREN/TEPA grafting. *Journal of Hazardous Materials* **2010,** *175* (1-3), 928-938.

80. Ma, X.; Zhou, B.; Gao, W.; Qu, Y.; Wang, L.; Wang, Z.; Zhu, Y., A recyclable method for production of pure silica from rice hull ash. *Powder Technology* **2012,** *217*, 497-501.

81. Mochidzuki, K.; Sakoda, A.; Suzuki, M.; Izumi, J.; Tomonaga, N., Structural behavior of rice husk silica in pressurized hot-water treatment processes. *Industrial & Engineering Chemistry Research* **2001,** *40* (24), 5705-5709.

82. Bansal, V.; Ahmad, A.; Sastry, M., Fungus-mediated biotransformation of amorphous silica in rice husk to nanocrystalline silica. *Journal of the American Chemical Society* **2006,** *128* (43), 14059-14066.

83. Estevez, M.; Vargas, S.; Castano, V. M.; Rodriguez, R., Silica nano-particles produced by worms through a bio-digestion process of rice husk. *Journal of Non-Crystalline Solids* **2009,** *355* (14-15), 844-850.

84. Espindola-Gonzalez, A.; Martinez-Hernandez, A. L.; Angeles-Chavez, C.; Castano, V. M.; Velasco-Santos, C., Novel Crystalline SiO_2 Nanoparticles via Annelids Bioprocessing of Agro-Industrial Wastes. *Nanoscale Research Letters* **2010,** *5* (9), 1408-1417.

85. Chandrasekhar, S.; Satyanarayana, K. G.; Pramada, P. N.; Raghavan, P.; Gupta, T. N., Processing, properties and applications of reactive silica from rice husk - an overview. *Journal of Materials Science* **2003,** *38* (15), 3159-3168.

86. Kumar, V.; Sinha, S.; Saini, M. S.; Kanungo, B. K.; Biswas, P., Rice husk as reinforcing filler in polypropylene composites. *Reviews in Chemical Engineering* **2010,** *26* (1-2), 41-53.

87. Habeeb, G. A.; Bin Mahmud, H., Study on Properties of Rice Husk Ash and Its Use as Cement Replacement Material. *Materials Research-Ibero-American Journal of Materials* **2011,** *13* (2), 185-190.

88. Proctor, A.; Palaniappan, S., Soy oil lutein adsorption by rice hull ash. *Journal of the American Oil Chemists Society* **1989,** *66* (11), 1618-1621.

89. Adhikari, C.; Proctor, A.; Blyholder, G. D., Diffuse-reflectance fourier-transform infrared-spectroscopy of phospholipid adsorption onto silicic-acid. *Journal of the American Oil Chemists Society* **1995,** *72* (3), 337-341.

90. Chaves, M. R. M.; Dockal, E. R.; Souza, R. C. R.; Buchler, P. M., Biogenic modified silica as a sorbent of cadmium ions: Preparation and characterization. *Environmental Technology* **2009,** *30* (7), 663-671.

91. Ren, Y.; Yue, B.; Gu, M.; He, H., Progress of the Application of Mesoporous Silica-Supported Heteropolyacids in Heterogeneous Catalysis and Preparation of Nanostructured Metal Oxides. *Materials* **2010,** *3* (2), 764-785.

92. Maksimchuk, N. V.; Zalomaeva, O. V.; Skobelev, I. Y.; Kovalenko, K. A.; Fedin, V. P.; Kholdeeva, O. A., Metal-organic frameworks of the MIL-101 family as heterogeneous single-site catalysts. *Proceedings of the Royal Society a-Mathematical Physical and Engineering Sciences* **2012,** *468* (2143), 2017-2034.

93. Ahmed, A. E.; Adam, F., The benzylation of benzene using aluminium, gallium and iron incorporated silica from rice husk ash. *Microporous and Mesoporous Materials* **2009,** *118* (1-3), 35-43.

94. Artkla, S.; Wantala, K.; Srinameb, B. O.; Grisdanurak, N.; Klysubun, W.; Wittayakun, J., Characteristics and photocatalytic degradation of methyl orange on Ti-RH-MCM-41 and TiO_2/RH-MCM-41. *Korean Journal of Chemical Engineering* **2009,** *26* (6), 1556-1562.

95. Artkla, S.; Kim, W.; Choi, W.; Wittayakun, J., Highly enhanced photocatalytic degradation of tetramethylammonium on the hybrid catalyst of titania and MCM-41 obtained from rice husk silica. *Applied Catalysis B-Environmental* **2009,** *91* (1-2), 157-164.

96. Chareonpanich, M.; Nanta-Ngern, A.; Limtrakul, J., Short-period synthesis of ordered mesoporous silica SBA-15 using ultrasonic technique. *Materials Letters* **2007,** *61* (29), 5153-5156.

97. Chiarakorn, S.; Areerob, T.; Grisdanurak, N., Influence of functional silanes on hydrophobicity of MCM-41 synthesized from rice husk. *Science and Technology of Advanced Materials* **2007,** *8* (1-2), 110-115.

98. Li, D.; Zhu, X., Short-period synthesis of high specific surface area silica from rice husk char. *Materials Letters* **2011,** *65* (11), 1528-1530.

99. Li, D. W.; Chen, D. Y.; Zhu, X. F., Reduction in time required for synthesis of high specific surface area silica from pyrolyzed rice husk by precipitation at low pH. *Bioresource Technology* **2011,** *102* (13), 7001-7003.

100. Singh, S. K.; Mohanty, B. C.; Basu, S., Synthesis of SiC from rice husk in a plasma reactor. *Bulletin of Materials Science* **2002,** *25* (6), 561-563.

101. Wang, S. B.; Peng, Y. L., Natural zeolites as effective adsorbents in water and wastewater treatment. *Chemical Engineering Journal* **2010,** *156* (1), 11-24.

102. Martinez, V.; Valencia, M. F.; Cruz, J.; Mejia, J. M.; Chejne, F., Production of beta-SiC by pyrolysis of rice husk in gas furnaces. *Ceramics International* **2006,** *32* (8), 891-897.

103. Zhu, D.; Gao, M.; Zhang, S.; Wu, H.; Pan, Y.; Liu, Y.; Pan, H.; Oliveira, F. J.; Vieira, J. M., A high-strength SiC_w/SiC-Si composite derived from pyrolyzed rice husks by liquid silicon infiltration. *Journal of Materials Science* **2012,** *47* (12), 4921-4927.

104. Wu, H. Y.; Gao, M. X.; Zhu, D.; Zhang, S. C.; Pan, Y.; Pan, H. G.; Liu, Y. F.; Oliveira, F. J.; Vieira, J. M., SiC whisker reinforced multi-carbides composites prepared from B_4C and pyrolyzed rice husks via reactive infiltration. *Ceramics International* **2012,** *38* (5), 3519-3527.

105. Krishnarao, R. V.; Mahajan, Y. R., Effect of acid treatment on the formation of SiC whiskers from raw rice husks. *J. European Ceram. Soc.* **1995,** *15* (12), 1229-1234.

106. Raman, V.; Parashar, V. K.; Bahl, O. P., Influence of boric acid on the synthesis of silicon carbide whiskers from rice husks and polyacrylonitrile. *J. Mater. Sci. Lett.* **1997,** *16* (15), 1252-1254.

107. Mizuki, E.; Okumura, S.; Saito, H.; Murao, S., Formation of silicon-carbide from rice husks using enzymatic methods for carbon control. *Bioresource Technology* **1993,** *44* (1), 47-51.

108. Javed., S. H.; S., T.; M., S.; Zafar., M.; Kazmi., M., Characterization of Silica from Sodium Hydroxide Treated Rice Husk. *Journal of Pakistan Institute of Chemical Engineers* **2009,** *37*, 97-101.

109. Hashishin, T.; Iwanaga, H.; Yamamoto, Y., Effects of impurities on the growth of SiC whiskers from silica-containing natural substances. *Journal of the Ceramic Society of Japan* **2002,** *110* (7), 644-648.

110. Janghorban, K.; Tazesh, H. R., Effect of catalyst and process parameters on the production of silicon carbide from rice hulls. *Ceramics International* **1999,** *25* (1), 7-12.

111. Wang, Q.; Guo, M.; Han, M., A Study on the Rate-determining Step of Growing SiC Whisker. *Journal of The Chinese Ceramic Society* **1997,** *44* (1), 47.

112. Krishnarao, R. V.; Godkhindi, M. M., Effect of Si_3N_4 additions on the formation of SiC whiskers from rice husks. *Ceramics International* **1992,** *18* (3), 185-191.

113. Silva, P. C.; Figueiredo, J. L., Production of SiC and Si_3N_4 whiskers in $C+SiO_2$ solid mixtures. *Materials Chemistry and Physics* **2001,** *72* (3), 326-331.

114. Krishnarao, R. V., Effect of cobalt catalyst on the formation of SiC from rice husk silica-carbon black mixture. *Journal of Materials Science* **1995,** *30* (14), 3645-3651.

115. Krishnarao, R. V., Effect of cobalt chloride treatment on the formation of SiC from burnt rice husks. *J. European Ceram. Soc.* **1993,** *12* (5), 395-401.

116. Wang., W.; Martin., J. C.; Huang., R.; Huang., W.; Liu., A.; Han., A.; Sun., L., Synthesis of silicon complexes from rice husk derived silica nanoparticles. *RSC Advances* **2012,** (2), 9036-9041.

117. Carassiti, L.; Jones, A.; Harrison, P.; Dobson, P. S.; Kingman, S.; MacLaren, I.; Gregory, D. H., Ultra-rapid, sustainable and selective synthesis of silicon carbide powders and nanomaterials via microwave heating. *Energy Environ. Sci.* **2011,** *4* (4), 1503-1510.

118. Satapathy, L. N.; Ramesh, P. D.; Agrawala, D.; Roy, R., Microwave synthesis of phase-pure, fine silicon carbide powder. *Materials Research Bulletin* **2005,** *40* (10), 1871-1882.

119. Qadri, S. B.; Imam, M. A.; Fliflet, A. W.; Rath, B. B.; Goswami, R.; Caldwell, J. D., Microwave-induced transformation of rice husks to SiC. *Journal of Applied Physics* **2012,** *111* (7).

120. Nayak, B. B.; Mohanty, B. C.; Singh, S. K., Synthesis of silicon carbide from rice husk in a dc arc plasma reactor. *Journal of the American Ceramic Society* **1996,** *79* (5), 1197-1200.

121. Singh, S. K.; Stachowicz, L.; Girshick, S. L.; Pfender, E., Thermal plasma synthesis of SiC from rice hull (husk). *J. Mater. Sci. Lett.* **1993,** *12* (9), 659-660.

122. Sharma, N. K.; Williams, W. S.; Zangvil, A., Formation and Structure of Silicon Carbide Whiskers from Rice Hulls. *Journal of the American Ceramic Society* **1984,** *67* (11), 715-720.

123. Motojima, S.; Hamamoto, T.; Iwanaga, H., Preparation of micro-coiled SiC fibers by chemical vapor deposition and their morphology. *J. Cryst. Growth* **1996,** *158* (1-2), 79-83.

124. Andersson, C. H.; Warren, R., Silicon-carbide fibers and their potential for use in composite-materials .1. *Composites* **1984,** *15* (1), 16-24.

125. Satapathy, A.; Jha, A. K.; Mantry, S.; Singh, S. K.; Patnaik, A., Processing and Characterization of Jute-Epoxy Composites Reinforced with SiC Derived from Rice Husk. *Journal of Reinforced Plastics and Composites* **2010,** *29* (18), 2869-2878.

126. Maeda, E.; Komatsu, M., The thermoelectric performance of silicon carbide semiconductor made from rice hull. In *Covalent Ceramics Iii - Science and Technology of Non-Oxides*, Hepp, A. F.; Kumta, P. N.; Sullivan, J. J.; Fischman, G. S.; Kaloyeros, A. E., Eds. Materials Research Soc: Pittsburgh, 1996; Vol. 410, pp 77-81.

127. Takeda, S.; Pai, C. H.; Seo, W. S.; Koumoto, K.; Yanagida, H., Thermoelectric properties of porous beta-SiC fabricated from rice hull ash. *Nippon Seramikkusu Kyokai Gakujutsu Ronbunshi-Journal of the Ceramic Society of Japan* **1993,** *101* (7), 814-818.

128. Prasad, B. K.; Das, S.; Jha, A. K.; Modi, O. P.; Dasgupta, R.; Yegneswaran, A. H., Factors controlling the abrasive wear response of a zinc-based alloy silicon carbide particle composite. *Compos. Pt. A-Appl. Sci. Manuf.* **1997,** *28* (4), 301-308.

129. An, Z.; Xia, Y. K.; Ren, Z. M.; Han, M. F.; Jia, R. H.; Guo, M. X., Pilot studies of Separation and purification of SiC whisker. *High Technology Letter* **1995,** *5* (7), 6.

130. Russell, L. M.; Johnson, L. F.; Hasselman, D. P. H.; Ruh, R., Thermal-conductivity diffusivity of silicon-carbide whisker reinforced mullite. *Journal of the American Ceramic Society* **1987,** *70* (10), C226-C229.

131. Nutt, S. R., Defects in silicon-carbide whiskers. *Journal of the American Ceramic Society* **1984,** *67* (6), 428-431.

132. Montalvo, S.; Guerrero, L.; Borja, R.; Sanchez, E.; Milan, Z.; Cortes, I.; de la la Rubia, M. A., Application of natural zeolites in anaerobic digestion processes: A review. *Applied Clay Science* **2012,** *58*, 125-133.

133. Olsbye, U.; Svelle, S.; Bjorgen, M.; Beato, P.; Janssens, T. V. W.; Joensen, F.; Bordiga, S.; Lillerud, K. P., Conversion of Methanol to Hydrocarbons: How Zeolite Cavity and Pore Size Controls Product Selectivity. *Angewandte Chemie-International Edition* **2012,** *51* (24), 5810-5831.

134. Zheng, Y. G.; Li, X. G.; Dutta, P. K., Exploitation of Unique Properties of Zeolites in the Development of Gas Sensors. *Sensors* **2012,** *12* (4), 5170-5194.

135. Coronas, J., Present and future synthesis challenges for zeolites. *Chemical Engineering Journal* **2010,** *156* (2), 236-242.

136. Chal, R.; Gerardin, C.; Bulut, M.; van Donk, S., Overview and Industrial Assessment of Synthesis Strategies towards Zeolites with Mesopores. *Chemcatchem* **2011,** *3* (1), 67-81.

137. Bajpai, P. K.; Rao, M. S.; Gokhale, K., Synthesis of mordenite type zeolite using silica from rice husk ash. *Industrial & Engineering Chemistry Product Research and Development* **1981,** *20* (4), 721-726.

138. Rawtani, A. V.; Rao, M. S.; Gokhale, K., Synthesis of zsm-5 zeolite using silica from rice husk ash. *Industrial & Engineering Chemistry Research* **1989,** *28* (9), 1411-1414.

139. Hemalatha, P.; Bhagiyalakshmi, M.; Ganesh, M.; Palanichamy, M.; Murugesan, V.; Jang, H. T., Role of ceria in CO_2 adsorption on NaZSM-5 synthesized using rice husk ash. *Journal of Industrial and Engineering Chemistry* **2012,** *18* (1), 260-265.

140. Naskar, M. K.; Kundu, D.; Chatterjee, M., A Facile Hydrothermal Conversion of Rice Husk Ash to ZSM-5 Zeolite Powders. *Journal of the American Ceramic Society* **2012,** *95* (3), 925-930.

141. Mohamed, M. M.; Zidan, F. I.; Thabet, M., Synthesis of ZSM-5 zeolite from rice husk ash: Characterization and implications for photocatalytic degradation catalysts. *Microporous and Mesoporous Materials* **2008,** *108* (1-3), 193-203.

142. Ali, I. O.; Hassan, A. M.; Shaaban, S. M.; Soliman, K. S., Synthesis and characterization of ZSM-5 zeolite from rice husk ash and their adsorption of Pb2+ onto unmodified and surfactant-modified zeolite. *Separation and Purification Technology* **2011,** *83*, 38-44.

143. Pacheco-Malagon, G.; Sanchez-Flores, N. A.; Saniger-Blesa, J.; Banos, L.; Perez-Romo, P.; Valente, J. S.; Guzman-Castillo, M. D.; Hernandez-Beltran, F.; Fripiat, J. J., New synthesis technique of supported ZSM-5 using organo-alumino-silicic gels. *Microporous and Mesoporous Materials* **2007,** *100* (1-3), 70-76.

144. Kordatos, K.; Gavela, S.; Ntziouni, A.; Pistiolas, K. N.; Kyritsi, A.; Kasselouri-Rigopoulou, V., Synthesis of highly siliceous ZSM-5 zeolite using silica from rice husk ash. *Microporous and Mesoporous Materials* **2008,** *115* (1-2), 189-196.

145. Katsuki, H.; Furuta, S.; Watari, T.; Komarneni, S., ZSM-5 zeolite/porous carbon composite: Conventional- and microwave-hydrothermal synthesis from carbonized rice husk. *Microporous and Mesoporous Materials* **2005,** *86* (1-3), 145-151.

146. Ali, I. O.; Ali, A. M.; Shabaan, S. M.; El-Nasser, K. S., Isomorphous substitution of Fe in the framework of aluminosilicate MFI by hydrothermal synthesis and their evaluation in p-nitrophenol degradation. *Journal of Photochemistry and Photobiology a-Chemistry* **2009,** *204* (1), 25-31.

147. Fernandes, A. A.; Frajndlich, E. U.; Riella, H. G., A low cost ZSM-5 zeolite obtained rice hull ash. In *Advanced Powder Technology Iv*, Salgado, L.; Filho, F. A., Eds. 2005; Vol. 498-499, pp 676-680.

148. Bhagiyalakshmi, M.; Anuradha, R.; Palanichamy, M.; Jang, H. T., Dexterous template-free synthesis of ferrisilicate with MFI morphology using rice husk ash. *Journal of Non-Crystalline Solids* **2010,** *356* (23-24), 1204-1209.

149. Vempati, R. K.; Borade, R.; Hegde, R. S.; Komarneni, S., Template free ZSM-5 from siliceous rice hull ash with varying C contents. *Microporous and Mesoporous Materials* **2006,** *93* (1-3), 134-140.

150. Corma, A.; Fornes, V.; Melo, F.; Perezpariente, J., Zeolite-beta - structure, activity, and selectivity for catalytic cracking. *Acs Symposium Series* **1988,** *375*, 49-63.

151. Wu, Y.; Tian, F.; Liu, J.; Song, D.; Jia, C.; Chen, Y., Enhanced catalytic isomerization of alpha-pinene over mesoporous zeolite beta of low Si/Al ratio by NaOH treatment. *Microporous and Mesoporous Materials* **2012,** *162*, 168-174.

152. Prasetyoko, D.; Ramli, Z.; Endud, S.; Hamdan, H.; Sulikowski, B., Conversion of rice husk ash to zeolite beta. *Waste Management* **2006,** *26* (10), 1173-1179.

153. Cheng, Y.; Lu, M.; Li, J.; Su, X.; Pan, S.; Jiao, C.; Peng, M., Synthesis of MCM-22 zeolite using rice husk as a silica source under varying-temperature conditions. *Journal of Colloid and Interface Science* **2012,** *369*, 388-394.

154. Wang, S. B.; Li, H.; Xu, L. Y., Application of zeolite MCM-22 for basic dye removal from wastewater. *Journal of Colloid and Interface Science* **2006,** *295* (1), 71-78.

155. Wittayakun, J.; Khemthong, P.; Prayoonpokarach, S., Synthesis and characterization of zeolite NaY from rice husk silica. *Korean Journal of Chemical Engineering* **2008,** *25* (4), 861-864.

156. Yusof, A. M.; Nizam, N. A.; Rashid, N. A. A., Hydrothermal conversion of rice husk ash to faujasite-types and NaA-type of zeolites. *Journal of Porous Materials* **2010,** *17* (1), 39-47.

157. Saceda, J. J. F.; de Leon, R. L.; Rintramee, K.; Prayoonpokarach, S.; Wittayakun, J., Properties of silica from rice husk and rice husk ash and their utilization for zeolite y synthesis. *Quimica Nova* **2011,** *34* (8), 1394-U289.

158. Dalai, A. K.; Pradhan, N. C.; Rao, M. S.; Gokhale, K., Synthesis and characterization of NaX and Cu-exchanged NaX zeolites from silica obtained from rice husk ash. *Indian Journal of Engineering and Materials Sciences* **2005,** *12* (3), 227-234.

159. Petkowicz, D. I.; Rigo, R. T.; Radtke, C.; Pergher, S. B.; dos Santos, J. H. Z., Zeolite NaA from Brazilian chrysotile and rice husk. *Microporous and Mesoporous Materials* **2008,** *116* (1-3), 548-554.

160. Azizi, S. N.; Yousefpour, M., Synthesis of zeolites NaA and analcime using rice husk ash as silica source without using organic template. *Journal of Materials Science* **2010,** *45* (20), 5692-5697.

161. Ghasemi, Z.; Younesi, H., Preparation and Characterization of Nanozeolite NaA from Rice Husk at Room Temperature without Organic Additives. *Journal of Nanomaterials* **2011**.

162. Yusof, A. M.; Malek, N., Removal of Cr(VI) and As(V) from aqueous solutions by HDTMA-modified zeolite Y. *Journal of Hazardous Materials* **2009,** *162* (2-3), 1019-1024.

163. Hemalatha, P.; Palanichamy, M.; Murugesan, V.; Kwon, S. B.; Park, D.; Cho, Y.; Jang, H. T., CO_2 Adsorption over Zinc Oxide Impregnated NaZSM-5 Synthesized Using Rice Husk Ash. *Asian Journal of Chemistry* **2011,** *23* (6), 2806-2810.

164. Riley, F. L., Silicon nitride and related materials. *Journal of the American Ceramic Society* **2000,** *83* (2), 245-265.

165. Rhodes, W. H.; Natansohn, S., Powders for advanced structural ceramics. *American Ceramic Society Bulletin* **1989,** *68* (10), 1804-1812.

166. Yu, G. E.; Edirisinghe, M. J.; Finch, D. S.; Ralph, B.; Parrick, J., Synthesis of alpha-silicon nitride powder from a polymeric precursor. *J. European Ceram. Soc.* **1995,** *15* (6), 581-590.

167. Cannon, W. R.; Danforth, S. C.; Flint, J. H.; Haggerty, J. S.; Marra, R. A., Sinterable ceramic powders from laser-driven reactions .1. Process description and modeling. *Journal of the American Ceramic Society* **1982,** *65* (7), 324-330.

168. Qi, Y. X.; Li, M. S.; Wang, C. G.; Bai, Y. J.; Zhu, B.; Wang, Y. X., Low-temperature preparation of silicon nitride via chemical metathesis route. *Materials Letters* **2004,** *58* (26), 3345-3347.

169. Luyjew, K.; Tonanon, N.; Pavarajarn, V., Mesoporous silicon nitride synthesis via the carbothermal reduction and nitridation of carbonized Silica/RF gel composite. *Journal of the American Ceramic Society* **2008,** *91* (4), 1365-1368.

170. Tan, G.; Miao, H.; Ren, H.; Yu, Z.; Li, J.; Li, H., Synthesizing silicon nitride whiskers by solvothermal and carbothermal methods. In *High-Performance Ceramics V, Pts 1 and 2*, Pan, W.; Gong, J. H., Eds. 2008; Vol. 368-372, pp 868-870.

171. Chaudhuri, M. G.; Ahmadullah, S.; Dey, R.; Das, G. C.; Mukherjee, S.; Mitra, M. K., Novel technique for synthesis of silicon nitride nanowires. *Advances in Applied Ceramics* **2011,** *110* (4), 211-214.

172. Rahman, I. A., Preparation of Si_3N_4 by carbothermal reduction of digested rice husk. *Ceramics International* **1994,** *20* (3), 195-199.

173. Kuskonmaz, N.; Sayginer, A.; Toy, C.; Acma, E.; Addemir, O.; Tekin, A., Studies on the formation of silicon nitride and silicon carbide from rice husk. *High Temperature Materials and Processes* **1996,** *15* (1-2), 123-127.

174. Liou, T. H.; Chang, F. W., The nitridation kinetics of pyrolyzed rice husk. *Industrial & Engineering Chemistry Research* **1996,** *35* (10), 3375-3383.

175. Weimer, A. W.; Cassiday, J. R.; Susnitzky, D. W.; Black, C. K.; Beaman, D. R., Carbothermal nitridation synthesis of alpha-Si_3N_4 powder from pyrolysed rice hulls. *Journal of Materials Science* **1996,** *31* (22), 6005-6013.

176. Rahman, I. A., The formation of different Si_3N_4 phases in the presence of V_2O_5 during carbothermal reduction of untreated and acid treated rice husk. *Ceramics International* **1998,** *24* (4), 293-297.

177. Mansour, N. A. L.; Hanna, S. B., Silicon-carbide and nitride from rice hulls .2. Effect of iron on the formation of silicon-carbide. *Transactions and Journal of the British Ceramic Society* **1979,** *78* (6), 132-136.

178. Rahman, I. A.; Riley, F. L., The Control of Morphology in Silicon Nitride Powder Prepared from Rice Husk. *J. European Ceram. Soc.* **1989,** *5*, 11-22.

179. Hashishin, T.; Iwanaga, H.; Yamamoto, Y., Effect of impurities on silicon nitride whiskers synthesized from silica-containing natural substances. *Journal of Materials Research* **2003,** *18* (12), 2760-2764.

180. Real, C.; Alcala, M. D.; Criado, J. M., Synthesis of silicon nitride from carbothermal reduction of rice husks by the constant-rate-thermal-analysis (CRTA) method. *Journal of the American Ceramic Society* **2004,** *87* (1), 75-78.

181. Pavarajarn, V.; Precharyutasin, R.; Praserthdam, P., Synthesis of Silicon Nitride Fibers by the Carbothermal Reduction and Nitridation of Rice Husk Ash. *Journal of the American Ceramic Society* **2010,** *93* (4), 973-979.

182. Rubio, E.; Rodriguez-Lugo, V.; Fuentes, R.; Castano, V. M., Synthesis of alpha-Si(3)N(4) whiskers from rice hulls. *Research Journal of Chemistry and Environment* **2008,** *12* (3), 63-67.

183. Malkov, A. V.; Gordon, M. R.; Stoncius, S.; Hussain, J.; Kocovsky, P., Desymmetrization of Cyclic meso-Epoxides with Silicon Tetrachloride Catalyzed by PINDOX, a Chiral Bipyridine Mono-N-oxide. *Organic Letters* **2009,** *11* (23), 5390-5393.

184. Gresback, R.; Nozaki, T.; Okazaki, K., Synthesis and oxidation of luminescent silicon nanocrystals from silicon tetrachloride by very high frequency nonthermal plasma. *Nanotechnology* **2011,** *22* (30).

185. Luo, Z.; Cai, X.; Hong, R. Y.; Wang, L. S.; Feng, W. G., Preparation of silica nanoparticles using silicon tetrachloride for reinforcement of PU. *Chemical Engineering Journal* **2012,** *187*, 357-366.

186. Chen, J. M.; Chang, F. W., The chlorination kinetics of rice husk. *Industrial & Engineering Chemistry Research* **1991,** *30* (10), 2241-2247.

187. Okutani, T.; Nakata, Y.; Ishikawa, K.; Takeda, K., Preparation of $SiCl_4$ from rice hull ashes .2. Effect of alkaline and alkaline-earth metal salt additives on chlorination of rice hull ashes. *Nippon Seramikkusu Kyokai Gakujutsu Ronbunshi-Journal of the Ceramic Society of Japan* **1991,** *99* (4), 315-319.

188. Andreoli, M.; Luca, G. T.; Seo, E. S. M., Characteristics of rice husks for chlorination reaction. *Materials Letters* **2000,** *44* (5), 294-298.

189. Seo, E. S. M.; Andreoli, M.; Chiba, R., Silicon tetrachloride production by chlorination method using rice husk as raw material. *Journal of Materials Processing Technology* **2003,** *141* (3), 351-356.

190. Singh, R.; Dhindaw, B. K., Production of High-purity silicon for use in solar cells. *in sun, Mankind's Future Source of Energy: Proceedings of the International Solar Energy Congress* **1978**, 776-781.

191. Banerjee, H. D.; Sen, S.; Acharya, H. N., Investigations on the production of silicon from rice husks by the magnesium method. *Materials Science and Engineering* **1982,** *52* (2), 173-179.

192. Bose, D. N.; Govindacharyulu, P. A.; Banerjee, H. D., Large grain polycrystalline silicon from rice husk. *Solar Energy Materials* **1982,** *7* (3), 319-321.

193. Hunt, L. P.; Dismukes, J. P.; Amick, J. A.; Schei, A.; Larsen, K., Rice hulls as a raw-material for producing silicon. *Journal of the Electrochemical Society* **1984,** *131* (7), 1683-1686.

194. Mishra, P.; Chakraverty, A.; Banerjee, H. D., Production and purification of silicon by calcium reduction of rice-husk white ash. *Journal of Materials Science* **1985,** *20* (12), 4387-4391.

195. Larbi, K. K.; Barati, M.; McLean, A., Reduction behaviour of rice husk ash for preparation of high purity silicon. *Canadian Metallurgical Quarterly* **2011,** *50* (4), 341-349.

196. Romano, J. S.; Rodrigues, F. A., Titanium-bearing dicalcium silicates from rice hull ash: Synthesis and properties. *Journal of the American Ceramic Society* **2007,** *90* (7), 2259-2261.

197. Pyon, K. R.; Han, K. S.; Lee, B. H., Formation and color properties of vanadium doped $ZrSiO_4$ ceramic pigments. *Journal of Ceramic Processing Research* **2011,** *12* (3), 279-288.

198. Chatterjee, M.; Naskar, M. K., Sol-gel synthesis of lithium aluminum silicate powders: The effect of silica source. *Ceramics International* **2006,** *32* (6), 623-632.

199. Ng, Y. C.; Jei, C. Y.; Shamsuddin, M., Titanosilicate ETS-10 derived from rice husk ash. *Microporous and Mesoporous Materials* **2009,** *122* (1-3), 195-200.

200. Sayan, P.; Titiz-Sargut, S.; Ozgul-Yucel, S.; Kiran, B., Physical and Adsorptive Characterization of Precipitated Magnesium Silicate from Rice Hull Ash Silica. *Chemical Engineering & Technology* **2011,** *34* (9), 1497-1506.

201. Rodrigues, F. A., Synthesis of chemically and structurally modified dicalcium silicate. *Cement and Concrete Research* **2003,** *33* (6), 823-827.

202. Davidovits, J., Global Warming Impact on the Cement and Aggregates Industries. *5th International Global Warming Conference* **1994,** *6* (2), 263-278.

203. Singh, N. B., Hydrothermal synthesis of (beta-dicalcium silicate beta-Ca_2SiO_4). *Progress in Crystal Growth and Characterization of Materials* **2006,** *52* (1-2), 77-83.

204. Lin, Z.; Rocha, J.; Navajas, A.; Tellez, C.; Coronas, J.; Santamaria, J., Synthesis and characterisation of titanosilicate ETS-10 membranes. *Microporous and Mesoporous Materials* **2004,** *67* (1), 79-86.

205. Pang, X. A.; Zhuang, X. L.; Tang, Z. H.; Chen, X. S., Polylactic acid (PLA): Research, development and industrialization. *Biotechnology Journal* **2010,** *5* (11), 1125-1136.

206. Mussatto, S. I.; Dragone, G.; Guimaraes, P. M. R.; Silva, J. P. A.; Carneiro, L. M.; Roberto, I. C.; Vicente, A.; Domingues, L.; Teixeira, J. A., Technological trends, global market, and challenges of bio-ethanol production. *Biotechnology Advances* **2010,** *28* (6), 817-830.

207. FAO Cereal Supply and Demand Brief. *Food and Agriculture Organization (FAO) of the United Nations* **2012**.

208. Kumar, P.; Barrett, D. M.; Delwiche, M. J.; Stroeve, P., Methods for Pretreatment of Lignocellulosic Biomass for Efficient Hydrolysis and Biofuel Production. *Ind. Eng. Chem. Res.* **2009,** *48* (Copyright (C) 2012 American Chemical Society (ACS). All Rights Reserved.), 3713-3729.

209. Li, Y.; Ding, X. F.; Guo, Y. P.; Rong, C. G.; Wang, L. L.; Qu, Y. N.; Ma, X. Y.; Wang, Z. C., A new method of comprehensive utilization of rice husk. *Journal of Hazardous Materials* **2011,** *186* (2-3), 2151-2156.

210. Singh, A.; Pant, D.; Korres, N. E.; Nizami, A.-S.; Prasad, S.; Murphy, J. D., Key issues in life cycle assessment of ethanol production from lignocellulosic biomass: Challenges and perspectives. *Bioresource Technology* **2010,** *101* (13), 5003-5012.

211. Moon, H. C.; Jeong, H. R.; Kim, D. H., Bioethanol production from acid-pretreated rice hull. *Asia-Pac. J. Chem. Eng.* **2012,** *7* (2), 206-211.

212. Saha, B. C.; Cotta, M. A., Lime pretreatment, enzymatic saccharification and fermentation of rice hulls to ethanol. *Biomass & Bioenergy* **2008,** *32* (10), 971-977.

213. Abbas, A.; Ansumali, S., Global Potential of Rice Husk as a Renewable Feedstock for Ethanol Biofuel Production. *BioEnergy Res.* **2010,** *3* (4), 328-334.

214. Anda, M.; Shamshuddin, J.; Fauziah, C. I.; Omar, S. R. S., Increasing the Organic Matter Content of an Oxisol using Rice Husk Compost: Changes in Decomposition and Its Chemistry. *Soil Sci. Soc. Am. J.* **2010,** *74* (4), 1167-1180.

215. Safiuddin, M.; Jumaat, M. Z.; Salam, M. A.; Islam, M. S.; Hashim, R., Utilization of solid wastes in construction materials. *Int. J. Phys. Sci.* **2010,** *5* (13), 1952-1963.

216. Prasara-A, J.; Grant, T., Comparative life cycle assessment of uses of rice husk for energy purposes. *Int. J. Life Cycle Assess.* **2011,** *16* (6), 493-502.

217. Adam, F.; Appaturi, J. N.; Iqbal, A., The utilization of rice husk silica as a catalyst: Review and recent progress. *Catal. Today* **2012,** *190* (1), 2-14.

218. Kavitha, N.; Balasubramanian, M.; Vashistha, Y. D., Synthesis and Characterization of Nano Silicon Carbide Powder from Agricultural Waste. *Transactions of the Indian Ceramic Society* **2011,** *70* (3), 115-118.

219. Swatloski, R. P.; Spear, S. K.; Holbrey, J. D.; Rogers, R. D., Dissolution of cellose with ionic liquids. *Journal of the American Chemical Society* **2002,** *124* (18), 4974-4975.

220. Wang, H.; Gurau, G.; Rogers, R. D., Ionic liquid processing of cellulose. *Chem. Soc. Rev.* **2012,** *41* (4), 1519-1537.

221. Meng, Z.; Zheng, X.; Tang, K.; Liu, J.; Qin, S., Dissolution of natural polymers in ionic liquids: A review. *E-Polymers* **2012**, 1-29.

222. Zhu, S. D.; Wu, Y. X.; Chen, Q. M.; Yu, Z. N.; Wang, C. W.; Jin, S. W.; Ding, Y. G.; Wu, G., Dissolution of cellulose with ionic liquids and its application: a mini-review. *Green Chemistry* **2006,** *8* (4), 325-327.

223. Yang, D. L.; Fan, T. X.; Zhou, H.; Ding, J.; Zhang, D., Biogenic Hierarchical TiO_2/SiO_2 Derived from Rice Husk and Enhanced Photocatalytic Properties for Dye Degradation. *Plos One* **2011,** *6* (9).

224. Lynam, J. G.; Reza, M. T.; Vasquez, V. R.; Coronella, C. J., Pretreatment of rice hulls by ionic liquid dissolution. *Bioresource Technology* **2012,** *114*, 629-36.

225. Teck Nam, A.; Yoon, L. W.; Lee, K. M.; Ngoh, G. C.; Chua, A. S. M.; Lee, M. G., Efficiency of ionic liquids in the dissolution of rice husk. *Bioresources* **2011,** *6* (4), 4790-4800.

226. Patel, M.; Karera, A., Sic whisker from rice husk - microscopic study. *Powder Metallurgy International* **1991,** *23* (1), 30-32.

227. Ge, X. M.; Burner, D. M.; Xu, J. F.; Phillips, G. C.; Sivakumar, G., Bioethanol production from dedicated energy crops and residues in Arkansas, USA. *Biotechnology Journal* **2011,** *6* (1), 66-73.

228. Li, W. Y.; Sun, N.; Stoner, B.; Jiang, X. Y.; Lu, X. M.; Rogers, R. D., Rapid dissolution of lignocellulosic biomass in ionic liquids using temperatures above the glass transition of lignin. *Green Chemistry* **2011,** *13* (8), 2038-2047.

229. Huffman, G. P.; Shah, N.; Zhao, J. M.; Huggins, F. E.; Hoost, T. E.; Halvorsen, S.; Goodwin, J. G., In-Situ XAFS Investigation of K-Promoted Co Catalysts. *Journal of Catalysis* **1995,** *151* (1), 17-25.

230. Kamijo, N.; Umesaki, N., Laboratory Soft-X-ray XAFS - the Local-Structure of K_2O-SiO_2 Glasses. *Jpn. J. Appl. Phys. Part 1 - Regul. Pap. Short Notes Rev. Pap.* **1993,** *32*, 658-660.

231. Bassett, D. R.; Boucher, E. A.; Zettlemoyer, A. C., The effect of alkali halides and silver nitrate on the crystallization of silica powders. *Journal of Materials Science* **1972,** *7* (12), 1379-1382.

232. Krishnarao, R. V.; Subrahmanyam, J.; Kumar, T. J., Studies on the formation of black particles in rice husk silica ash. *J. European Ceram. Soc.* **2001,** *21* (1), 99-104.

233. Goh, C. S.; Tan, K. T.; Lee, K. T.; Bhatia, S., Bio-ethanol from lignocellulose: Status, perspectives and challenges in Malaysia. *Bioresource Technology* **2010,** *101* (13), 4834-4841.

234. Tengerdy, R. P.; Szakacs, G., Bioconversion of lignocellulose in solid substrate fermentation. *Biochem. Eng. J.* **2003,** *13* (2-3), 169-179.

235. Kuhad, R. C.; Singh, A., Lignocellulose biotechnology - current and future-prospects. *Crit. Rev. Biotechnol.* **1993,** *13* (2), 151-172.

236. Huddleston, J. G.; Visser, A. E.; Reichert, W. M.; Willauer, H. D.; Broker, G. A.; Rogers, R. D., Characterization and comparison of hydrophilic and hydrophobic room temperature ionic liquids incorporating the imidazolium cation. *Green Chemistry* **2001,** *3* (4), 156-164.

237. Simmons, B. A.; Singh, S.; Holmes, B. M.; Blanch, H. W., Ionic Liquid Pretreatment. *Chem. Eng. Prog.* **2010,** *106* (3), 50-55.

238. Zhao, Y. N.; Han, C. S., Permeation of Solvents Through Disk Type Rice Husk Silica Membrane Modified with Alkyl Silylation Reagents. *Journal of Nanoscience and Nanotechnology* **2011,** *11* (8), 7254-7257.

239. Nakata, Y.; Suzuki, M.; Okutani, T.; Kikuchi, M.; Akiyama, T., Preparation and properties of SiO_2 from rice hulls. *Nippon Seramikkusu Kyokai Gakujutsu Ronbunshi-Journal of the Ceramic Society of Japan* **1989,** *97* (8), 842-849.

240. Iler, R. K., Coagulation of colloidal silica by calcium-ions, mechanism, and effect of particle-size. *Journal of Colloid and Interface Science* **1975,** *53* (3), 476-488.

241. Ahmaruzzaman, M., A review on the utilization of fly ash. *Progress in Energy and Combustion Science* **2010,** *36* (3), 327-363.

242. Ananthanarayanan, A.; Tricot, G.; Kothiyal, G. P.; Montagne, L., A Comparative Overview of Glass-Ceramic Characterization by MAS-NMR and XRD. *Critical Reviews in Solid State and Materials Sciences* **2011,** *36* (4), 229-241.

243. Rawlings, R. D.; Wu, J. P.; Boccaccini, A. R., Glass-ceramics: Their production from wastes-a review. *Journal of Materials Science* **2006,** *41* (3), 733-761.

244. Xia, L.; Wen, G. W.; Song, L.; Wang, X. Y., Sol-gel synthesis and crystallization behaviour of beta-spodumene. *Journal of Sol-Gel Science and Technology* **2009,** *52* (1), 134-139.

245. Arvind, A.; Kumar, R.; Deo, M. N.; Shrikhande, V. K.; Kothiyal, G. P., Preparation, structural and thermo-mechanical properties of lithium aluminum silicate glass-ceramics. *Ceramics International* **2009,** *35* (4), 1661-1666.

246. El-Diasty, F.; Abdel-Baki, M.; Wahab, F. A. A.; Darwish, H., Dispersion and thermal properties of lithium aluminum silicate glasses doped with Cr3+ ions. *Applied Optics* **2006,** *45* (30), 7818-7825.

247. Xu, H. W.; Heaney, P. J.; Navrotsky, A.; Topor, L.; Liu, J., Thermochemistry of stuffed quartz-derivative phases along the join $LiAlSiO_4$-SiO_2. *American Mineralogist* **1999,** *84* (9), 1360-1369.

248. Abdulkadyrov, M. A.; Belousov, S. P.; Patrikeev, A. P.; Patrikeev, V. E.; Semenov, A. P., Fabricating the optical elements of compound mirrors for large astronomical telescopes. *J. Opt. Technol.* **2013,** *80* (4), 214-218.

249. Westerhoff, T.; Jedamzik, R.; Hartmann, P. In *Zero expansion glass ceramic ZERODUR® roadmap for advanced lithography*, 2013; pp 86832H-86832H-11.

250. Roy, R.; Agrawal, D. K.; McKinstry, H. A., Very low thermal-expansion coefficient materials. *Annual Review of Materials Science* **1989,** *19*, 59-81.

251. Bach, H.; Krause, D., *Low Thermal Expansion Glass Ceramics*. Second Edition ed.; 2006; p 51-59.

252. Naskar, M. K.; Chatteljee, M., A novel process for the synthesis of lithium aluminum silicate powders from rice husk ash and other water-based precursor materials. *Materials Letters* **2005,** *59* (8-9), 998-1003.

253. Wang, M. C., The Effect of TiO_2 Addition on the Preparation and Phase-Transformation for Precursor Beta-Spodumene Powders. *Journal of Materials Research* **1994,** *9* (9), 2290-2297.

254. Morsi, S. M.; Pakzad, A.; Amin, A.; Yassar, R. S.; Heiden, P. A., Chemical and nanomechanical analysis of rice husk modified by ATRP-grafted oligomer. *Journal of Colloid and Interface Science* **2011,** *360* (2), 377-385.

255. Wang, W.; Martin, J. C.; Huang, R.; Huang, W.; Liu, A.; Han, A.; Sun, L., Synthesis of silicon complexes from rice husk derived silica nanoparticles. *Rsc Advances* **2012,** *2* (24), 9036-9041.

256. Murthy, M. K.; Kirby, E. M., Infrared Study of Compounds and Solid Solutions in the System Lithia–Alumina–Silica. *Journal of the American Ceramic Society* **1962,** *45* (7), 324-329.

257. Phillips, B. L.; Xu, H. W.; Heaney, P. J.; Navrotsky, A., Si-29 and Al-27 MAS-NMR spectroscopy of beta-eucryptite ($LiAlSiO_4$): The enthalpy of Si,Al ordering. *American Mineralogist* **2000,** *85* (1), 181-188.

258. Roy, B. N., Spectroscopic Analysis of the Structure of Silicate Glasses along the Joint $xMAlO_2$-$(1–x)SiO_2$(M = Li, Na, K, Rb, Cs). *Journal of the American Ceramic Society* **1987,** *70* (3), 183-192.

259. Lin, M. H.; Wang, M. C., Crystallization Behavior of Beta-Spodumene in the Calcination of Li_2O-Al_2O_3-SiO_2-ZrO_2 Gels. *Journal of Materials Science* **1995,** *30* (10), 2716-2721.

260. Ghosh, N. N.; Pramanik, P., *Aqueous sol-gel synthesis of spodumene and eucryptite powders*. Maney: London, ROYAUME-UNI, 1997; Vol. 96.

261. Samanta, A. K.; Dhargupta, K. K.; Ghatak, S., Retention of SiC during development of SiC-MxSiyOz composites M = Al, Zr, Mg by reaction bonding in air. *J. European Ceram. Soc.* **2000,** *20* (12), 1883-1894.

262. Zaera, F., Nanostructured materials for applications in heterogeneous catalysis. *Chem. Soc. Rev.* **2013,** *42* (7), 2746-2762.

263. Zhang, S.; Nguyen, L.; Zhu, Y.; Zhan, S.; Tsung, C.-K.; Tao, F., In-Situ Studies of Nanocatalysis. *Accounts of Chemical Research* **2013,** *46* (8), 1731-1739.

264. Bonati, M. L. M.; Douglas, T. M.; Gaemers, S.; Guo, N., Synthesis, Characterization, and Catalytic Properties of Novel Single-Site and Nanosized Platinum Catalysts. *Organometallics* **2012,** *31* (15), 5243-5251.

265. Wang, S. N.; Zhang, M. C.; Zhong, L. W.; Zhang, W. Q., A strategy to immobilize noble metal nanoparticles on silica microspheres. *Journal of Molecular Catalysis a-Chemical* **2010,** *327* (1-2), 92-100.

266. Zhu, J.; Wang, T.; Xu, X.; Xiao, P.; Li, J., Pt nanoparticles supported on SBA-15: Synthesis, characterization and applications in heterogeneous catalysis. *Applied Catalysis B: Environmental* **2013,** *130–131* (0), 197-217.

267. Li, Z.-X.; Shi, F.-B.; Li, L.-L.; Zhang, T.; Yan, C.-H., A facile route to ordered mesoporous-alumina-supported catalysts, and their catalytic activities for CO oxidation. *Physical Chemistry Chemical Physics* **2011,** *13* (7), 2488-2491.

268. Li, A.; Zhao, J. X.; Pierce, D. T., Silica nanoparticles for template synthesis of supported Pt and Pt–Ru electrocatalysts. *Journal of Colloid and Interface Science* **2010,** *351* (2), 365-373.

269. Jiang, H. L.; Akita, T.; Ishida, T.; Haruta, M.; Xu, Q., Synergistic Catalysis of Au@Ag Core-Shell Nanoparticles Stabilized on Metal-Organic Framework. *Journal of the American Chemical Society* **2011,** *133* (5), 1304-1306.

270. Zhou, X.; Wu, T.; Hu, B.; Jiang, T.; Han, B., Ru nanoparticles stabilized by poly(N-vinyl-2-pyrrolidone) grafted onto silica: Very active and stable catalysts for hydrogenation of aromatics. *Journal of Molecular Catalysis A: Chemical* **2009,** *306* (1–2), 143-148.

271. Huang, L.; Wang, Z.; Ang, T. P.; Tan, J.; Wong, P. K., A novel SiO_2 supported Pd metal catalyst for the Heck reaction. *Catal Lett* **2006,** *112* (3-4), 219-225.

272. Li, W.; Zhao, D., Extension of the Stöber Method to Construct Mesoporous SiO_2 and TiO_2 Shells for Uniform Multifunctional Core–Shell Structures. *Advanced Materials* **2013,** *25* (1), 142-149.

273. Liz-Marzan, L. M.; Giersig, M.; Mulvaney, P., Synthesis of nanosized gold-silica core-shell particles. *Langmuir* **1996,** *12* (18), 4329-4335.

274. Zhang, L. X.; Shi, J. L.; Yu, J.; Hua, Z. L.; Zhao, X. G.; Ruan, M. L., A New In-Situ Reduction Route for the Synthesis of Pt Nanoclusters in the Channels of Mesoporous Silica SBA-15. *Advanced Materials* **2002,** *14* (20), 1510-1513.

275. Gill, C. S.; Price, B. A.; Jones, C. W., Sulfonic acid-functionalized silica-coated magnetic nanoparticle catalysts. *Journal of Catalysis* **2007,** *251* (1), 145-152.

276. Zhang, Q.; Zhang, T. R.; Ge, J. P.; Yin, Y. D., Permeable silica shell through surface-protected etching. *Nano Letters* **2008,** *8* (9), 2867-2871.

277. Lu, Y.; Mei, Y.; Drechsler, M.; Ballauff, M., Thermosensitive Core–Shell Particles as Carriers for Ag Nanoparticles: Modulating the Catalytic Activity by a Phase Transition in Networks. *Angewandte Chemie International Edition* **2006,** *45* (5), 813-816.

278. Kuroda, K.; Ishida, T.; Haruta, M., Reduction of 4-Nitrophenol to 4-Aminophenol over Au nanoparticles deposited on PMMA. *Journal of Molecular Catalysis A: Chemical* **2009,** *298* (1–2), 7-11.

279. Premkumar, T.; Lee, K.; Geckeler, K. E., Shape-tailoring and catalytic function of anisotropic gold nanostructures. *Nanoscale Research Letters* **2011,** *6*.

280. Datta, K. K. R.; Kulkarni, C.; Eswaramoorthy, M., Aminoclay: a permselective matrix to stabilize copper nanoparticles. *Chemical Communications* **2010,** *46* (4), 616-618.

281. El-Bahy, Z. M.; Mahmoud, K. H., Dielectric characterization and catalytic activity studies of nickel chloride doped carboxymethyl cellulose films. *Spectrochimica Acta Part A: Molecular and Biomolecular Spectroscopy* **2012,** *92* (0), 105-112.

282. Bonacchi, S.; Genovese, D.; Juris, R.; Montalti, M.; Prodi, L.; Rampazzo, E.; Zaccheroni, N., Luminescent Silica Nanoparticles: Extending the Frontiers of Brightness. *Angewandte Chemie-International Edition* **2011,** *50* (18), 4056-4066.

283. Zhang, C.; Lin, J., Defect-related luminescent materials: synthesis, emission properties and applications. *Chem. Soc. Rev.* **2012,** *41* (23), 7938-7961.

284. Pan, W.; Wang, N. H.; Li, G. F.; Ning, G. L., Monodisperse, Luminescent Silica Spheres Synthesized by a New Method. In *Advanced Material Science and Technology, Pts 1 and 2*, Tan, Y.; Ju, D. Y., Eds. 2011; Vol. 675-677, pp 1093-1096.

285. Rossi, L. M.; Shi, L.; Quina, F. H.; Rosenzweig, Z., Stöber Synthesis of Monodispersed Luminescent Silica Nanoparticles for Bioanalytical Assays. *Langmuir* **2005,** *21* (10), 4277-4280.

286. Green, W. H.; Le, K. P.; Grey, J.; Au, T. T.; Sailor, M. J., White phosphors from a silicate-carboxylate sol-gel precursor that lack metal activator ions. *Science* **1997,** *276* (5320), 1826-1828.

287. Ishikawa, Y.; Sato, K.; Kawasaki, S.; Ishii, Y.; Matsumura, A.; Muto, S., White light emission from amorphous silicon-oxycarbide materials. *Physica Status Solidi a-Applications and Materials Science* **2012,** *209* (6), 1022-1025.

288. Ishikawa, Y.; Kawasaki, S.; Ishi, Y.; Sato, K.; Matsumura, A., White Photoluminescence from Carbon-Incorporated Silica Fabricated from Rice Husk. *Japanese Journal of Applied Physics* **2012,** *51* (1).

289. Ishikawa, Y.; Vasin, A. V.; Salonen, J.; Muto, S.; Lysenko, V. S.; Nazarov, A. N.; Shibata, N.; Lehto, V. P., Color control of white photoluminescence from carbon-incorporated silicon oxide. *Journal of Applied Physics* **2008,** *104* (8).

290. Matsumura, A.; Ishii, Y.; Sato, K.; Ishikawa, Y.; Kawasaki, S., White light emitting Mesoporous Carbon-silica Nanocomposite. *IOP Conference Series: Materials Science and Engineering* **2011,** *18* (10), 102019 (4 pp.)-102019 (4 pp.).

291. Ishikawa, Y.; Ishii, Y.; Satoh, K.; Matsumura, A.; Kawasaki, S., Preparation of light emitting material by thermal treatment of rice husks. *IOP Conference Series: Materials Science and Engineering* **2011,** *18* (10), 102015 (4 pp.)-102015 (4 pp.).

292. Hayakawa, T.; Hiramitsu, A.; Nogami, M., White light emission from radical carbonyl-terminations in Al_2O_3-SiO_2 porous glasses with high luminescence quantum efficiencies. *Applied Physics Letters* **2003,** *82* (18), 2975-2977.

293. Yoldas, B. E., Thermochemically induced photoluminescence in sol-gel-derived oxide networks. *Journal of Non-Crystalline Solids* **1992,** *147–148* (0), 614-620.

294. Lin, P. Y.; Hsieh, C. W.; Kung, M. L.; Hsieh, S. C., Substrate-Free Self-Assembled SiOx-Core Nanodots from Alkylalkoxysilane as a Multicolor Photoluminescence Source for Intravital Imaging. *Scientific Reports* **2013,** *3*.

295. Davies, G. L.; McCarthy, J. E.; Rakovich, A.; Gun'ko, Y. K., Towards white luminophores: developing luminescent silica on the nanoscale. *Journal of Materials Chemistry* **2012,** *22* (15), 7358-7365.

296. Andreola, F.; Barbieri, L.; Bondioli, F., Agricultural waste in the synthesis of coral ceramic pigment. *Dyes and Pigments* **2012,** *94* (2), 207-211.

297. Andreola, F.; Barbieri, L.; Bondioli, F.; Cannio, M.; Ferrari, A. M.; Lancellotti, I., Synthesis of chromium containing pigments from chromium galvanic sludges. *Journal of Hazardous Materials* **2008,** *156* (1-3), 466-471.

298. Sahu, K. K.; Alex, T. C.; Mishra, D.; Agrawal, A., An overview on the production of pigment grade titania from titania-rich slag. *Waste Management & Research* **2006,** *24* (1), 74-79.

299. Hajjaji, W.; Seabra, M. P.; Labrincha, J. A., Evaluation of metal-ions containing sludges in the preparation of black inorganic pigments. *Journal of Hazardous Materials* **2011,** *185* (2–3), 619-625.

300. Abreu, M. A.; Toffoli, S. M., Characterization of a chromium-rich tannery waste and its potential use in ceramics. *Ceramics International* **2009,** *35* (6), 2225-2234.

301. Bondioli, F.; Andreola, F.; Barbieri, L.; Manfredini, T.; Ferrari, A. M., Effect of rice husk ash (RHA) in the synthesis of (Pr,Zr)SiO_4 ceramic pigment. *J. European Ceram. Soc.* **2007,** *27* (12), 3483-3488.

302. Pyon, K. R.; Lee, B. H., The influence of firing conditions on the color properties of Pr-$ZrSiO_4$ pigments synthesized using rice husk ash. *Journal of the Korean Ceramic Society* **2009,** *46* (4), 397-404.

303. Della, V. P.; Junkes, J. A.; Rambo, C. R.; Hotza, D., Synthesis of the ceramic pigment victoria green ($Ca_3Cr_2Si_3O_{12}$) from $CaCO_3.Cr_2O_3$ and SiO_2. *Quimica Nova* **2008,** *31* (5), 1004-1007.

304. Herrera, G.; Montoya, N.; Alarcon, J., Microstructure of Fe-$ZrSiO_4$ solid solutions prepared from gels. *J. European Ceram. Soc.* **2012,** *32* (1), 227-234.

305. Cannio, M.; Bondioli, F., Mechanical activation of raw materials in the synthesis of Fe_2O_3-$ZrSiO_4$ inclusion pigment. *J. European Ceram. Soc.* **2012,** *32* (3), 643-647.

306. Akdemir, S.; Ozel, E.; Suvaci, E., Stability of zircon pigments in water and diethylene glycol media: The case of turquoise V-$ZrSiO_4$. *Ceramics International* **2013,** *39* (2), 1909-1915.

307. Bondioli, F.; Ferrari, A. M.; Leonelli, C.; Manfredini, T., Syntheses of Fe_2O_3/silica red inorganic inclusion pigments for ceramic applications. *Materials Research Bulletin* **1998,** *33* (5), 723-729.